Neural Control and Biomechanics of Flight Initiation in *Drosophila melanogaster*

Thesis by
Gwyneth M. Card

In Partial Fulfillment of the Requirements
for the Degree of
Doctor of Philosophy

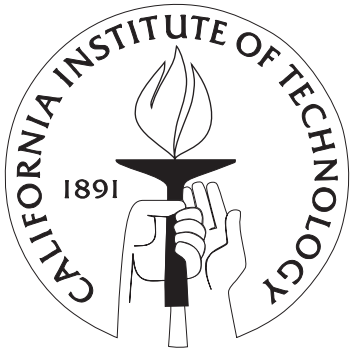

California Institute of Technology
Pasadena, California
2009

(Defended December 1, 2008)

To my parents

Who showed me what was possible

And then held my hand as I toddled along my way.

Acknowledgements

This thesis would not have been possible without the inspiration and guidance of my advisor, Michael Dickinson. I am especially grateful for his patient support, enthusiasm, and mentoring (including the occasional look of horror at my experimental use of rubber bands). I have learned a great deal from his example of excellence.

I would like to thank the rest of my committee, Mark Konishi, Joel Burdick, and John Dabiri, for their time and helpful suggestions. I especially appreciated the opportunity for feedback from both the biology and engineering perspectives.

I am most grateful to David King for his permission to reproduce his beautiful images of Dipteran cervical connective cross-sections shown in figure 1.3 and for his timely and patient help extracting detailed scaling information about these images from his data archives.

All my labmates have been unparalleled companions on this journey, and it is only with the help of their suggestions, expertise, conversation, and encouragement that I have made it this far. In particular, I am thankful to Seth Budick for teaching me how to poot my first fly; Rosalyn Sayaman for introducing me to the world of hand-digitization; Doug Altschuler for helping with the design of my initial camera rig; Mike Reiser for his sound advice and use of his modular visual displays; Allen Wong for his prowess with genetic tools and his patience in teaching; Andrew Straw for both his scientific and computer expertise; Francisco Zabala for carrying on the torch of fly biomechanics; Will Dickson for his willingness to lend a helping hand, be it with milling, math, or good company (and especially for our discussions on object rotation); Gaby Maimon and Wyatt Korff for their generous offers of help in the darkest hours, continual optimism, and excellent company on the dance floor; a big thanks to Jasper Simon and Alice Robie, whose care and helpful

suggestions I especially appreciated throughout our tenure together as grad students in the Dickinson Lab. Thanks also to Timothy Chung and Tim Tayler, whose collaboration greatly enriched my Caltech experience, and to the volunteers—Kimmi, Kavi, Lina, and Christin—for whose hours helping out in the lab I am grateful.

My parents, to whom this thesis is dedicated, deserve a special thanks for their continued support and encouragement. I still hope that some day I will grow up to be just like them. And thanks to my sister, Tiffany, for her enduring belief in the power of fruit flies and for knowing just what ray of sunshine to send her big sis as encouragement.

And finally, thanks to Stephen. Collectively we have now made it through the writing of five theses, and I think the team is just starting to hit its stride. Thanks for your patience through the long nights and endless noodles; for your proofreading and discussion; and for taking care of me during all the in-between times.

Abstract

In response to abrupt visual stimulation, the fruit fly, *Drosophila melanogaster*, quickly initiates flight. This rapid takeoff is believed to be a reflex coordinated by a pair of large descending interneurons (the "giant fibers"). However, it has been difficult to evoke escapes in wild-type flies, and thus flight initiation behavior in the unrestrained wild-type fly is poorly described. I have taken advantage of recent advances in high-speed videography to capture video sequences of *Drosophila* flight initiation at the temporal resolution of 6,000 frames per second. A three-dimensional kinematic analysis of takeoff sequences indicates that wing use during the jumping phase of flight initiation is essential for stabilizing flight. During voluntary takeoffs, flies raise their wings prior to leaving the ground, resulting in a stable, controlled takeoff. In contrast, during visually-elicited escapes flies pull their wings down close to their body during the takeoff jump, resulting in tumbling flights that are faster but less steady. The takeoff kinematics suggest that the power delivered by the legs is substantially greater during these escapes than during voluntary takeoffs. Thus, I show that the two types of *Drosophila* flight initiation result in different flight performances once the fly is airborne, and that these performances are distinguished by a trade-off between speed and stability. I also determined that flies can use visual information to plan a jump directly away from a looming threat. This is surprising, given the simple architecture of the giant fiber pathway thought to mediate escape. I found that approximately 200 ms before takeoff, flies begin a series of postural adjustments that determine the direction of their escape. These movements position their center of mass so that leg extension will push them away from the looming stimulus. These preflight movements are not the result of a simple feed-forward motor program because their magnitude and direction depend on the

flies' initial postural state. Furthermore, flies plan a takeoff direction even in instances when they choose not to jump. This sophisticated motor program is evidence for a form of rapid, visually mediated motor planning in a genetically accessible model organism.

Preface

For centuries we have been fascinated by the mystery of our own minds. Where do our thoughts come from? How do we process information? What guides our actions? Neuroscientists have come to appreciate the generality of this question: humans are not the only animals in which an assemblage of neurons assimilates information about the world and generates appropriate behavioral responses. In fact, this feat of cognitive processing is perhaps even more impressive from an organism, such as the fly, in which a brain with far fewer neurons than the human brain prescribes a rich behavioral repertoire that ensures the fly's survival.

Traditionally, neuroscientists have been divided in their approaches to answer the broad question "how does the brain work?" In one camp are those who advocate studying more complex brains, like our own, and in the other are those who believe we should start by understanding the basic functions of simpler brains. The first approach has the advantages that findings are directly applicable to treatment of human disorders and that studying a more complex system allows one to investigate more sophisticated cognitive processes. The second approach benefits from smaller, more tractable systems that permit neural circuit analysis at the level of individual cells and specific synaptic connections. Indeed some great success stories have come from simple creatures. General principles for how neurons are connected to produce circuit properties, such as lateral inhibition and habituation, were discovered in the horseshoe crab and sea slug respectively. Central pattern generating circuits, the basis for most coordinated movement, are best described in the stomatogastric ganglion of the lobster.

Both traditional approaches, however, have lacked systems in which we can analyze

an entire behavioral circuit, at the level of the neuron or populations of neurons, from sensory input to coordinated muscle output, especially with regard to central processing areas. There are many examples of systems that focus on either the sensory or motor components this process. To take just a few examples, sensory processing has been worked out in exquisite detail in both primate vision (Kaas and Collins, 2004) and barn owl sound localization (Knudsen and Konishi, 1978), and these systems have become important models for how information is coded in the brain. On the motor side, researchers have discovered how to decode motor planning areas of the primate cortex, information that could be used in the design of a new generation of prosthetic limbs (Andersen et al., 2004). And in simpler systems, such as the leech, we now know the exact circuits of motor- and interneurons that coordinate the leech's different modes of locomotion (swimming, crawling, retraction, etc.; Briggman et al., 2006).

The time is ripe to take advantage of our extensive knowledge of sensory and motor systems in order to evaluate how these components interact, at the systems-level, to generate appropriate behavioral responses to the environment. Beyond our accumulated knowledge of system components, the coming of age of model organisms has now provided us with the tool kit necessary to pursue this more integrative approach. After 100 years of studying *Drosophila melanogaster* (fruit fly) and *Mus musculus* (house mouse) and about 30 years investigation of *Caenorhabditis elegans* (round worm) and *Danio rerio* (zebrafish) we now have model organisms in which detailed neuroanatomy as well as sensory and motor physiology are known for the same system in which molecular genetic tools enable *in situ* visualization and *in vivo* manipulation of small, targeted groups of cells.

The main tool still lacking from this arsenal is the rigorous quantification of the behavior that arises from the known sensory and motor architectures of model organisms. A systems level analysis requires that one have detailed measures of the systems output to guide investigation of its components. For example, it is impossible to determine how neurons of a circuit contribute to a behavior without well-quantified parameters of the "normal" behavior to which one can compare mutant or otherwise perturbed systems.

This thesis is a first step down a path that proposes to use the flight initiation behavior of

the fruit fly, *Drosophila melanogaster*, as a model system in which to connect neural function to behavioral output across many levels of analysis. *Drosophila* is a particularly promising organism in which to try "cracking behavioral circuits" (Olsen and Wilson, 2008) because fly molecular genetic tools are the most highly developed, electrophysiological monitoring of identified cells, though challenging, is possible, and calcium imaging of brain activity is rapidly coming online. Furthermore, as this thesis proposes, the behavioral repertoire of *Drosophila* is turning out to be more sophisticated than we could have imagined. Recent development of high-speed video techniques now enable us to view the world at a fly's timescale, and we see that, in mere blinks of the human eye, flies are performing intricate calculations about their environment and planning appropriate responses, whether its escaping a predator, avoiding a collision with another fly, or traversing challenging terrain.

Several labs have already identified promising behaviors and approaches with *Drosophila* in order to begin teasing apart the neural circuits coordinating the fruit fly's diverse behavioral repertoire. *Drosophila* optomotor responses (Katsov and Clandinin, 2008), gap-crossing behaviors (Pick and Strauss, 2005), egg-laying choices (Yang et al., 2008), aggressive displays (Vrontou et al., 2006), and courtship rituals (Manoli et al., 2005) have all been examined to this end. From these studies researchers have ascertained that the central complex plays a key role in coordinating aspects of walking (Strauss, 2002) and that separate motion processing streams in the fly's visual system coordinate different optomotor behaviors (Katsov and Clandinin, 2008). This approach has also revealed that the neuromodulator octopamine modifies male courtship behavior and that a single neuron in the octopaminergic system is able to provide integration of multisensory cues that may be essential to proper expression of courtship behavior (Certel et al., 2007). A challenge of working with these previously described fly behaviors, however, is that little is known about the many of the neural components of these systems. Even with a visual behavior such as the optomotor response, a great deal is known about visual processing in the fly's optic lobes, but it is unclear how much central processing, if any, is required to generate the optomotor reflex and how this information is then relayed to thoracic motor centers that coordinate leg movement.

The genesis of this thesis was the suggestion of my advisor, Michael Dickinson, that flight initiation of the fruit fly might be good behavioral system in which to connect neural function to behavioral output. From what was known at the time, *Drosophila* flight initiation was an attractive system because the fly performed two distinct kinds of takeoff: one that was visually stimulated and coordinated by an identified reflex circuit, the giant fiber pathway, and one that was coordinated by an unknown but distinct pathway (reviewed in the following introduction). What I found in the course of this thesis work was a system far more complicated than previously imagined, but, I believe, quite amenable to the circuit-cracking techniques currently being developed for the fruit fly—perhaps bringing us one small step closer to understanding how our own brains work.

Contents

List of Figures

List of Tables

Chapter 1

Introduction

The ability to escape predation is one of the most important determinants of an animal's fitness. Perhaps no other behavior, besides reproduction itself, relates so directly to evolutionary success. Thus it is not surprising that neural circuits mediating escape responses tend to be fast, efficient, and highly conserved among organisms. This simplicity and stereotypy, together with the comparative ease of eliciting escape behaviors in a lab setting, has made escape a valuable model for researchers interested in elucidating the neural circuits that mediate behavior. Most physiological preparations, however, require that the animal be restrained, or even anesthetized, in order to record from its muscles or neurons. Consequently, though escape circuits are well-studied pathways, very little is known about how they are actually used in the life of an organism.

The escape circuit of the fruit fly, *Drosophila melanogaster*, is of special interest because of the molecular genetic and physiological tools now available to neuroscientists for monitoring and purturbation of specific neural pathways. For example, enhancer trap lines of a GAL4/UAS system (Brand and Perrimon, 1993) allow simultaneous expression of a gene whose activation is specific to a small group of adult neurons (the driver) and a gene inserted into the genome by researchers (the reporter). By selecting a specific reporter gene, researchers can manipulate the cells of the driver line in different ways, e.g., silence them, visualize their activity by monitoring internal calcium levels, or even photoactivate them in unrestrained animals (for a review, see Duffy, 2002).

Furthermore, years of studying the *Drosophila* escape circuit as a model for general neurobiological mechanisms as diverse as synaptogenesis, habituation, and epilepsy mean that the anatomy, development, and physiology of the circuit are well known. Despite this attention, however, we still do not know how the circuitry is used in the real world by the fly.

This thesis examines the unrestrained escape response of *Drosophila melanogaster* to naturalistic stimuli. We find that it is useful for the fly to have a separate mechanism to initiate flight during escape and nonurgent situations because there is a trade-off in takeoff performance between speed and stability. Further, I find that the escape response used by *Drosophila* to avoid a looming object, such as an approaching predator, is much more complicated and directed than previously thought, and I present some of the first evidence suggesting that, in a natural setting, the known escape circuit is not sufficient to explain the entire escape response.

1.1 Giant Fibers and Escape

One reason escape behaviors are of such interest to neuroethologists is that in many animals they are mediated by simple pathways involving giant fibers. Giant fibers (GFs) are neurons whose axons are considerably larger in diameter than any other fibers in the nervous system of the animal to which they belong. Such cells were observed in arthropods as early as 1879 (Krieger, 1879) and even earlier in annelids, such as the earthworm (Leydig, 1860, cited in Friedländer, 1889). By the start of the twentieth century, giant fibers had been found in a range of invertebrates (for a list see Johnson, 1924), however there was some debate as to whether they were part of the nervous system or had a structural function (Claparede, 1869; Johnson, 1924). Ultimately, their similarity to other neurons in the nerve cord, connection to cell bodies, and branching structure marked them out as neurons, and in the 1920s Johnson (1924; 1926) showed that they had a neural function: electrical stimulation of crayfish lateral and medial giant fibers produced a ventral tail flip. The giant axons of the squid, identified by Young in 1936, were later famously used by Hodgkin and Huxley (1939)

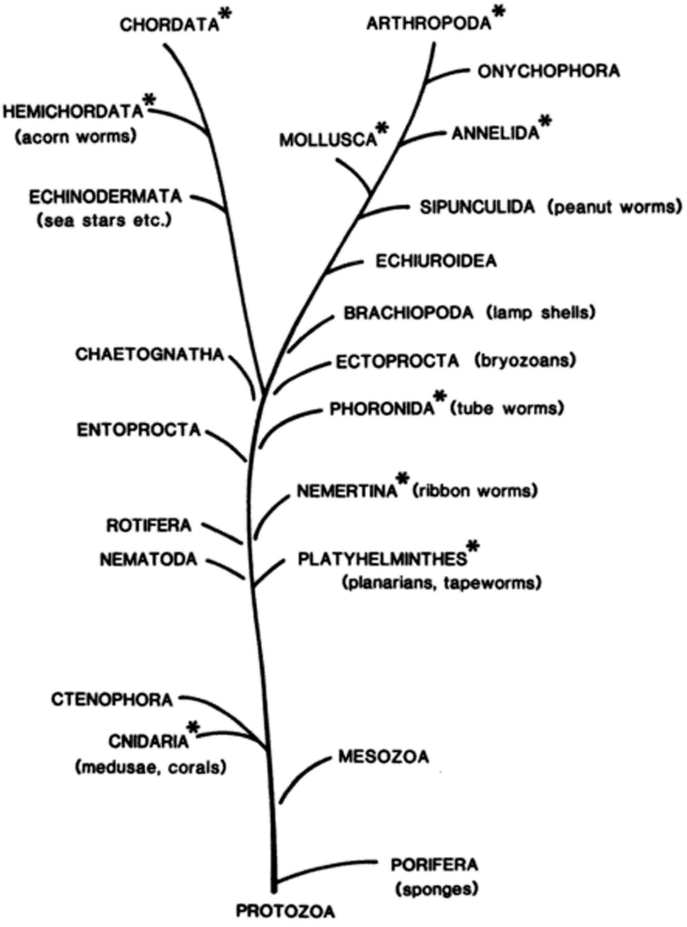

Figure 1.1. Phylogenetic tree showing evolutionary relationships of animal phyla. Phyla marked with an asterisk include species that have giant fibers. Reproduced from Bullock (1984).

to determine the ionic basis of the action potential, the mechanism of electric transmission used by neurons for rapid communication. In the last 70 years, studies using giant systems have contributed to the core knowledge of neurobiology on every level including cell and membrane properties, synaptogenesis, mechanisms of neural integration, regeneration and plasticity, and system organization (Bullock, 1984). Giant fibers are now know to occur across a wide range of phyla, including jellyfish, insects, and lower vertebrates, though they are notably absent from others including reptiles, birds, and mammals (figure 1.1).

The exact relationship between giant fibers and escape behaviors remains unclear. The discontinously large size of the fibers indicates that they should have a fast conduction

velocity (Offner et al., 1940; Rushton, 1951; Hodgkin, 1954; Hartline and Colman, 2007; Bullock and Horridge, 1965), and, in fact, the fastest recorded impulse (210 m s^{-1}) was recorded in the giant fiber of a shrimp at (at 22℃; Fan et al., 1961; Kusano, 1965; Kusano and LaVail, 1971; Kusano, 1966). This speed suggested to researchers early on that GFs should play a role in rapid maneuvers such as a predatory strike or escape. Of the many GF systems examined so far, all seem to be involved in escape behavior (for a review, see Eaton, 1984), though examples range from fish, in which Mauthner cells are believed to start or accelerate an escape "C-start" to *Drosophila* where the GFs are considered a command neuron for rapid flight initiation.

1.2 The Giant Fiber System (GFS) of *Drosophila*

1.2.1 A Historical Perspective

Insect giant fibers (GFs) were first observed in *Drosophila* in 1948 when Power examined the nervous structure of the thoracic ganglion in a winged insect for the first time. In his description of the GFs, Power wrote,

> *There are several groups of large fibers in the nervous system of* Drosophila *... but none of these approach the size of the two giant fibers ... When they were first observed by the author 4 or 5 years ago, he could not accept the fact, which now seems clear, that they are true giant nerve fibers.*

Power's observations suggest that, though the *Drosophila* giant fibers are diminutive in absolute terms (4–6 µm in diameter; Power, 1948; Coggeshall et al., 1973) they qualify as true giant fibers because they are still considerably larger than the next largest cells in the *Drosophila* nervous system. In other words it is relative, not absolute, size that qualifies a fiber as "giant." Power makes the further point that even the truly giant fibers of the squid *Loligo*, which reach 0.6–1 mm in the adult, are only 4.3 µm in diameter in newly hatched squid, which have roughly the same body length as an adult *Drosophila*.

Power described the course of the bilaterally paired giant fibers as they descended from the brain, through the central connective in the neck, to their outputs in the thoracic

ganglion. His staining technique, using gold- and silver-impregnated whole mounts, did not enable him to determine the origin of the GF in the brain, so he described only the middle and distal portions of the neurons. Power also described the GF as branching in the mesothoracic neuromere of the thoracic ganglion and exiting out the posterior dorsal mesothoracic nerve to directly innervate the large muscle that extended the jumping legs (tergotrochanteral muscle, TTM). This description of the GF as a motor neuron was supported in later work by Levine and Tracey (1973), who intracellularly filled the GF with cobalt dye. It was not until the electron microscopy studies of Tanouye and Wyman in 1980 that it became clear that the giant fibers were not themselves motor neurons. Instead they make a set of extended synaptic connections in the thoracic ganglion with the TTM motor neuron and an interneuron (the peripherally synapsing interneuron, PSI) that innervates all five motor neurons of the wing depressor muscles (dorsal longitudinal muscles, DLMs). It later became clear that earlier staining techniques could not differentiate the TTM motor neuron and PSI interneuron from the GF because the neurons are connected by electrical synapses, through which small dye molecules can pass (Pitman et al., 1972; Politoff et al., 1974; Strausfeld and Obermayer, 1976).

After their discovery, initial interest in the giant fibers was focused on their possible role in the starting mechanism for flapping flight. The stretch-activation mechanism for powering flight had already been described (see section 1.2.5; Pringle, 1949; Roeder, 1951), but it was unclear how the oscillation of the wing depressor and elevator muscles was started. The tergotrochanteral muscle (TTM), the first muscle triggered by GF activation, was under scrutiny as the potential starter muscle because its location in the thorax indicated it might be bifunctional and could both extend the fly's middle legs and elevate its wings (Williams and Williams, 1943; Boettiger and Furshpan, 1952; Mulloney, 1969; Nachtigall and Wilson, 1967; Pringle, 1957). The direct connection between the GF and TTM raised the possibility that the GF-TTM pathway was the start mechanism. While it remains unclear at present whether TTM activation is sufficient to start the flight motor, there is increasing evidence that flapping can commence without GF or TTM activity (Nachtigall and Wilson, 1967; Bennet-Clark and Ewing, 1968; Levine and Tracey, 1973; Heide, 1968).

Detailed analysis of the *Drosophila* GF pathway continued in the 1980s when Robert Wyman, John Thomas, David King and others focused on the system as a model for the study of the genes and gene products essential to determining precise neural connectivity. Wyman and colleagues meticulously described the anatomy and physiology of the 8 neurons and 20 muscles involved in the thoracic Giant Fiber System (GFS; figure 1.2) and developed a rapid screening protocol to identify flies with deficiencies at GFS synapses. Mutagenized flies were screened for defective jump reflexes by putting them in a flask turned upside down in a beaker. Flies were able to walk along the walls of the flask and naturally walked upward to populate the flask walls and ceiling. A light-off stimulus, previously demonstrated to activate the GF in white-eyed flies (Levine, 1974), was delivered to the flask full of flies, causing those with normal GF reflexes to jump off the walls and fall down out of the flask (Thomas and Wyman, 1982; Wyman and Thomas, 1983; Thomas and Wyman, 1984). A later varient on this protocol added a *curved* wing deficiency to the genome so that jumping flies were not able to fly back onto the flask walls (Wyman et al., 1984). In this way, only those flies with a defect in their jump reflex were left in the flask and collected. Subsequent physiological tests then determined whether the defect was in the sensory processing pre-synaptic to the GFs in the brain or was part of the known GFS anatomy in the thorax. After using this method to mutagenize and screen over 100,000 flies, Thomas and Wyman (1982; 1984) identified three mutants that demonstrated precise deficiencies in GFS synapses: *bendless*, *passover*, and *gfA*. Further investigation of these mutants has led to general discoveries of the molecular basis of neural development and function as described in the following section.

1.2.2 Contributions of *Drosophila* GFS Studies to Neurobiology

The three GFS mutants originally identified by the forward genetics approach of Thomas and Wyman (1982; 1984) provide some of the best examples of how analysis of this simple system has led to discoveries with relevance to all nervous systems.

In *bendless* mutants, the GF arborize normally in the brain, but in the T2 neuromere of the thoracic ganglion they fail to make the normal turn away from the midline towards

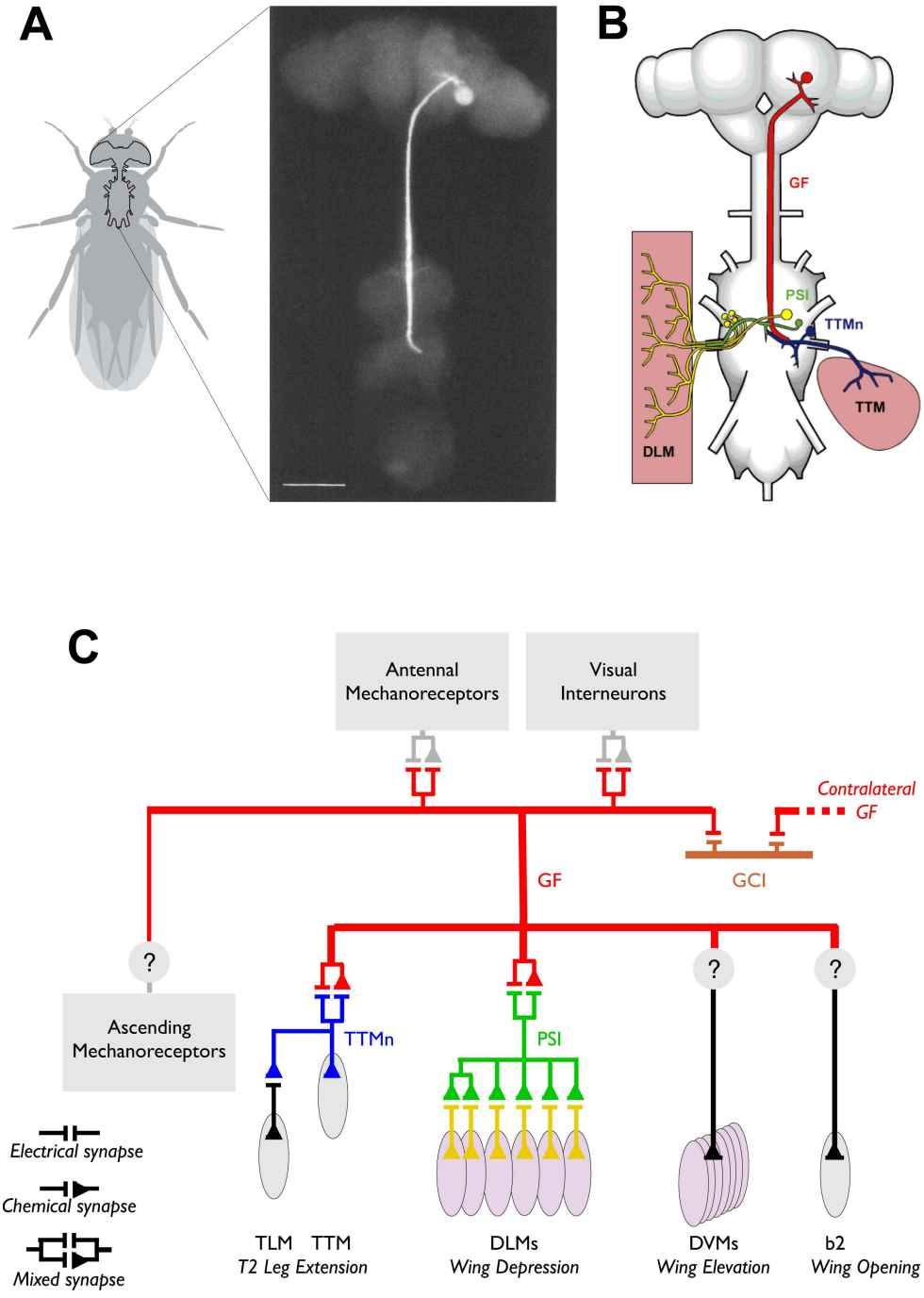

Figure 1.2. The giant fiber system of *Drosophila*. (A) Fluorescent photomicrograph of a GF in a shaking-B2 mutant (adapted from Phelan et al., 1996); (B) Morphology of the GF and its primary synaptic partners, the TTMn and the PSI (from Blagburn et al., 1999); (C) Schematic of the GFS and its known and hypothesized inputs and outputs.

their connection point with the TTM motor neuron (TTMn, Thomas and Wyman, 1982). Disruption of the normal GF-TTMn synapse is evident from the delayed TTM response to GF stimulation (Thomas and Wyman, 1984; Oh et al., 1994). It was not until a full decade after isolation of the mutant, however, that molecular tools had developed enough to determine that the *bendless* gene encoded a ubiquitin-conjugating protein (Muralidhar and Thomas, 1993; Oh et al., 1994). Ubiquitination is an enzyme-mediated process that marks a protein for degredation (for review see Murphey and Godenschwege, 2002). The *Drosophila bendless* mutation provided the first clue that ubiquitin may play a critical role in the assembly of neural networks, and we now know that ubiquitin trafficking of cell surface proteins is important for growth-cone pathfinding as well as the formation and upkeep of synapses (for reviews see Hicke, 2001; Hegde and Diantonio, 2002).

When the GF is stimulated extracellularly in the brain, *passover* mutants have abnormally long latencies of TTM response, and the normal DLM activation is absent (Thomas and Wyman, 1984; Baird et al., 1990). The disruption in the pathway must be at the synapses with the GF because stimulation of TTM and DLM motorneurons still activate the muscles normally (Thomas and Wyman, 1984). Furthermore, in these mutants Lucifer yellow or cobalt dye fails to pass between the GF and any of its presynaptic or postsynaptic partners as it does in wild-type flies, even though GF morphology in *passover* and wild-type flies is essentially identical (Sun and Wyman, 1996; Phelan et al., 1996; Jacobs et al., 2000). Further investigations of the cause of the *passover* mutation, and an independently identified mutation in the same gene, *shaking-B* (Homyk et al., 1980; Baird et al., 1990) led to the discovery of a novel family of proteins that form gap junctions in invertebrates (Krishnan et al., 1993; Phelan et al., 1996; Trimarchi and Murphey, 1997; Phelan et al., 1998). These proteins share structure and function with the four-pass transmembrane gap junction proteins found in vertebrates, the connexins, but have very different primary amino acid sequences, implying the two sets of proteins are not homologous (Bauer et al., 2005). The new class of proteins were thus named Innexins (for invertebrate connexin analogues; Phelan et al., 1998) and helped solve the mystery of why, until that time, no sequence coding for connexin proteins could be found in the newly sequenced genomes of

either the fruit fly or worm (for a review, see Phelan and Starich, 2001).

The *gfA* mutants were orginially characterized by their normal TTM-activation but abnormally long DLM-activation latencies in response to GF stimulation (Thomas and Wyman, 1984). No problem was found in the neuromuscular junction between DLM motor neurons and DLMs, and each DLM fiber could fail independently, so Thomas and Wyman surmised the disruption was likely to be in the PSI-DLM motor neuron connection. Only recently, did Fayyazuddin and coworkers (2006) finally show that the *gfA* gene codes for a nicotinic acetylcholine receptor ($D\alpha7$), which is present at PSI-DLM motor neuron synapses, but also localizes to GF dendrites where cholinergic synapses presumeably mediate visual input to the GF. Thus, lack of $D\alpha7$ in *gfA* mutants can explain both the aberrant DLM response and the behavioral phenotype which does not jump in response to a light-off stimulus.

Beyond these initial examples, the GFS has been important as a model central synapse for the characterization of membrane channels involved in the propagation of normal action potentials, including the Na^+ channel mutant, *paralyzed* (Siddiqi and Benzer, 1976) and the K^+ channel mutant, *Shaker* (Tanouye et al., 1981). The *Drosophila* GFS also played a key role in the characterization of the dynamin mutant, *shibire* (Ikeda et al., 1976). Currently the GFS is used to investigate the mechanisms of synaptic plasticity (Engel and Wu, 1996; Engel and Wu, 1998; Engel et al., 2000) and seizure disorders in the hopes of finding a treatment for human epilepsies (Pavlidis et al., 1994; Pavlidis and Tanouye, 1995; Kuebler and Tanouye, 2000; Kuebler et al., 2001; Lee and Wu, 2002; Zhang et al., 2002).

1.2.3 Anatomy of the GFS

The giant fibers are a pair of bilaterally symmetric interneurons that are clearly identifiable in the *Drosophila* CNS by their size and unique morphology. The cell bodies of the GFs are large, 24–29 µm in diameter, and reside near the posterior border of the brain, dorsal to the esophageal canal (Koto et al., 1981; Phelan et al., 1996). A 60 µm neurite projects anteriorly to connect the cell body to the main GF axon. The dendritic arbor of the GF in the brain has three main branches. The largest of these runs ventrally (in relation to the neuroaxis)

to the ipsilateral protocerebral lobe near the anterior edge of the brain. Here it extends numerous short, spiny processes into the antennal glomerulus (Koto et al., 1981). Cobalt staining from backfills of the neuropil containing the GF suggest that it receives first order input from the mechanoreceptors of the Johnston's organ as well as other antennal afferents (Strausfeld and Singh, 1980; Strausfeld and Bassemir, 1983; Bacon and Strausfeld, 1986; Sun and Wyman, 1996). The two other dendrites are smaller. One projects ventrolaterally where it is cobalt-coupled via gap junctions to a set of retinotopically arrayed small fibers (Col-A neurons) from the lobula region of the optic lobe (Strausfeld and Bassemir, 1983; Strausfeld et al., 1984). The second small dendrite projects dorsomedially to contact a trio of giant commissural interneurons (GCIs), which extend to the contralateral side of the brain. (Koto et al., 1981; Phelan et al., 1996). Intracellular injection of Lucifer Yellow dye into one of the GFs often passes both into the GCIs and into the contralateral GF, indicating that these neurons are connected with electrical synapses (Phelan et al., 1996; Strausfeld and Obermayer, 1976; Benshalom and Dagan, 1985). The GF axons continue posteriorly to the rear of the brain where they turn dorsally, part around the esophagus, and then exit the brain along the dorsal midline of the cervical connective (Power, 1948; Koto et al., 1981; Phelan et al., 1996).

The cervical connective is a thin bundle of axons that traverses the fly's neck ventrally to connect the brain to the thoracic ganglion. In cross section, the GFs are clearly visible as the largest fibers, with diameters ranging from 4–8 µm (Power, 1948; Phelan et al., 1996; figure 1.3⋆). The GFs enter the thorax from their dorsal position in the central connective, continue their path posteriorly down the midline of the animal, and then begin to descend ventrally. Thus when they reach the mesothoracic (T2) neuromere they are roughly in the center of the ganglion along a dorsal-ventral axis (Power, 1948). The GFs are remarkable because during their descent from the back of the brain, through the cervical connective and the first half of the thoracic ganglion, their axons are unbranched. In the anterior region of the T2 neuromere, however, the fibers make a sharp lateral bend away from each other (Power, 1948; Levine and Tracey, 1973; Koto et al., 1981; Phelan et al., 1996; Thomas and Wyman, 1982). At the point of this turn, the GF axons send out a tuft of

small spines towards each other (King and Wyman, 1980; Koto et al., 1981; Phelan et al., 1996), and it is suggested that this is a second place, besides via the GCIs in the brain, where the fibers are electrically coupled. Evidence for this comes from the observation that dye will spread between the two fibers even when the GCIs and regions of the CNS anterior to the dye injection site are gently crushed (Phelan et al., 1996).

The GFs make two main synaptic contacts in the mesothoracic neuromere: the peripherally synapsing interneuron (PSI), which traverses the midline to excite all five motorneurons of the contralateral wing depressor muscles (dorsolateral muscles, DLMs), and the motor neuron of the main jump muscle, the tergotrochanteral muscle (TTM). Both the GF-TTMn and GF-PSI synapses pass dye, indicating that they are gap junctions (Power, 1948; Levine and Tracey, 1973; Strausfeld and Bassemir, 1983), but if electrical synapses are eliminated by a mutation that prevents the formation of gap junctions, then stimulating the GFs still produces a long latency response in the muscles (Allen et al., 1999; Blagburn et al., 1999; Baird et al., 1990). The conclusion based on these observations is that both of these contacts are made with mixed electrical/chemical synapses.

The GF makes extensive contact with the ipsilateral PSI near the point of the GF bend in the T2 neuromere. The PSI axon then projects dorsally and crosses the midline to exit the ganglion in the contralateral posterior dorsal mesothoracic nerve (PDMN). Cross sections of the nerve show that here the PSI is surrounded by the five large motorneurons of the DLMs (Ikeda et al., 1980; Wyman et al., 1984). These motor neurons press in on the PSI, giving it an irregular shape in profile and forming numerous cholinergic synapses with the interneuron. Electron micrographs also show reciprocal synapses of the DLMs

Figure 1.3. Cross sections of the cervical connective for a range of Dipteran species (and one section of a Cuttlefish stellar nerve). The scale bars shown below each section represent 25 μm; the two *Drosophila* sections (marked with $\star$) have interior scale bars of 10 μm. Unless otherwise noted, the images are from King (2007) and show cross sections through the anterior thorax. Thus the large-diameter fibers seen in the lateral areas of the cross-section are motor neurons rather than descending interneurons as shown in the rest of the section (motor neurons are indicated by brackets in some sections). Sections are listed by the Dipteran family to which they belong, see Appendix A for detailed species information. Row 1: Tipulidae, Psychodidae, Tabanidae, Rhagionidae; Row 2: Asilidae, Bombyliidae, Bombyliidae, Empididae; Row 3: Dolichopodidae, Syrphidae, Micropezidae, Lauxaniidae, Sphaeroceridae; Row 4: Drosophilidae ($\star$*Drosophila melanogaster*; from J. Coggshall, in King, 2007), Drosophilidae ($\star$*Drosophila melanogaster*; by Bruce Boschek, in Wyman et al., 1984), Ephydridae, Row 5: Anthomyiidae, Muscidae, Muscidae (King, 1983), Glossinidae; Row 6: Glossinidae (King, 1983), Sarcophagidae (King, 1983), Tachinidae, Cuttlefish (*Sepia officinalis*, stellar nerve; Young, 1936)

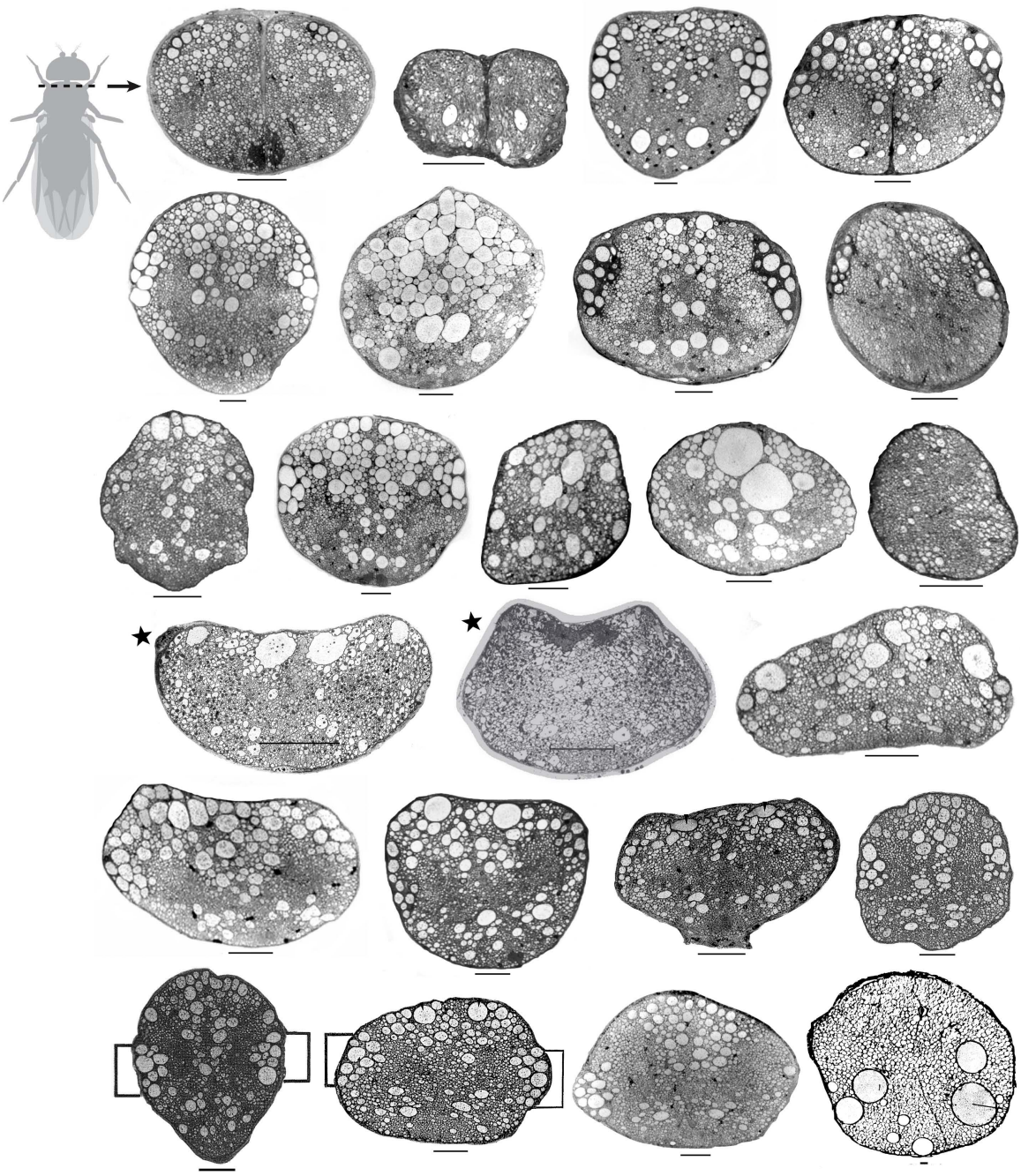

Figure 1.3. See p. 11 for caption.

back onto the PSI. These are fewer in number and observed to have synaptic vesicles of a different size (and hence probably a different neurotransmitter) in comparison to the forward synapses. The PSI terminates about 20 µm into the PDMN, and after this point the DLMns increase in diameter (from 1-3 µm to 3-5 µm) and continue out of the nerve to contact all six wing depressor muscles (note two of the wing depressor muscles are innervated by a single motorneuron, (King and Tanouye, 1983; King and Wyman, 1980). Besides their contact with the ipsilateral GF in the ganglion, the bilateral PSI pair also have an extensive area of mutual contact near the midline, and they also each directly contact the ipsilateral TTM (King and Wyman, 1980). The interneurons also have an extensive dendritic arbor within the anterior thoracic ganglion. Thus the PSIs could integrate sensory information coming into the thoracic ganglion and activate the TTMs and DLMs bilaterally without the requirement of GF activity (Coggshall, 1978; Phelan et al., 1996).

After its bend and contact with the PSI, the GF continues 25–30 µm laterally where its distal tip contacts the motorneuron of the TTM (TTMn). The TTMn is the largest of three axons presumed to innervate the TTM, which acts as an extensor of the mesothoracic jumping legs. Its 10-15 µm diameter cell body can be found ventral to the GF axon bend. The TTMn has two branches before it leaves the ganglion through the PDMN. One branch extends dorsomedially from the cell body to contact the tip of the GF, the other projects posteriorly and branches distally at the T2-T3 boundary (Power, 1948; Phelan et al., 1996).

The assembly of all GFS contacts is completed within the first two days of pupation. The GF and TTMn are actually born early in development, during embryogenesis, but GF and TTMn axon pathfinding does not begin until the larval period (Allen et al., 1998; Jacobs et al., 2000; Murphey et al., 2003), and it ends about 24 hours after puparium formation. In the next 24 hour period, functional synapses between the GFS components are formed (Phelan et al., 1996). In the final 55-100 hours of pupation, dendritic growth continues and the synapes of the GFS are stabilized (Allen et al., 1998; Murphey et al., 2003; Hummon and Costello, 1987; for a review, see Allen et al., 2006). Though the neural connections of the GFS are complete at the time of eclosion, the fly does not demonstrate an escape response during the first few hours post eclosion (Harvey et al., 2008; Hammond

and O'Shea, 2007b), and when the GFS is stimulated directly, the jumping legs of newly eclosed flies produce only 65% of the jumping force observed in older flies.

1.2.4 Physiology of the GFS

A unique feature of the GFS, which has made it amenable to studies of physiological mutants (see section 1.2.2), is that, due to their large size, the GFs are the first descending neurons triggered by gross electrical stimulation across the brain (Levine and Tracey, 1973; Tanouye and Wyman, 1980; Tanouye and King, 1983; Hummon and Costello, 1989; Trimarchi and Schneiderman, 1993; Trimarchi and Schneiderman, 1995a) or cervical connective (Levine and Tracey, 1973). The prediction that larger fibers have lower activation thresholds is supported by both classical theory and evidence in larger insects (Hursh, 1939; Dagan and Parnas, 1970; O'Shea, personal communication in Levine and Tracey, 1973). Early experimenters observed that the lowest threshold response to a voltage induced across the brain was a stereotyped "triadic" muscle activation pattern of the TTM, DLM, and DVM muscles. They observed that when the voltage was increased, the latency of the responses to the stimulation decreased by about 3 ms, although the relative timing of evoked potentials in the muscles remained the same (Levine and Tracey, 1973). They interpreted this short-latency response to be the motor output of direct GF stimulation, and the long-latency response to be the result of stimulating the presynaptic inputs to the GF in the brain. Later studies, in which intracellular recordings of the GF were made simultaneously with brain stimulation, confirmed that this method does invoke a spike in the GF, followed by the characteristic timing of DLM activation (Tanouye and Wyman, 1980). These researchers were not able to record TTM muscle activity simultaneously with intracellular GF recordings as the strong contraction of the TTM muscle dislodged their electrode, so all successful recordings had the TTM removed. However, a later study using extracellular recording of the GF in the neck connective showed that brain stimulation triggers a spike in the cervical connective, presumably the GF, as well as the expected TTM and DLM responses (Trimarchi and Schneiderman, 1995a). Furthermore, intracellular injection of current into the GF drives the TTM and DLM mus-

cles with the same latencies as brain stimulation, indicating that activation of the GF alone can produce the observed triadic muscle response (Tanouye and Wyman, 1980; Thomas and Wyman, 1982).

The Triadic Motor Response

When the GF is activated, either by gross stimulation of the brain or cervical connective, or by intracellular current injection, the TTM is always the first muscle to respond. Its latency to the stimulus is 0.81 ± 0.07 (SD) ms (Tanouye and Wyman, 1980). The DLMs are activated next with a latency of 1.25 ± 0.10 (SD) ms (Tanouye and Wyman, 1980). The firing of all six DLM fibers is tightly synchronized, with only 0.22–0.27 ms latency between DLMa and DLMd. The evoked potentials in the DVMs, which fire last, have a larger variability in their latency to the stimulus and the fibers fire more asynchronously: 3.31 ± 0.8 ms for DVMI, 2.94 ± 0.7 ms for DVMII, and 2.03 ± 0.23 ms for DVMIII (Tanouye and Wyman, 1980). Besides the stereotyped timing of the evoked muscle potentials, another feature of the triadic muscle response is the high following frequencies of the TTM and DLM responses. If the stimulation across the brain is given as a train of pulses, DVM fibers stop responding at frequencies above 0.2–3 Hz. DLM fibers, however, can respond to the pulses one-to-one up to 30–100 Hz, and the TTM muscle can follow up to 300 Hz (Levine and Tracey, 1973; Tanouye and Wyman, 1980). The triadic muscle response has been recorded repeatedly in multiple studies and is remarkably consistant, although the voltage required to initiate the triad using brain stimulation does vary considerably between preparations. Measurements of the muscle triad in wild-type and mutant flies from a number of studies are summarized in Table 1.1.

Other Motor Output of the GFS

Although recording from the GF itself is a challenge (it is large relative to other fibers in the neck connective but still small relative to available electrophysiological methods) the robustness of the triadic muscle response has given researchers a tool with which to further investigate the input and output of the GFS. To determine which of the fly's other thoracic

Table 1.1. The GFS traidic muscle response

GF stimulation method	GF recording method	TTM latency (ms)	DLM latency (ms)	DVM latency (ms)	Max TTM following freq. (Hz)	Max DLM following freq. (Hz)	Fly genotype	Ref.
Extr. brain	none	0.81 ± 0.07	1.25 ± 0.10	3.31 ± 0.8 (I) 2.94 ± 0.7 (II) 2.03 ± 0.23 (III)	> 100	> 100	Hochi-R	[1]
Extr. brain	none	0.9–1.1, 0.1 var	1.2–1.3, 0.1 var	2.3–2.5, 7–8 var	–	–	Canton-S, Oregon-R	[2]
Extr. brain	none	0.84 ± 0.01	1.33 ± 0.01	$3.36 + /0.04$ (Ic)	–	–	Canton-S	[3]
Extr. brain	extracel.	0.864	–	–	–	–	*bw;st*	[4]
Intracellular	–	0.9	1.3	–	–	–	Canton-S	[5]
Extr. brain	intracel.	0.88 ± 0.09	1.30 ± 0.04	–	–	–	Canton-S	[5]
Extr. brain	none	–	1.13 ± 0.05	–	–	–	Canton-S	[6]
Intracellular	intracel.	0.8	1.2	–	–	–	*bw;st*	[7]
Extr. brain	none	1.06 ± 0.03	1.43 ± 0.02	–	–	–	Oregon-R	[8]
Extr. brain	none	0.88, 0.003 var	1.31, 0.021 var	–	–	–	Canton-S	[9]
Extr. brain	none	0.78 ± 0.12	1.24 ± 0.10	–	97 ± 11	81 ± 26	Canton-S	[10]
Extr. brain	none	0.96 ± 0.05	1.54 ± 0.08	4.45 ± 1.06 (I) 4.47 ± 0.86 (II) 2.17 ± 0.16 (III)	300 (6 stim)	100 (9 stim)	Canton-S	[11]
Extr. brain	none	0.83 ± 0.04	1.42 ± 0.11	–	100%@250	51.7%@250	*w*; c17/CyO	[12]
Extr. brain	none	0.86 ± 0.10	1.39 ± 0.14	–	88.3%@250	55%@250	*w*; A307/CyO	[12]
Extr. brain	none	0.81 ± 0.07	1.25 ± 0.10	–	> 100	137 ± 14.7	+/+	[13]
Extr. brain	intracel.	2.31 ± 0.44	1.29 ± 0.10	–	–	–	*bendless*	[5]
Extr. brain	intracel.	1.50 ± 0.18	No response	–	–	–	*passover*	[5]
Extr. brain	intracel.	0.87 ± 0.09	3.21 ± 0.94	–	–	–	*gfA*	[5]
Extr. brain	none	1.76 ± 0.27*	No response*	–	–	–	*pas* mutants	[8]
Extr. brain	none	0.97, 0.015 var	1.64, 0.028 var	–	–	–	*shi* (44 hr)	[9]
Extr. brain	none	1.01 ± 0.25	1.30 ± 0.23	–	–	–	*bithorax*	[10]
Extr. brain	none	2.67 ± 0.68	1.45 ± 0.11	4.08 ± 0.72 (I) 5.29 ± 1.59 (II) 2.33 ± 0.18 (III)	(Can't follow moderate frequencies)	(Follows high frequencies)	ben^1	[11]
Extr. brain	none	1.36 ± 0.55	1.53 ± 0.20	–	39.1%@250	60%@250	*w*;c17/UAS-*Gl*	[12]
Extr. brain	none	2.68 ± 0.52	2.33 ± 0.41	–	10%@250	16%@250	*w*;A307/UAS-*Gl*	[12]
Extr. brain	none	1.36 ± 0.05	1.48 ± 0.09	–	< 1	22 ± 9.2	cpo^{EGI}/cpo^{cp1}	[13]
Extr. brain	none	1.46 ± 0.24	1.45 ± 0.05	–	< 1	14 ± 4.8	cpo^{EGI}/cpo^{cp2}	[13]

[1] Tanouye and Wyman, 1980; [2] Levine and Tracey, 1973; [3] Trimarchi and Schneiderman, 1993; [4] Trimarchi and Schneiderman, 1995a; [5] Thomas and Wyman, 1984; [6] Tanouye and King, 1983; [7] Thomas and Wyman, 1982; [8] Baird et al., 1990, *See reference for other examples; [9] Hummon and Costello, 1987; [10] Schneiderman et al., 1993; [11] Oh et al., 1994; [12] Allen et al., 1999; [13] Glasscock and Tanouye, 2005;

muscles are stimulated by the GFS, researchers can stimulate the brain at the lowest voltage necessary to elicit the triadic muscle response and simultaneously record from the muscle in question. If a muscle is stimulated at this same low threshold of GF activation, it is assumed that it is driven by the GF pathway. Using this methodology, Tanouye and King (1983) ascertained that neither of the direct flight muscles that cause wing elevation (*pa1*, *pa2* in the notation of Zalokar, 1947; I1, III1 in the notation of Heide, 1971) are driven by the GF pathway. One direct wing opener (*pa3* or b2) is activated at the same threshold as the GF pathway, while the other (*pa4* or b1) is not. The activated muscle, b2, is driven with a latency of 1.28 ± 0.10 ms from the stimulus pulse, which is just after the DLMs (indirect wing depressors) about 1 ms before the DVMs (indirect wing elevators). The latency of b2 activation indicates that there could be 1-2 chemical synapses between the GF and the b2 motor neuron.

Using the same technique, Trimarchi and Schneiderman (1993) have also shown that the tibia levator muscle (TLM), a muscle intrinsic to the leg, whose action extends the mesothoracic legs at the femur-tibia joint, is also activated at the same threshold as the triadic muscle response. Like b2, The TLM responds to brain stimulation just after the DLMs (mean latency 1.46 ± 0.02 ms after GF stimulation). In mutant flies with dysfunctional connections between the GF and the TTM that abnormally lengthen the TTM response time, the TLM response is also delayed. Yet in these cases the time between TTM and TLM firing remains about the same. Trimarchi and Schneiderman (1993) thus speculated that the TTM motor neuron (TTMn) itself may innervate the TLM motor neuron (TLMn). Though a functional connection between these two motor neurons has yet to be confirmed, neurites of the TTMn and TLMn do overlap in two regions of the T2 neuromere (Trimarchi and Schneiderman, 1993).

Sensory Activation of the GFS

It has proven difficult to activate the GF of wild-type *Drosophila* using sensory stimuli (Levine and Tracey, 1973; Kaplan and Trout, 1974; Nakashima-Tanaka and Matsubara, 1979; Trimarchi and Schneiderman, 1995b). Levine and Tracey (1973) originally found that

the only stimulus to reliably evoke a triadic muscle response in tethered wild-type flies was a puff of air directed at the antennae. However, several groups have shown that white-eyed mutant *Drosophila*, which lack the eye pigment that keeps photons entering one ommatidia from stimulating a neighboring region of the eye, readily elicit a triadic muscle response to flashes of light (Levine, 1974) or shadow stimuli (Trimarchi and Schneiderman, 1995b). In one study, researchers recorded the GF extracellularly in the neck during a shadow stimulus. The first spike recorded after stimulation, presumably the GF, occurred with the expected latency before TTM activation (0.85 ms, Trimarchi and Schneiderman, 1995a). Further evidence that flashes of light stimulate the GF in white-eyed flies come from experiments in which the fly is exposed to high-frequency stroboscopic flashes of light. The strobing frequencies at which different GF pathway muscles can no longer follow the stimulus one to one are similar to the brain stimulation frequencies at which the muscles can no longer follow: DVMs can follow light flashes up to 0.2–2.0 flashes per second, and DLMs follow up to 10–20 flashes per second. Several different mutant strains of white-eye flies exist, each with a mutation in a different part of the red eye pigment synthesizing pathway, yet all these mutants respond with about equal frequency to light-on or light-off stimuli. This indicates that the sensitivity of the white-eyed mutant GF pathway is unlikely to be a mutation in the pathway per se, but rather an effect that the loss of pigment itself has on amplifying the incoming visual stimulus. Normal, red-eyed flies do occasionally show a GF response to light flashes (Levine, 1974; Trimarchi and Schneiderman, 1995b), indicating that visual input to the GF is probably also present in wild-type flies, even if it is usually below the threshold to activate the pathway.

A second type of mutant in which flashes of light induce a GF-like response are *hyperkinetic* mutants (Hk^1). These mutants are known as "shakers" because their legs shake when anesthetized with diethyl ether. This mutation has been traced to motorneurons in each of the three leg pairs, which fire endogenously at a rate similar to that of the "shaking." *Hyperkinetic* mutants initiate flight (unrestrained flies) or produce a triadic muscle response (tethered flies) when shown flashes of light (Kaplan and Trout, 1974; Levine, 1974). Furthermore this response is mediated by sensory input from the ommatidia

and not the ocelli, since the response is normal if the ocelli are occluded but absent when both compound eyes are painted over. Both eyes must be covered, however, to abolish activity in either GF. Experiments with *hyperkinetic* mutants indicate that the GF may also receive ascending input from the tarsi. Tarsal contact with a piece of paper increased the probability that a tethered Hk^1 fly presented with a flash of light would produce a triadic muscle response 100-fold over trials in which the fly's tarsi were free. Tarsal contact also increased the likelihood that blowing on the fly would elicit the GF triad. Pulling the paper away without any wind or visual stimulus did not elicit the triadic muscle response, though the fly would often start to fly (Levine, 1974).

As the previous observation suggests, while visual and tactile stimuli have been indicated as activators of the GF pathway, other physiological evidence suggests that the fly has at least one alternate mechanism for initiating flight that does not involve the giant fibers. Levine and Tracey (1973) first suggested that there must be a non-GF flight initiating pathway when they observed that blowing on a tethered fly sometimes produced the GF-mediated muscle triad, but sometimes just stimulated a characteristic burst of DVM firing before the flight motor started. Trimarchi and Schneiderman (1995b) subsequently demonstrated that while shadow stimuli and brain stimulation induce the muscle triad response in white-eyed flies, the muscle response was more variable for trials in which a fly "voluntarily" kicked away the substrate (a Styrofoam ball) that it was holding (without any overt stimulation) or was induced to do so by exposure to an aversive benzaldehyde odor. Furthermore, the time between the first spike in the neck connective after stimulation, recorded extracellularly, and the onset of TTM firing had the same distribution and median value for the shadow response or brain stimulation, but was much more variable and, on average, shorter for odor-induced flight initiations, even those odor-induced starts that used muscle patterns very similar to the GF triad. In fact, 30% of odor presentations did not elicit a spike in the cervical connective before activation of the jump and flight muscles, compared to just 3% of trials with the shadow stimulus.

1.2.5 Sensors and Actuators of the GFS

As suggested by its anatomy and physiology, the GFS of *Drosophila* receives input from at least two modalities of sensor (visual and mechanosensory) and sends outputs to muscles of at least two types of appendage (legs and wings).

Visual Input

The compound eye of the fly is composed of about 700 individual structures (ommatidia), each of which has its own lens and set of 8 photoreceptors. The photoreceptors from each ommatidia project into the optic lobe where the visual information is organized in retinotopic columns of neurons and this structure is relayed through three layers of neuropil: the lamina, medulla, and lobula complex (Borst and Haag, 2002). The lobula complex itself is composed of two distinct regions, the lobula and the lobula plate. The lobula plate is one of the most comprehensively studied regions of an insect central nervous system as it occupies the dorsal surface of the brain, making it easy to access through the back of the head, and it contains several groups of giant motion-sensitive interneurons, which are relatively easy to record from. Many studies have shown that these large cells respond to particular patterns of wide-field motion that match the optic flow a fly would experience during specific self-rotations of its body (Reichardt, 1987; Hausen, 1984; Krapp et al., 1998; Franz and Krapp, 2000) In contrast, the Col-A cells that provide input to the GF have their dendrites in the lobula proper, and they have been shown to respond to visual contrast (a "light-on" stimulus) rather than motion (Gilbert and Strausfeld, 1991). Flies have a second array of photoreceptors, the occelli, located anterior and medial to the compound eyes, but covering these visual sensors appears to have no effect on the responses of the GFS (Levine, 1974).

Mechanoreception

The GFs have been shown to receive input from mechanoreceptors on at least two different parts of the body. Input from the tarsi when the legs are in contact with the ground increases the response rate of the GFs (Levine, 1974; Bacon and Strausfeld, 1986), however

little is known about which mechanoreceptors mediate this input. More is known about the antennal mechanoreceptors to which the GFs are dye coupled (Strausfeld and Singh, 1980; Strausfeld and Bassemir, 1983; Bacon and Strausfeld, 1986; Sun and Wyman, 1996). The Johnston's organ (JO) is a highly developed mechanoreceptor located in the second segment of the *Drosophila* anteannae (for a review, see Eberl and Boekhoff-Falk, 2007). It is the largest fly chordotonal organ, comprising 227 scolopidia sensor units and nearly 500 neurons (Kamikouchi et al., 2006). The JO responds to displacement of the third antennal segment relative to the second and is mulitifunctional. In *Drosophila* it has been shown to mediate hearing (Eberl et al., 2000) and play a role in gravitactic behavior (Armstrong et al., 2006). From behavioral studies (Budick and Dickinson, 2006) and by analogy with larger flies (Burkhardt, 1960; Gronenberg and Strausfeld, 1990) it is presumed that the JO detects air currents during flying and/or walking.

Wing Muscles

Insect flight muscles can be divided into two classes, "steering" muscles and "power" muscles, that are functionally and morphologically distinct (Pringle, 1949; Roeder, 1951; Boettiger, 1960). Power muscles drive the oscillatory motions of the wingstroke and thus produce the work necessary for flight. These muscles are composed of unusually large muscle fibers, which, in some species, can reach up to 2 mm in diameter. The muscles are rich in mitochondria (20%–40% by volume) in order to serve the aerobic needs of flight and so may be distinguished by their pinkish-brown color (Josephson, 2006). These muscles were originally referred to as "fibrillar" because their large fibrils can easily be seen under a microscope (Tiegs, 1955). Power muscles are distinct from most striated muscle because they are indirect and asynchronous. They are indirect because they do not attach to the wing directly, but rather to the thorax wall. One set, the dorsal longitudinal muscles (DLMs), consists of six muscles pairs attached from the anterior end of the scutum to the postnotum and mesophragma in a stack, one on top of the other from the dorsum down (Miller, 1950; Levine and Hughes, 1973). Contraction of these muscles along the fore-aft axis of the thorax causes an upward bowing of the scutum, depressing the wings, which are suspended

from the scutum (Pringle, 1968; Tiegs, 1955; Josephson, 2006). A second set, the dorsoventral muscles (DVMs), run from the scutum to three different ventral attachment points. Contraction of these muscles deforms the scutum, elevating the wings. Alternating contractions of the DLMs and DVMs thus cause the wings to flap rhythmically. The extremely rapid wingstroke of insects, up to 1,000 Hz in the smallest fliers (Sotavalta, 1953; Josephson, 2006), however, is only possible because the power muscles are asynchronous, meaning they do not need to receive neural input for each contraction. Instead the muscles need only be primed by motorneuron activation, which releases calcium, and can then be activated by stretching of the muscle itself (Pringle, 1949). In the case of insect flight, contraction of the DLMs indirectly stretches the DVMs and vice versa.

In contrast to the power muscles, the smaller steering muscles are synchronous, and fire one to one with their innervating motorneuron. There are 13 pairs of control muscles that attach directly onto the base of the wing (Dickinson and Tu, 1997; Williams and Williams, 1943; Nachtigall and Wilson, 1967; Heide, 1971). Activation of these direct steering muscles alters the attitude of the wing during the wingstroke by adjusting the wingstroke amplitude and wing angle of attack. The specific action of each muscle, however, depends not only on its anatomical attachment points, but also on what phase of the wingstroke it is activated and on which other steering muscles are also activated (Dickinson and Tu, 1997; Balint and Dickinson, 2001; Balint and Dickinson, 2004). The b2 is the only direct steering muscle known to be activated by the GFS.

Leg Muscles

The first and most robust response to GFS activity is contraction of the tergotrochanteral muscle (TTM). The TTM is the largest of the synchronous muscles in the fly. It extends from the lateral edge of the scutum to the trochanter of the mesothoracic leg (Miller, 1950; Schouest et al., 1986). Though it traverses the thorax parallel to the DVMs, the TTM is not fibrillar. Rather it consists of 22 anatomically distinct tubular fibers (Miller, 1950; Pringle, 1968) arranged to form a flattened tube that is twisted into a slight helix (Levine and Hughes, 1973). Activation of the TTM directly extends the femur at the femur-coxa

joint. The mesothoracic legs are the only leg pair attached to such a thoracic muscle (though Miller (1950) suggests that one of the DVMs, DVMII, was ancestrally a prothoracic leg muscle that has been transformed into a fibrillar flight muscle), and it is suggested that this muscle provides the main force during jumping in *Drosophila* (Mulloney, 1969; Zumstein et al., 2004; Nachtigall and Wilson, 1967; Williams and Williams, 1943; Elliott et al., 2007).

The only intrinsic leg muscle demonstrated to be part of the GFS so far is the tibia levator muscle (TLM) of the mesothoracic leg (Trimarchi and Schneiderman, 1993). This muscle is intrinsic to the femur and attaches at the trochanter and femur-tibia joint (Miller, 1950); (Soler, 2004). TLM contraction extends the femur-tibia joint. The motor neuron of this muscle, the TLMn, has extensive arborizations in the lateral leg neuromere (Trimarchi and Schneiderman, 1993). Trimarchi and Schneiderman (1993) hypothesized that the TTMn innervated the TLMn directly, but a direct anatomical connection between the TTMn and TLMn has yet to be observed.

1.2.6 The GFS and Escape Behavior

If stimulation of the GFs results in fast and stereotyped activation of wing and leg muscles, what does this mean for the actual behavior of the animal? Tanouye and King (1983) observed that, in a tethered preparation, brain stimulation of the GF drove prominent wing opening movements. In response to a single pulse, the fly opened and elevated its wings to an angle of about 45° with its body, then lowered them to the resting position. A train of pulses could keep the wings raised indefinitely. Others have demonstrated that in response to a flash of light, shadow stimulus, or strong gustatory input, tethered flies holding onto an object, such as a piece of tissue or small Styrofoam ball will kick the object away as though they were taking off from the ground (Levine and Wyman, 1973; Levine, 1974; Trimarchi and Schneiderman, 1995b). Not until recently, however, has it been unequivocally demonstrated that exciting the giant fiber pathway causes flight initiation in an unrestrained fly. Lima and Miesenbock (2005) expressed ATP-gated ion channels ($P2X_2$) in specific parts of the GFS. They then injected these flies with ATP molecules trapped

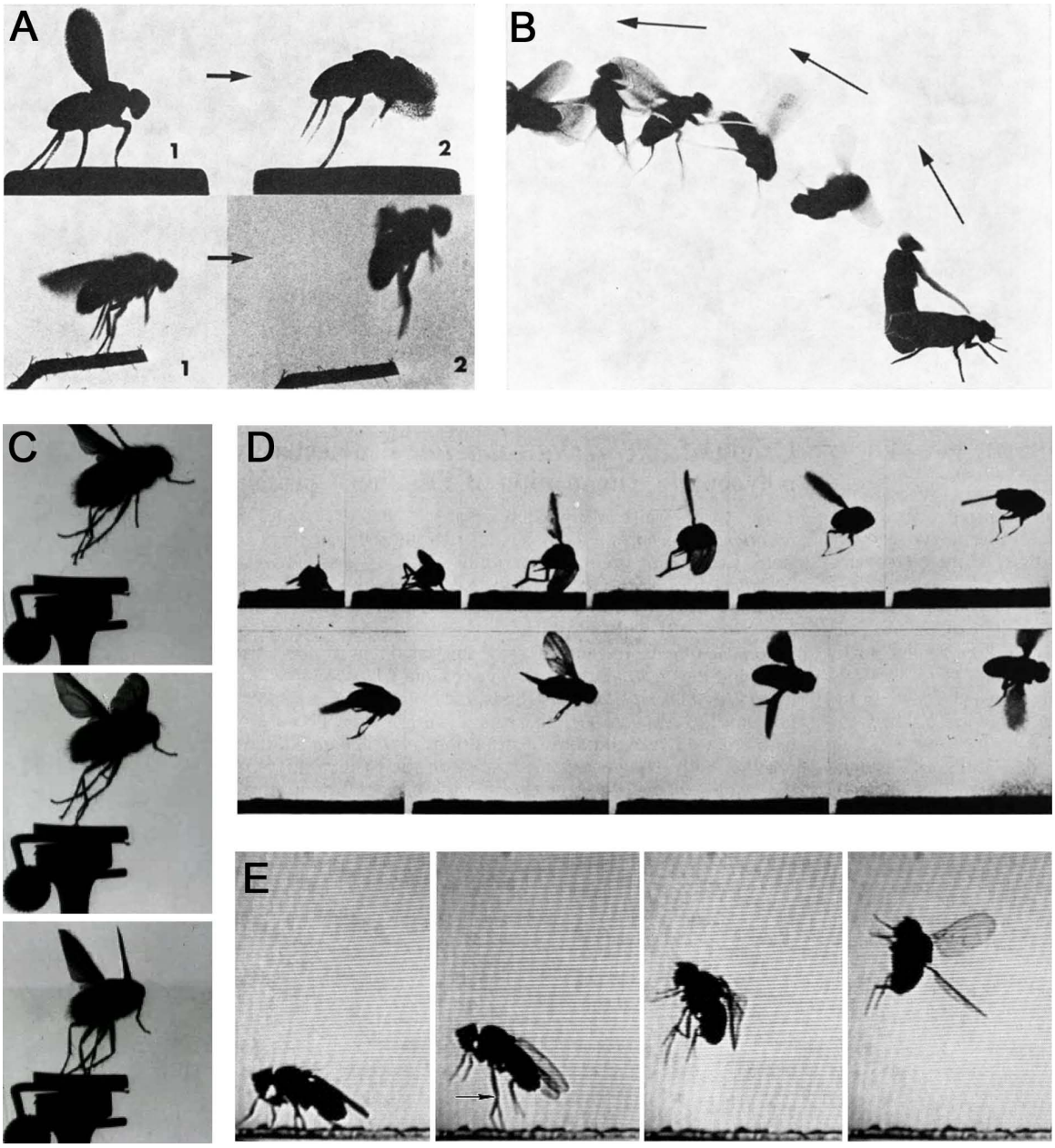

Figure 1.4. (A) Kaplan and Trout (1974), Canton-S (top), Hk^1 (bottom); (B) Kaplan and Trout (1974), Hk^1; (C) species unknown, Étienne-Jules Marey and Lucien Bull, circa 1903; (D) Williamson et al. (1974), *y w* Hk^1 *para12*; (E) Trimarchi and Schneiderman (1993), *bw;st*; next page: Trimarchi and Schneiderman (1995c), *bw;st*, (F) "Voluntary," (G) "Escape," sequences start in lower right panel.

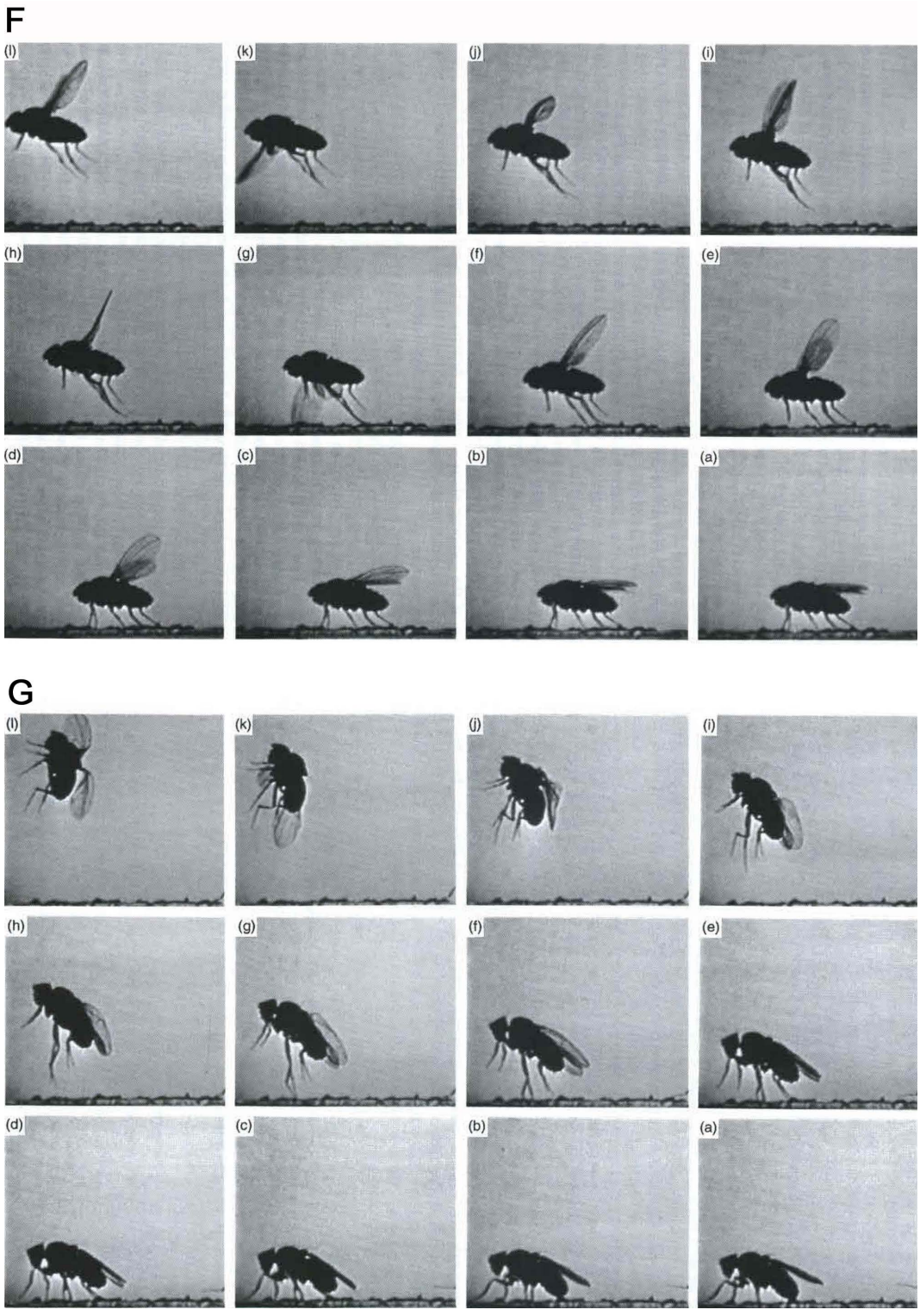
F
(l)
(k)
(j)
(i)
(h)
(g)
(f)
(e)
(d)
(c)
(b)
(a)
G
(l)
(k)
(j)
(i)
(h)
(g)
(f)
(e)
(d)
(c)
(b)
(a)

in a molecular cage that would change conformation and release them upon exposure to light. When a blue laser light was focused on these flies, presumably uncaging the ATP and depolarizing the GFs, the flies initiated flight.

Imaging the extremely rapid escape responses of unrestrained flies, however, has historically been a technological challenge. Very little is known about how freely moving flies use the GFS in real world situations. Few studies have examined the flight initiation of unrestrained *Drosophila*, and these have primarily used mutant stocks as their test subjects (figure 1.4). Both *hyperkinetic* mutants (Kaplan and Trout, 1974) and several eye-pigment mutants with both brown- and white-eyed phenotypes (Nakashima-Tanaka and Matsubara, 1979; Trimarchi and Schneiderman, 1995c) take off in response to a hand waved in front of them or a light-off stimulus. These same stimuli, however, fail to elicit flight initiation in wild-type flies of many strains (Canton-S: Kaplan and Trout, 1974; Trimarchi and Schneiderman, 1995c; Hikone-H: Nakashima-Tanaka and Matsubara, 1979).

The earliest known photographic sequences of a fly taking flight (figure 1.4C) were taken by the French scientist Étienne-Jules Marey and his assistant Lucien Bull at the start of the twentieth century (Hassler, 2008). Nearly a century later, Kaplan and Trout (1974) took the first high-speed images of the jump response of *Drosophila* (figure 1.4A). They filmed (at 400 frames per second) *hyperkinetic* mutants responding to a hand waved in front of them, and observed that the flies kicked off the ground with their middle legs. The wings did not start beating until the fly was airborne, resulting in a tumbling flight. In contrast, when they induced wild type Canton-S *Drosophila* to takeoff by using a speaker to vibrate the platform they were standing on, the wild-type flies first raised their wings then executed the take off kick together with downward and forward wing motion. Kaplan and Trout observed that Hk^1 flies could also execute wing-first takeoffs and so surmised that the response to hand motion might be some aberrant behavior related to the *hyperkinetic* mutation.

Twenty years later, Trimarchi and Schneiderman (1995c) were able to capture fly takeoffs on film at 2,000 frames per second, and they concluded that flies do have at least two modes of takeoff (figure 1.4F, G). They observed that flies taking off without explicit stimulation

("voluntarily") first raise their wings to a ready position, then simultaneously depress their wings and extend their mesothoracic legs at the moment of takeoff, a similar takeoff to those observed by Kaplan and Trout (1974) in response to vibration. In contrast, white-eyed flies shown a shadow stimulus forgo the wing-raising phase of the takeoff and immediately extend their middle legs. The authors argued that the no-wing jump in response to visual stimulation was not an aberrant behavior of the white-eyed mutant as the same behavior had been observed by Kaplan and Trout (1974) in a completely different mutant phenotype, Hk^1. Comparing their behavioral results with their physiological studies, they found that the same shadow stimulus that elicited the escape takeoff in unrestrained flies elicited a triadic motor pattern and spike in the cervical connective identical to that caused by brain stimulation of the GF. Therefore they concluded that the GF mediated visually-induced escape behavior. In contrast, non-visual escapes (voluntary or odor-induced) produced a different behavior sequence in unrestrained flies and did not elicit a triadic muscle response or cervical connective spike with the appropriate timing in tethered preparations. Therefore the GF pathway does not coordinate these flight initiations and there must be a second pathway that coordinates takeoff.

1.2.7 Similarity with Giant Fibers in Other Flies

The GFS of *Drosophila* shares a remarkable anatomical and physiological similarity with circuits found in other flies, most notably larger Muscoid flies. Anatomical studies of *Musca domestica* (King and Valentino, 1983; Strausfeld et al., 1984; Bacon and Strausfeld, 1986; Milde and Strausfeld, 1990), *Calliphora vicina* (Mulloney, 1969; Strausfeld et al., 1984; Bacon and Strausfeld, 1986; Milde and Strausfeld, 1990), and *Sarcophaga bullata* (King and Valentino, 1983) show that these flies all possess a pair of large descending fibers that resemble the giant fibers of *Drosophila*. Like in *Drosophila*, these fibers are the largest fibers visible in cross sections of the neck connective: up to 32 µm diameter in *Calliphora*. The general shape and trajectory of the giant cells is also very similar in all flies. The cell body is located in the posterior area of the brain and from it the relatively few dendritic arbors extend into antennal and visual neuropils. The bilaterally symmetric fibers then

descend unbranched through the cervical connective in a dorsomedial location in the ventral nerve cord. Like in *Drosophila*, the GFs of *Calliphora* have been shown to make functional connections with the motoneuron of the ipsilateral TTM (Mulloney, 1969) and a connection resembling the unique synapses of the PSI with the DLM motoneurons has been observed in all three larger flies (Bacon and Strausfeld, 1986). The dendritic arbors of the GF are more easily visualized in the larger flies, and injection with cobalt dye clearly shows that the dendrites get first order sensory input from antennal mechanoreceptors of the first and second antennal segments and from the receptors of the Johnston's organ, as well as input from columnar (Col-A) interneurons from the lobula (Strausfeld and Bassemir, 1983; Strausfeld et al., 1984; Bacon and Strausfeld, 1986).

The main differences between the GFS of *Drosophila* and that of its larger relatives appears to be in the GF terminal in the thorax. Though the contact points between the GF and the TTM motoneuron are similar in all flies examined, it is unclear what connection the GF makes with the PSI. Not only have these central connections been difficult to visualize (King and Valentino, 1983), the DLMs , whose motoneurons we know do contact a PSI-like interneuron, do not respond to gross stimulation of the cervical connective in *Calliphora*, though the TTMs produce a spike as expected if the GFs are stimulated (Mulloney, 1969). Furthermore, the GFs in the larger flies are dye coupled to more thoracic outputs than in *Drosophila*. For example, the GFs couple to three pairs of interneurons that project to all six leg neuronmeres (Bacon and Strausfeld, 1986). Activation of all 6 legs during escape is supported by the observation of Mulloney (1969) that white-eyed *Calliphora* with their middle legs removed can still jump about half the height as flies with all legs intact.

As in *Drosophila*, there is evidence that the GF pathway is not required to mediate flight initiation. Holmqvist and Srinivasan (1991) showed that a range of purely visual stimuli will reliably elicit a jump response from wild-type *Musca*, as long as the visual stimulus has outward motion cues and increasing darkening contrast. In a follow up study, however, Holmqvist (1994) observed that a looming stimulus which reliably induces a housefly to jump does not cause a spike in the GF in a restrained preparation, despite activation of the TTM jump muscle and a reliably observed GF spike when the animal is stimulated

electrically in the brain.

Figure 1.3 shows transverse cross sections from the cervical connective in a range of different Dipteran flies. In the *Drosophila* cross sections, the GFs are clearly identifiable as the largest-diameter profiles. Large fibers in a similar dorso-medial location are also clear in cross section from the *Drosophila* relatives described above (*Musca* and *Sarcophoga*). Across the whole Dipteran order, however, there are clearly some species that have GFs, others that have many large fibers, and some that have no particularly large fibers. In some cases, such as the tsetse fly, the phylogenetic order suggests that the GFs were lost from an ancestor that likely possessed them (King, 1983).

Chapter 2

Performance Trade-offs in the Flight Initiation of *Drosophila melanogaster*

2.1 Summary

The fruit fly *Drosophila melanogaster* performs at least two distinct types of flight initiation. One kind is a stereotyped escape response to a visual stimulus that is mediated by the hard-wired giant fiber neural pathway, and the other is a more variable "voluntary" response that can be performed without giant fiber activation. Because the simpler escape takeoffs are apparently successful, it is unclear why the fly has multiple pathways to coordinate flight initiation. In this study we use high-speed videography to observe flight initiation in unrestrained wild-type flies and assess the flight performance of each of the two types of takeoff. Three-dimensional kinematic analysis of takeoff sequences indicates that wing use during the jumping phase of flight initiation is essential for stabilizing flight. During

This chapter previously published as G Card and MH Dickinson (2008a) Performance trade-offs in the flight initiation of *Drosophila*. *J Exp Biol* 211:341-53.

voluntary takeoffs, early wing elevation leads to a slower and more stable take- off. In contrast, during visually elicited escapes, the wings are pulled down close to the body during takeoff, resulting in tumbling flights in which the fly translates faster but also rotates rapidly about all three of its body axes. Additionally, we find evidence that the power delivered by the legs is substantially greater during visually elicited escapes than during voluntary takeoffs. Thus, we find that the two types of *Drosophila* flight initiation result in different flight performances once the fly is airborne, and that these performances are distinguished by a trade-off between speed and stability.

2.2 Introduction

The flight initiation behavior of *Drosophila melanogaster* is an attractive model system for the study of sensory-motor integration, as it is a tractable system in which different sensory modalities are believed to trigger different descending pathways to elicit a takeoff. During a spontaneous takeoff, or when stimulated by an attractive odor, a fly first raises its wings to a ready position that it may hold for several seconds. It then extends its mesothoracic legs while depressing its wings, thus coordinating a jump with the initial downstroke (Trimarchi and Schneiderman, 1995c; Hammond and O'Shea, 2007b). In contrast, strong visual stimuli, such as a rapid drop in luminance, cause a fly to quickly extend its middle legs, propelling itself off the ground in less than 5 ms without the aid of coordinated wing motion. This simpler visually elicited escape response is mediated by the well-characterized giant fiber (GF) interneurons (for a review, see Allen et al., 2006), whereas spontaneous or odor-induced takeoffs are thought to involve a separate descending pathway (Holmqvist, 1994; Trimarchi and Schneiderman, 1995a; Trimarchi and Schneiderman, 1995b).

The GFs are a pair of large interneurons that traverse the cervical connective, linking sensory regions of the fly's brain to motor centers in its thoracoabdominal ganglion. In the thorax, each giant fiber contacts the ipsilateral motorneuron of the fly's main jump muscle (the tergotrochanteral muscle, TTM) and the peripherally synapsing interneuron (PSI), which crosses the midline to innervate the motorneurons of all six indirect wing

depressors (dorsal longitudinal muscles, DLMs) (Allen et al., 2006). When contracted, the TTMs extend the femur of the fly's mesothoracic legs. Thus it is this middle pair of legs that provides the main leg force during both voluntary and escape jumps (Nachtigall and Wilson, 1967; Tanouye and Wyman, 1980). The GFs in *Drosophila* are thought to receive input primarily from visual areas of the brain (Kaplan and Trout, 1974; Levine, 1974; Thomas and Wyman, 1984; Holmqvist and Srinivasan, 1991), and it was demonstrated directly that a light-off stimulus activates the giant fiber in white-eyed *Drosophila* mutants (Trimarchi and Schneiderman, 1995c). However, in larger flies, such as the house fly *Musca domestica*, it has been shown that the GFs also receive mechanosensory input from the antennae, and possibly ascending input from the tarsal mechanoreceptors (Bacon and Strausfeld, 1986).

Activation of the GFs, either directly via a stimulating electrode or by a light-off stimulus, results in a stereotyped pattern of muscle potentials with characteristic latencies. As implied by the anatomy, giant fiber stimulation first elicits a TTM muscle spike, followed by activation of the DLMs (Tanouye and Wyman, 1980). Recently, Lima and Miesenbock coupled expression of the ligand-gated $P2X_2$ ion channel with injections of an optically caged agonist to drive GF activation in intact animals using pulses of light (Lima and Miesenbock, 2005). Freely moving animals initiated flight when the giant fibers were activated with light pulses, confirming that these neurons are sufficient to elicit an escape response.

Although the function of the GF pathway in the escape response seems clear, the anatomy and functional role of the other pathways that can initiate flight are not. Several lines of evidence suggest that both odor-induced and spontaneous takeoffs proceed without activation of the GFs, observations that argue for the existence of a separate descending pathway (Holmqvist, 1994; Trimarchi and Schneiderman, 1995a; Trimarchi and Schneiderman, 1995b). There is even evidence that the GFs are neither the only, nor even the first, descending pathway activated during visually elicited escape responses: contrary to previous observations, a recent study using high-speed imaging found that *Drosophila* begin to raise their wings before they start to jump in response to a looming visual stimulus (Hammond and O'Shea, 2007a). Because the GF pathway is not known to activate any wing-elevator muscles prior to the jump muscle, Hammond and O'Shea suggested that a

non-GF descending pathway that coordinates wing raising may be activated before the GF in response to a looming threat.

If the anatomical arrangement of the GF pathway is sufficient to generate a takeoff during escape responses, why are other pathways necessary to elicit other forms of flight initiation? A study using hummingbirds (Tobalske et al., 2004) found that different levels of motivation result in different takeoff performance. Thus, one possibility is that various types of takeoff behavior are optimized for different performance requirements, and that these are mediated by different neural circuits. In order to test this hypothesis, we used 3D high-speed video techniques to quantitatively analyze the body dynamics and performance of *Drosophila* during takeoffs initiated under different stimulus conditions. Our results suggest that different flight initiation circuits may have evolved to selectively emphasize either launch velocity or stability, two incompatible features of takeoff performance.

2.3 Materials and Methods

2.3.1 Animals

In all experiments we used 3-day old mated female *Drosophila Melanogaster* (Meigen) taken from the lab colony, which is descended from 200 wild-caught females. Flies were reared in incubators at 25℃, and tested at room temperature (22℃–25℃).

2.3.2 High-speed Videography

Three high-speed video cameras (Photron Ultima APX, San Diego, CA, USA) captured freely moving flies taking off in orthogonal views. Takeoffs were filmed at 6000 frames s^{-1} with 512×512 pixel resolution, using 50 mm Nikon lenses (Nikon USA, Melville, NY, USA) with (1:2) extension tubes to obtain the desired magnification. We calibrated the cameras using the Direct Linear Transform method (Abdel-Aziz and Karara, 1971). A single LED, mounted on a micromanipulator and moved to known positions in the filming volume, served as the calibration object.

To correctly position a fly in the focal planes of all three cameras simultaneously, we

focused each camera on the tip of a glass pipette fixed at an angle of approximately 45 from the horizontal. We introduced individual flies into the bottom of the pipette, and the animals crawled upward by positive geotaxis until they emerged at the tip, maximizing the probability that the fly was in focus in all three views at the start of the takeoff.

2.3.3 Voluntary Takeoffs

Upon emerging from the pipette tip, most flies chose to stand or groom themselves. At this point we began capturing images with the cameras set in a continuous capture mode. Those flies that walked off the pipette were not used. Flies were permitted to remain on the pipette undisturbed until they flew away. For convenience, we will term these unelicited takeoffs as 'voluntary' although we do not presume any complex cognitive processing by the fly's brain. We recorded voluntary takeoffs by manually post-triggering the camera to save all frames captured 1.7 s prior to the trigger point. Voluntary takeoffs occurred anywhere from 1 to 60 min after the fly climbed to the top of the pipette. In some cases, the flies were deprived of water for several hours before the experiment to increase the frequency of voluntary takeoffs.

2.3.4 Escape Responses

We triggered escape behaviors with a physical black disk falling on a collision course with the fly. The disk consisted of a 140 mm diameter foam board circle covered with black felt. A small hole in the center of the disk allowed it to slide 190 mm down a plastic rod angled 50° from the horizontal. The falling disk subtended a visual angle of 20° at its starting point and 40° at its final point in the fly's field of view. The disk thus provided a very strong looming stimulus to the fly, similar to the visual stimulation that might be created by a predator or approaching fly swatter. We have previously reported preliminary results indicating that this stimulus is effective for eliciting escapes in wild type *Drosophila* (Card et al., 2005). We started the falling disk manually by pulling on a long rod that acted as a block to keep the disk from descending. We triggered the disk within several seconds of the fly emerging onto the platform, but only after the fly had settled down into a

stationary position. As the disk fell, it passed a photodiode/detector pair, which generated an electrical pulse that served as the recording trigger. A plastic stopper prevented the disk from sliding off the end of the rod. The disk did bounce slightly when it hit the stopper, but in all experiments the escaping flies had left the substratum before the disk reached the end of the rod. We determined the time course of the falling disk by filming it with the high-speed video cameras and digitizing its position along the rod.

2.3.5 Clipped-wing Flies

To assess the role played by the wings during escape takeoffs, we filmed flies with their wings removed taking off in response to the falling disk. In these clipped-wing trials, we anesthetized individual flies by cooling them to 4°C using a Peltier system and then excised both wings at the wing hinge. We then isolated each fly in a small vial and left them to recover for at least 30 min before introducing them into the high-speed video apparatus. In order to capture the entire escape jump trajectory we used a slower recording (2000 frames s^{-1}) and lower camera lens magnification to film clipped-wing trials.

2.3.6 Analysis

To compare the coordinated action of wings and legs in the observed types of takeoff, we recorded the timing of wing and leg events from each video sequence. Most event timings were not normally distributed within each stimulus condition (Lillie test for normality, $P < 0.025$), so we use non-parametric statistics to report our findings: the median (med) is the middle value in our observed data range, and the interquartile range (IQR) is the range around the median including 50% of the data. To assess differences in body kinematics and flight performance between the two different types of takeoff, we digitized the long (abdomen to head) and transverse (left-to-right wing hinge) axes of the fly in each of the three orthogonally arranged cameras. Position data were smoothed using a zero-phase-lag 4th-order Butterworth filter (cut-off frequency 250 Hz, or 60 Hz for clipped-wing flies). As a rough guess, we estimated the center of mass (COM) of the fly as the point along the long body axis 50% of the distance from the head to the end of the abdomen. COM calculations

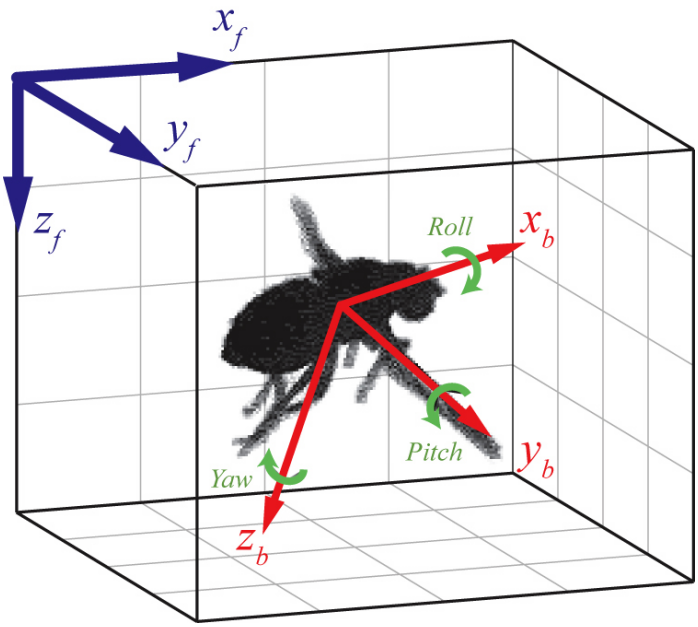

Figure 2.1. Definition of kinematic frames of reference. The fixed lab frame (x_f, y_f, z_f) is a right-handed coordinate system with the positive z_f-axis pointing down toward the ground. A second frame of reference (x_b, y_b, z_b) has its origin at the fly's center of mass with the x_b-axis oriented along the long body axis toward the animal's head, the y_b-axis oriented parallel to the fly's right wing, and the z_b-axis positioned perpendicular to the x_b- and y_b-axes and directed toward the ventral surface of the animal. Right-wing down rotation about the x_b-axis is positive roll, nose-up rotation around the y_b-axis is positive pitch, and a turn to the fly's right around the z_b-axis is positive yaw. For each video frame, a unit quaternion, $\boldsymbol{q}$, specifies the rotation from body-centered coordinates to the fixed lab coordinates necessary to achieve the attitude of the fly in that frame.

made from a 3D model of a fruit fly body and from 2D video images (assuming uniform density) confirmed that this is a reasonable estimate. COM velocities and accelerations were determined by fitting the smoothed position data with a cubic spline and taking the first and second derivatives of the spline without further smoothing (equivalent to applying the Central Difference Theorem).

Following the convention from aerodynamics described by Phillips (2002), we defined two frames of reference to describe the kinematic data: the fixed lab frame (x_f, y_f, z_f) and the animal's body-centered frame (x_b, y_b, z_b). In this scheme, rotations around the body-centered x_b, y_b and z_b axes are called roll, pitch and yaw, respectively (figure 2.1). Note that these body angles are distinct from an Euler angle system in which three successive rotations about non-orthogonal axes define the attitude of the rotated object. The three Euler rotation angles are sometimes also called roll, pitch and yaw (Schilstra and Hateren, 1999), but in our convention they are referred to as bank, elevation and heading (see section 2.3.7). As Euler angle schemes are subject to singularities ('gimbal lock') when rotations are large, a more convenient way to express the 3D rotation of a rigid body is with a quaternion. Quaternions are an extension of the complex number system for which a unit quaternion $\boldsymbol{q}$ can be thought of as representing a rotation of θ radians about a 3D axis defined by the vector $\boldsymbol{v}$ such that (Kuipers, 2002):

$$\boldsymbol{q} = \cos\frac{\theta}{2} + \boldsymbol{v}\sin\frac{\theta}{2}. \tag{2.1}$$

We determined roll, pitch and yaw velocities $\boldsymbol{omega}$ by expressing the three-dimensional rotations about the COM as unit quaternions, $\boldsymbol{q}$ and solving the equation:

$$\frac{d\boldsymbol{q}}{dt} = \frac{1}{2}\boldsymbol{q} \otimes \boldsymbol{\omega}, \tag{2.2}$$

where $\otimes$ indicates quaternion multiplication (Phillips, 2002). Angular position was then determined from the rotational velocities by a cumulative sum, and acceleration was calculated using the spline method described above. Because of the geometry of the glass pipette substrate from which the flies took off, some flies had initial 'roll' and 'pitch' angles relative

to the lab coordinate frame. These starting angles were added to the rotational velocity cumulative sum so that initial roll and pitch position values are expressed in the context of the lab frame. Initial yaw orientations were also arbitrary, but have no systematic implications for flight control, and so for calculating mean time courses they are expressed relative to starting position (i.e., initial yaw is always 0°). All digitization and analysis was performed using custom programs written in Matlab (Mathworks, Natick, MA, USA; see appendix B). Most kinematic parameters were normally distributed within stimulus condition groups (Lillie test, $P > 0.025$), so kinematic data are reported as mean ± s.e.m.

From the measured kinematic parameters, we can estimate the kinetic and potential energy of the fly during flight initiation. Translational kinetic energy KE_{trans} of a fly with mass, m and translational speed, v, is:

$$KE_{trans} = \frac{1}{2}mv^2. \tag{2.3}$$

Rotational kinetic energy, KE_{rot}, can be calculated as the vector product:

$$KE_{rot} = \frac{1}{2}\boldsymbol{I}\boldsymbol{\omega}^2, \tag{2.4}$$

where $\boldsymbol{I}$ is the moment of inertia tensor for an ellipsoid body, and $\boldsymbol{\omega}$ is the angular velocity vector. The potential energy PE of the fly is calculated from the fly's height off the substrate, z, and the acceleration due to gravity g, as:

$$PE = mgz. \tag{2.5}$$

We estimate the average total energy of the fly during the first 2 ms after takeoff as the sum of translational, rotational, and potential energies during this period.

2.3.7 A Note on Alternative Conventions for Describing Rotation

Any arbitrary attitude of the fly (orientation relative to the lab frame) can be uniquely described by a sequence of three rotations. In a rotation sequence common to aerodynamics,

the transformation from the lab-fixed coordinate frame to the fly body-centered coordinate frame is accomplished by a ZYX rotation sequence: first, the fly body is rotated by an angle ψ about the lab z_f-axis, then rotated by an angle θ about the new y_1-axis, and, finally, rotated by an angle ϕ about the x_2-axis, that is the x_f-axis after the first two rotations. The angles ψ, θ, and ϕ are commonly referred to as Euler angles, and we call them heading, elevation and bank, respectively. In order to uniquely describe an object's attitude, we must restrict the range of the Euler angles as follows: $-180° < \phi < 180°$, $-90° < \theta < 90°$ and $0° < \psi < 360°$. Thus while Euler angles are a useful scheme for defining the posture of an animal relative to the lab frame unambiguously, their use is limited when trying to describe large rotations, such as those observed during escape takeoff, because singularities occur when the elevation angle reaches $\pm 90°$ (a phenomenon often called 'gimbal lock'). For this reason we have chosen to express the rotational kinematics of the fly as roll, pitch and yaw rotations around the orthogonal x_b-, y_b- and z_b-body axes, respectively (figures 2.8, 2.9, and 2.12,). Note that Euler angles do not have a one-to-one relationship with roll, pitch and yaw (see Phillips, 2002). Expressing the kinematics in the body-centered coordinate frame has the advantage that this is the coordinate frame in which the fly itself senses the world. For example, neurons in the lobula plate of blowflies respond to specific self-motion rotations about different body-centered axes (Krapp et al., 1998; Kern et al., 2001). However, for comparison with other work, which has used Euler angles schemes to describe flight kinematics, in figure 2.10 we present the bank (ϕ), elevation (θ) and heading (ψ) angles in a ZYX-rotation scheme for the same data as shown in figure 2.9B.

2.4 Results

We analyzed 16 voluntary takeoffs and 27 escape responses captured on videotape. Our analysis excluded 25 additional takeoff sequences (4 voluntary, 21 escape) in which one or both of the fly's middle legs slipped on the pipette during leg extension.

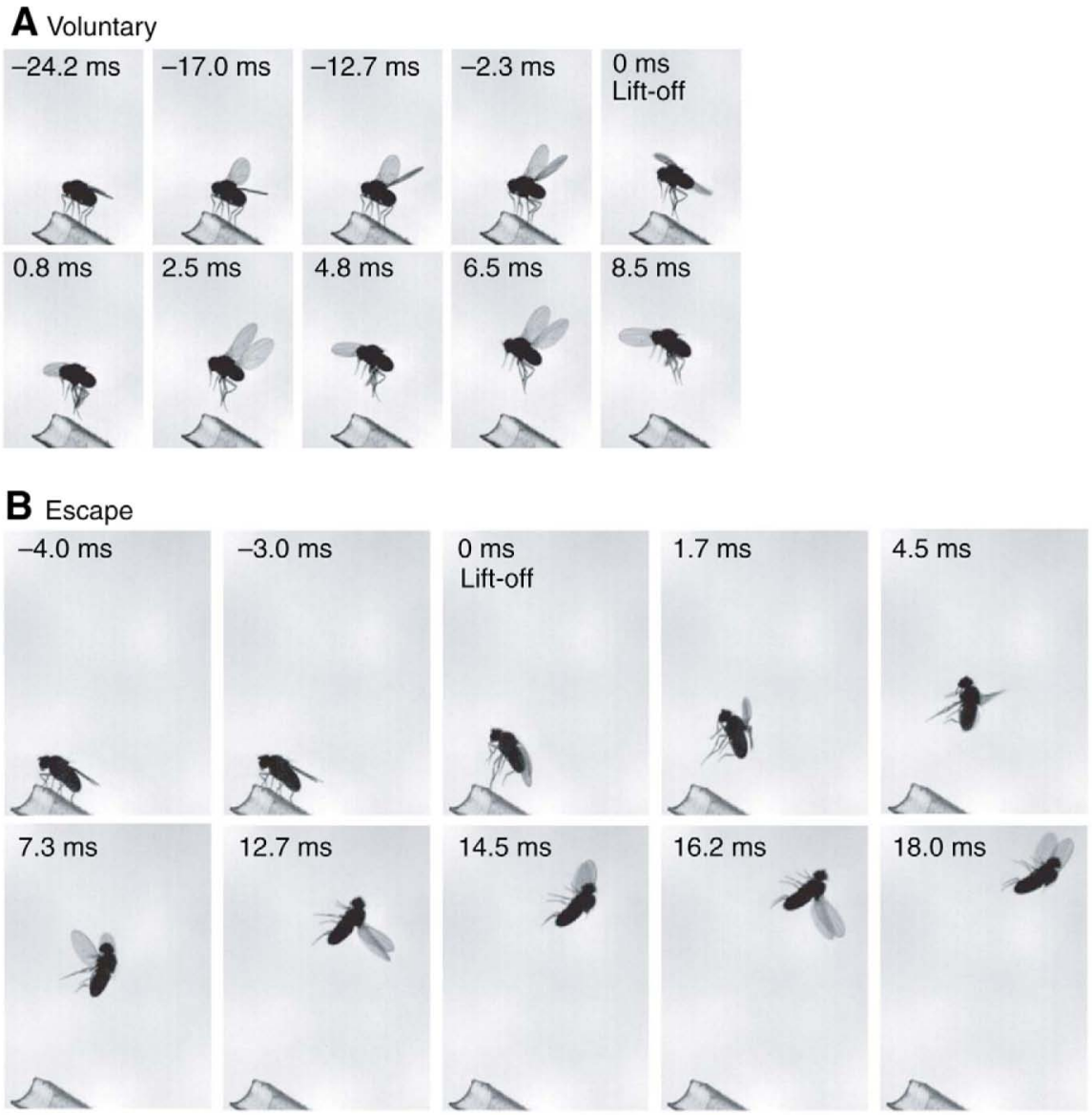

Figure 2.2. Video sequences for (A) voluntary and (B) escape takeoffs. Only one of the three camera views is shown. Times noted are ms from liftoff, the first frame in which both the fly's mesothoracic legs are no longer touching the substrate. For complete video sequences, see supplementary material Movies JEB1 and JEB2.

2.4.1 Voluntary Flight Initiations

As previously described (Trimarchi and Schneiderman, 1995c), we observed that flight initiations performed in the absence of any overt stimulus consisted of at least two distinct phases: wing raising and subsequently leg extension. First, the fly elevated and then supinated its wings so that the ventral surface of each wing faced out laterally with the leading edge forward. Second, the mesothoracic legs extended at the coxotrochanteral, femorotibial and tibiotarsal joints. The motion of the legs and wings were coordinated so that at the start of leg extension the wings elevated further (first upstroke), but then quickly depressed downward (first downstroke) as the legs completed their extension (figure 2.2A). figure 2.3 shows the relative timing of wing and leg motion for all voluntary takeoffs analyzed.

We found that the time between first wing-raising movements and the start of leg extension (41.7 ms, IQR = 46.3, N = 16, figure 2.3A) was substantially longer and more variable than previously reported (10.5 ± 5.4 ms, mean $\pm$ s.d., N = 4; Trimarchi and Schneiderman, 1995c. We also observed that the timing of wing raising varies not only from event to event, but from wing to wing. In other words, the fly typically did not raise the left and right wing in unison. In only three of the 16 voluntary takeoffs that we digitized did the wings begin to rise simultaneously within the resolution of our frame rate. This observation confirms a recent report (Hammond and O'Shea, 2007b). In our sample, 8/16 flies began flight initiation by raising the right wing first, whereas 5/16 flies began with the left. The first wing raised always corresponded with whichever wing happened to be on top at rest.

The median time lag between the start of top and bottom wing opening was 7.0 ms (IQR = 17.7). The duration of wing opening (interval from start of motion until wing stops in fully raised position) was not significantly different between right and left wings (right: 10.7 ms, IQR = 15.3; left: 11.5 ms, IQR = 11.3; $P = 0.75$, Kruskal-Wallis test).

2.4.2 Escape Responses

In our experiments, 95% of the flies stimulated with the falling black disk took off between the moment the stimulus was released ($t = 0$) and the time the stimulus reached the end of the rod ($t = 228$ ms, figure 2.5). Flies that initiated flight outside this time window were

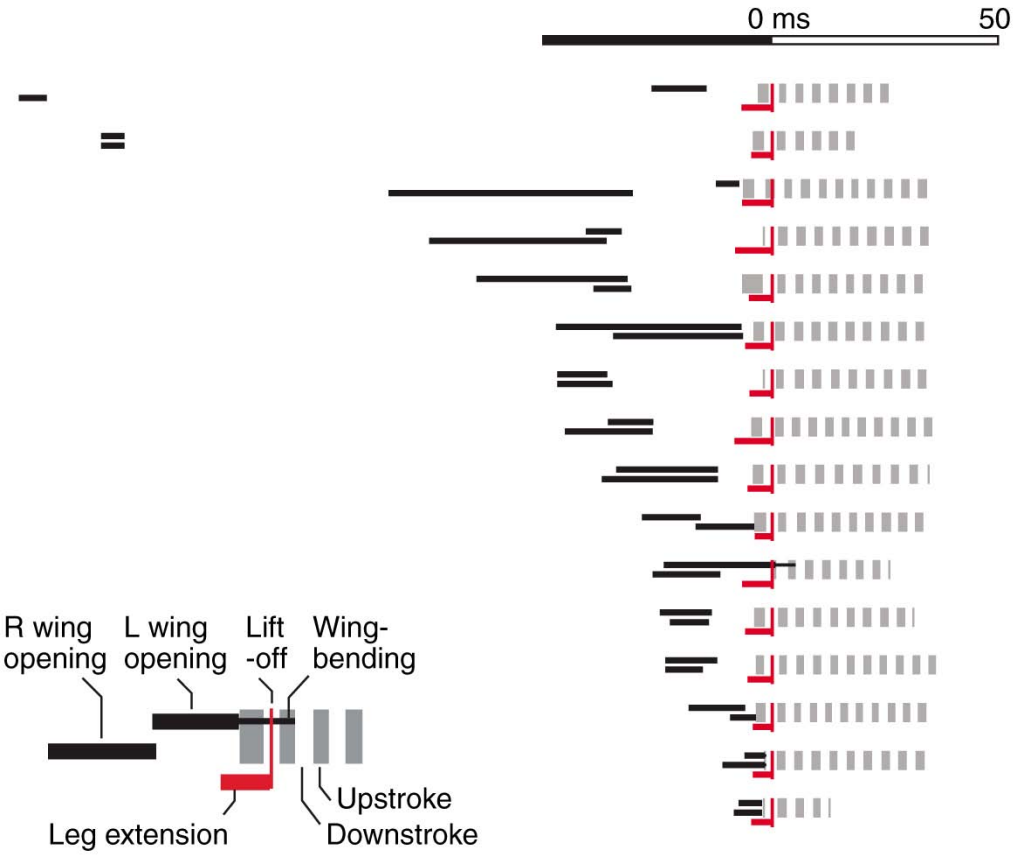

Figure 2.3. Voluntary flight initiation timelines of leg and wing events ($N = 16$). Each timeline represents the flight initiation sequence for an individual fly, and the timelines are aligned such that liftoff occurs at 0 ms. Black lines correspond to the duration of wing opening for left (L; upper black line) and right (R; lower black line) wings. The line starts at the time of first wing movement, and ends when the wing is in its fully raised position. In some cases, the wing had not reached its fully raised position when the wings began stroking, leading to wing bending on the upstroke. Wing bending is represented by a thinner black line, which ends at the time when the wing was successfully unfurled. The grey and white bands represent the periods of upstroke and downstroke, respectively. These bands end when the fly left the field of view of the cameras. The red line shows the period of mesothoracic leg extension. It starts when the legs first begin to move and ends when the legs stop extending, usually at the point of liftoff, shown by the thin vertical red line.

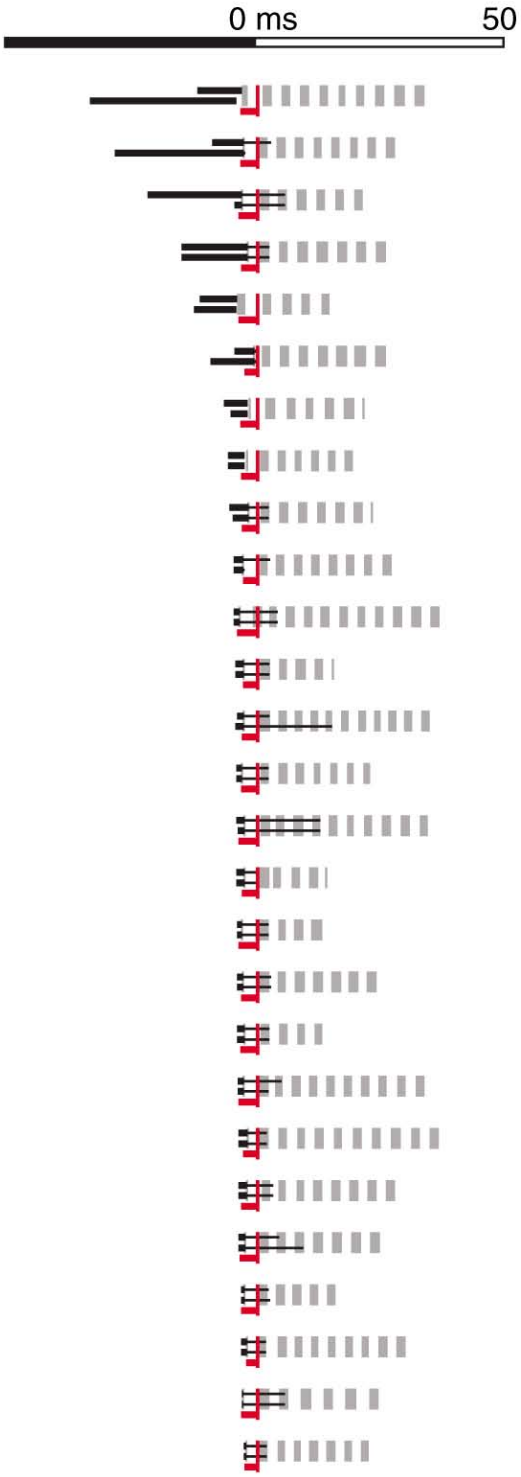

Figure 2.4. Escape flight initiation timelines of leg and wing events ($N = 27$). See figure 2.3 for description.

not considered to have responded to the disk stimulus and were discarded. A sample video sequence of an escape takeoff is shown in figure 2.2B, and timelines for all analyzed escape takeoffs are shown in figure 2.4.

From our data, it is clear that wing raising preceded leg extension in almost all (96%) escape responses. This agrees well with recent observations (Hammond and O'Shea, 2007a) in a similar preparation. In some cases, the wings were fully elevated prior to the jump and the overall pattern resembled a voluntary takeoff. In 80% of the cases (22/27) in which wing motion preceded leg extension, however, one or both wings never reached full extension before the legs began to kick, at which point the wings were pulled back against the body. As a consequence, most escape jumps occurred with the wings in the closed position, as originally observed (Trimarchi and Schneiderman, 1995c), and the flies attempted to open their wings only after they were fully airborne (figure 2.6).

Opening the wings completely after the jump often took several wing strokes to accomplish. During the first few upstrokes, the wings bent substantially at a flexure point that was distal to the actual wing hinge (figure 2.7; also figure 2.2B, fourth panel). This bending pattern contrasted sharply with the normal flight pattern in which the wings move smoothly about the hinge with little flexure (Fry et al., 2005). Wings displayed this peculiar upstroke-bending pattern for 2-6 strokes until they were successfully unfurled during a downstroke. Left and right wings could unfurl independently. In some cases one wing would continue to bend on the upstroke even after the other wing was fully open and flapping normally (figure 2.4).

For a subset of the escape responses (N = 17), we also measured the timing of the escape response relative to the action of the falling black disk stimulus. The median escape takeoff latency was 190.7 ms (IQR = 15.3) from the start of stimulus motion, and flies began wing motion within a range of 160-210 ms from the start of the stimulus (figure 2.5). During this period, the disk diameter had reached a size of 30°–40° in the fly's field of view. The rather large range in reaction times (∼50 ms) could be related to the fact that the flies oriented themselves roughly randomly when they emerged at the pipette tip, so that in some cases the disk approached from the front, whereas in other cases it fell toward the back or side

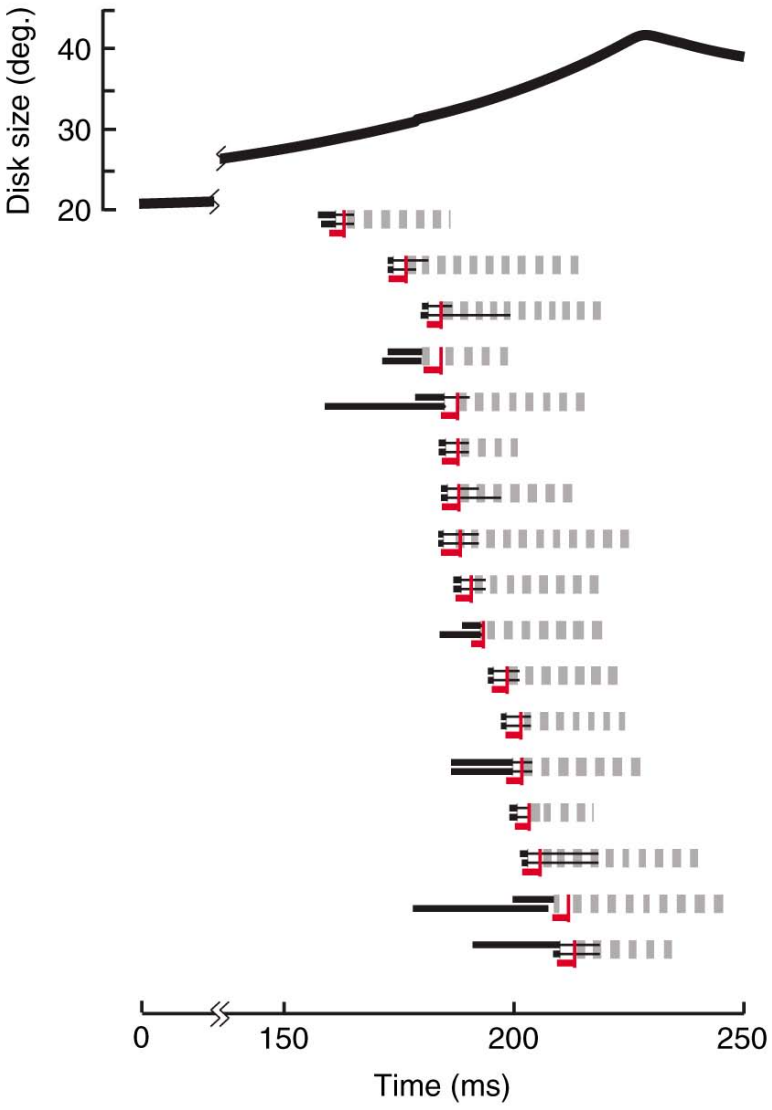

Figure 2.5. Latency of escape takeoffs. Timelines of the subset of escape responses for which latency was measured are plotted in relation to the angular size of the falling black disk stimulus in the fly. Timeline notation is as in figure 2.3 ($N = 17$).

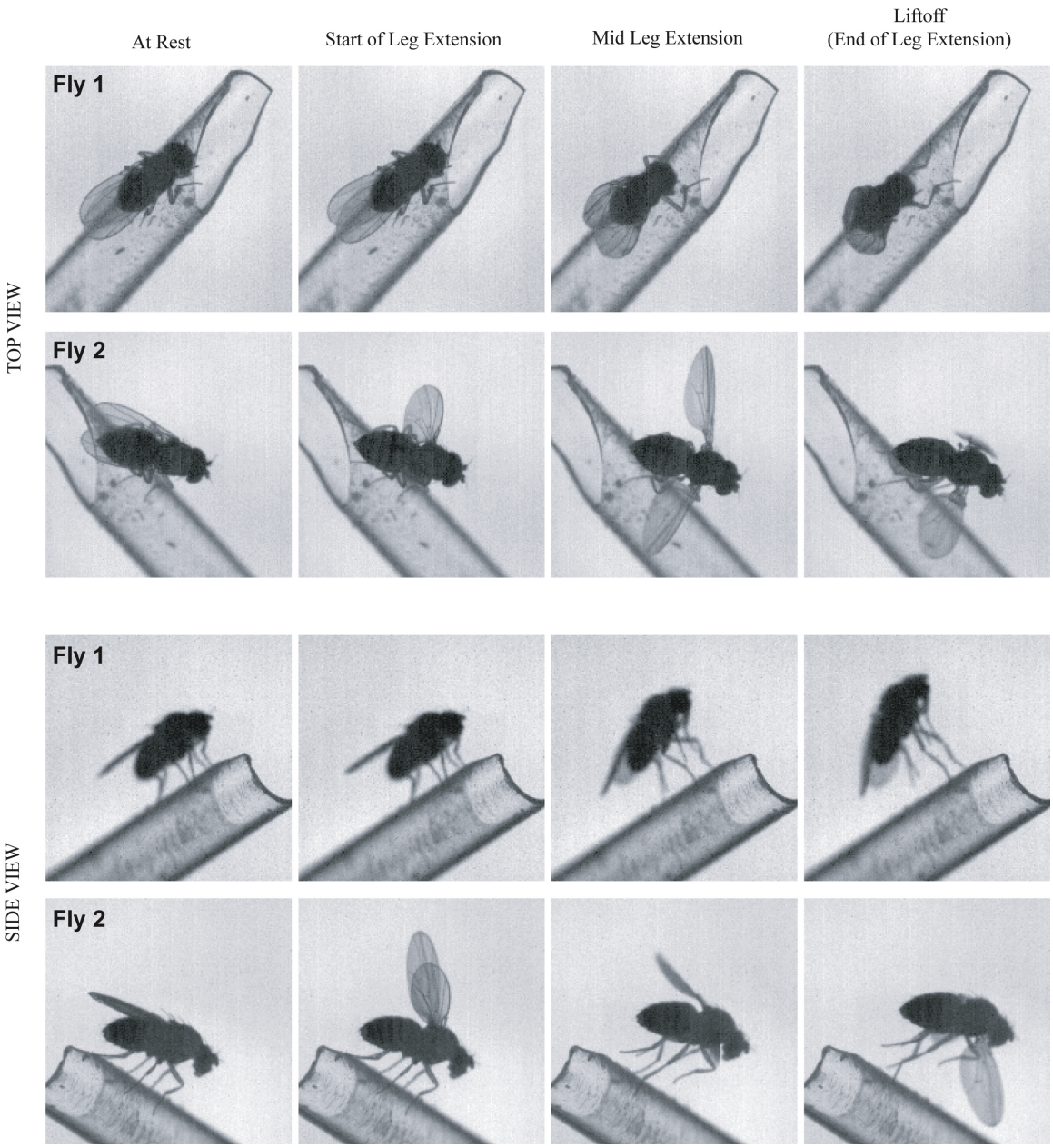

Figure 2.6. Comparison of wing position during leg extension for two different escape takeoffs. Fly 1 executes an escape in which the wings are not raised before the start of leg extension. The two different camera views (top and side) show that by mid-leg extension the wings are still closed along the back of the fly, a wing posture that the fly maintains even as its legs leave the substrate. Fly 2 executes an escape in which its wings were fully raised before the start of leg extension (these wing-open escapes are labeled **Esc. in figure 2.13). As the fly extends its legs, the wings flap down in a normal downstroke, similar to the wing motion during a voluntary takeoff. The result is that the wings are fully outstretched during the leg extension period.

Table 2.1. Timing of voluntary and escape takeoff events

Event	Median (IQR)		Significant difference	*P*-value*
	Voluntary	Escape		
Start of stimulus to lift-off (ms)	–	190.67 (15.29)	–	–
L–R wing interlatency (ms)	7.00 (17.67)	0.00 (0.58)	0	0.446
Left wing opening (ms)	11.50 (11.25)	–	–	–
Right wing opening (ms)	10.75 (15.25)	–	–	–
Wing–leg interval (ms)	34.83 (45.42)	1.00 (2.67)	1	<0.001
Leg-downstroke interval (ms)	3.33 (2.33)	0.67 (0.83)	1	<0.001
Leg extension (ms)	5.50 (2.00)	3.33 (0.46)	1	<0.001
Wing-beat frequency (Hz)†	261 (11.2)	277 (26.6)	1	0.001

*Kruskal–Wallis test.
†Average of first three strokes.

of the fly.

2.4.3 Comparison of Escape and Voluntary Takeoff Behaviors

We found significant differences between voluntary and escape takeoffs with respect to three temporal measures: wing-leg interval, leg-downstroke interval, and the period of leg extension (Table 2.1). The time between the start of wing opening and the onset of leg extension (wing-leg interval) was much longer and more variable for voluntary (34.83 ms, IQR = 45.4) compared to escape takeoffs (1.0 ms, IQR = 2.7) (see also Hammond and O'Shea, 2007a). The time between the start of leg extension and the start of the first downstroke (leg-downstroke interval) was also longer and more variable for voluntary (3.3 ms, IQR = 2.3) compared to escape takeoffs (0.67 ms, IQR = 0.83). This interval is of particular interest because a short latency between leg extensor and wing depressor muscle activation is a hallmark of the giant fiber pathway. In electrophysiological experiments, GF stimulation results in a short and fixed latency between TTM and DLM activation (0.44 ± 0.05 ms delay, Tanouye and Wyman, 1980; 0.4–0.8 ms, Trimarchi and Schneiderman, 1995b). Finally, voluntary takeoffs exhibited a significantly longer period of leg extension compared to escapes (5.5 ms, IQR = 2.0 vs. 3.3 ms, IQR = 0.46), similar to the difference recently reported (Hammond and O'Shea, 2007b).

Voluntary and escape takeoffs also differed significantly in the stroke frequency of the first several wing beats once airborne. For the first three strokes, flies taking off voluntarily flapped at an average rate of 261 Hz (IQR = 26.6) compared to 277 Hz (IQR = 11.2) for

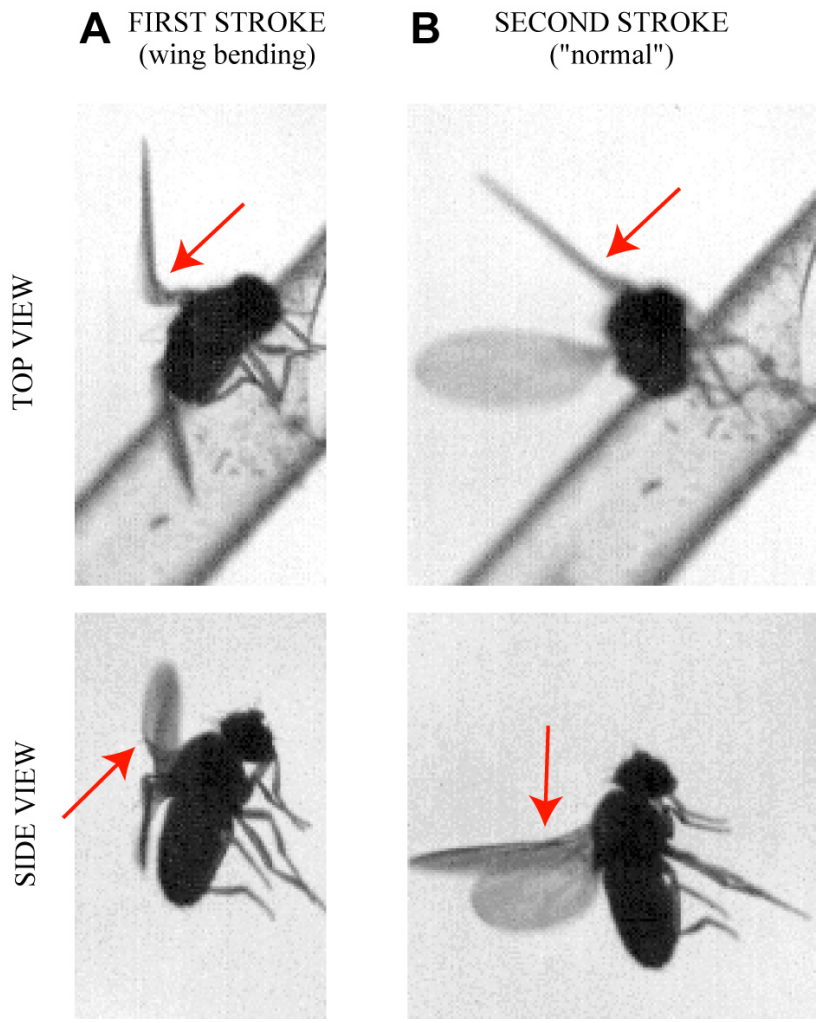

Figure 2.7. Wing bending during the first upstroke. The images show a comparison of wing shape during the first upstroke after takeoff (A) and the second upstroke (B) of an example escape takeoff. Two camera views are shown for each stroke (top and side views). The images show the fly's wing position 7 frames (1.2 ms) after the start of the respective upstrokes. The red arrows point to a flexure point along the left wing. The wing bends nearly 90° at this point during the first upstroke, but only minimal bend is evident during the second, more 'normal' upstroke (see also supplementary material Movie JEB3). The right wing also appears to bend in a similar fashion.

escaping flies. These wing beat frequencies are 20%–30% higher than the 200–220 Hz wing beat frequency measured for steadily hovering flies in free flight (Fry et al., 2005).

2.4.4 Flight Initiation Kinematics

To assess flight performance during and after flight initiation, we recorded voluntary and escape takeoffs in 3D using multiple camera views. figure 2.8 shows example trajectories for a voluntary takeoff (figure 2.8A) and an escape response (figure 2.8B). In both examples, the fly's center of mass (COM) was stationary immediately before the jump as the wings elevated, accelerated during the leg-extension period, and continued with positive translational velocity once airborne. The escaping fly also underwent notable rotational velocities about all three axes and in the air.

Figure 2.9 shows the mean (±s.e.m.) translational and rotational body kinematics for all 43 flies digitized. To enable pooling of results, we arbitrarily transformed each individual trajectory so that all first yawing and rolling motions were to the right. We did not transform the pitch angle in this way, because head-down pitch and head-up pitch have very different functional implications for flight. However, 39 out of 43 flies started takeoff with a head-up pitching motion, an observation that suggests that the ground reaction forces generated by the mesothoracic legs during the jump are typically oriented anterior to the fly's center of mass.

On average, both the horizontal and vertical components of center of mass acceleration during escapes were nearly twice those during voluntary takeoffs (figure 2.9A). Peak vertical acceleration was 57.0 m s^{-2} (IQR = 35.8) for voluntary takeoffs and 112 m s^{-2} (IQR = 47.8) for escapes ($P \ll 0.001$, Kruskal-Wallis test). Peak horizontal acceleration was 46.1 m s^{-2} (IQR = 28.8) and 107 m s^{-2} (IQR = 50.0) for voluntary takeoffs and escapes, respectively ($P \ll 0.001$, Kruskal-Wallis test). In both cases, the ratio of vertical to horizontal peak acceleration was close to 1, indicating the fly typically launched itself into the air with a takeoff angle of roughly 45° from the horizontal. If the fly were purely ballistic, this is the expected launch angle to maximize horizontal distance traveled.

A plot of the mean time courses for angular accelerations during voluntary takeoffs

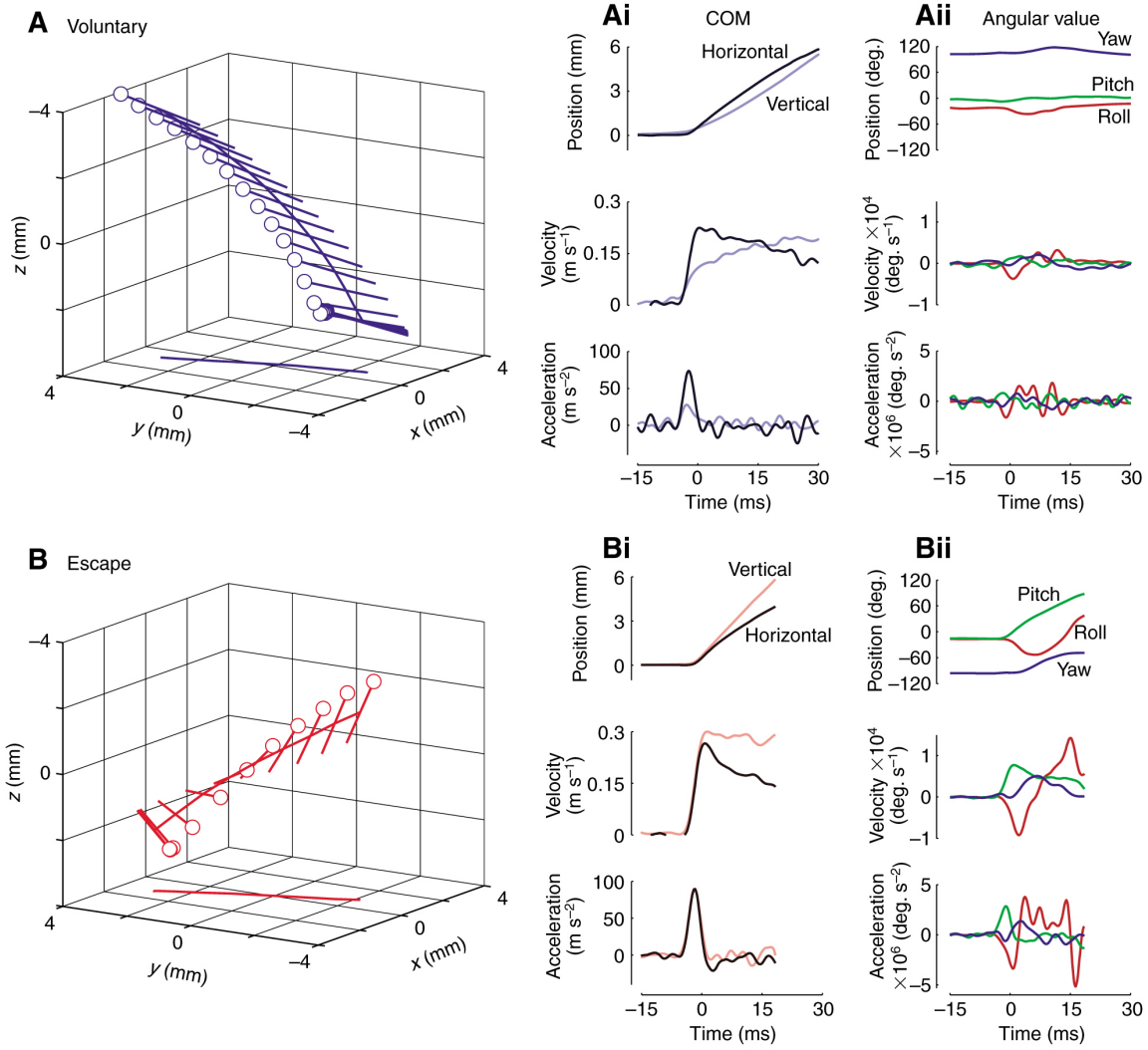

Figure 2.8. Example body kinematics for an (A) voluntary and (B) escape takeoff. Lollipop diagrams show the 3D position of the fly during takeoff. Lines represent the long axis of the fly, and the open circle represents the position of the fly's head. Positions are plotted every 2.5 ms. The center of mass (COM; Ai, Bi) was defined as the point along the long body axis of the fly 50% of the distance from the head to the tip of the abdomen. We defined the starting COM location of the animal to be the origin. Horizontal position of the COM is the Euclidian distance traveled in the horizontal (x-y) plane (parallel to the ground) from the starting position. Angular values (Aii, Bii) are expressed in a body-centered frame of reference. Roll, pitch and yaw position are the cumulative rotations around the x_b, y_b, and z_b body axes, respectively (see figure 2.1 for axes definitions). The fly for the roll, pitch and yaw angles associated with the rotation required to move the body-centered frame from alignment with the lab frame to alignment with the fly's starting position.

(figure 2.9B) show that both pitch and yaw accelerations reached a peak during leg extension but decayed quickly once the fly was airborne. In contrast, roll acceleration maintained a plateau for nearly 5 ms after liftoff, which suggests that the flies are generating roll actively with their wings. Mean peak velocities around all three axes were of similar magnitude, approximately 2000–3000 deg. s^{-1}. These values are comparable to maximum yaw velocity during saccade maneuvers in free-flying *Drosophila* (1800 deg. s^{-1}, Fry et al., 2003) and maximum roll velocity during a variety of maneuvers in free-flying houseflies (3000 deg. s^{-1}, Schilstra and Hateren, 1999). On average, roll and yaw velocities decayed after the first 10 ms of flight, whereas pitch velocities did not decline to zero until after 20 ms from lift- off.

Escape takeoffs produced substantially larger angular accelerations and higher rotational velocities around all three body axes compared to voluntary takeoffs, and the differences were most striking in roll. Average peak pitch and yaw velocities were twice as large for escapes compared to voluntary takeoffs (e.g., pitch: $5,710 \pm 661$ deg. s^{-1} escape vs. $2,370 \pm 350$ deg. s^{-1} voluntary), whereas peak roll velocity during escapes was more than three times that measured during voluntary takeoffs and reached values greater than 10,000 deg. s^{-1} (10,200±1,480 deg. s^{-1} escape vs. $2,860 \pm 1,090$ deg. s^{-1} voluntary). Further, instead of developing roll after takeoff, as in the voluntary case, initial roll acceleration during escape occurred almost entirely during leg extension. Because escaping flies do not have their wings open during leg extension, the large roll acceleration must be produced primarily by the legs. Once airborne, escaping flies underwent a significant roll deceleration that returned the fly to a roll displacement of similar magnitude to that of flies performing voluntary takeoffs by about 20 ms into the flight.

Figure 2.9: Average time courses for (A) translational and (B) rotational kinematic variables. Blue lines are mean values for voluntary takeoffs and red lines are mean values for escape responses. Shaded area around the mean shows the standard error. Time courses are aligned so that liftoff occurred at 0 ms. The yaw angular position was adjusted to start at 0°. Roll and pitch starting positions for each fly were defined as in figure 2.8. Roll and yaw values for position, velocity and acceleration have been adjusted as if all first rolling and yawing motions were to the fly's right. The dark grey region represents the median time of leg extension for escape takeoffs, and the light and dark grey regions together indicate the median time of leg extension for voluntary takeoffs. Individual flies did not remain in the field of view of our cameras for uniform amounts of time (see figures 2.3 and 2.11). The inset in the lower right hand corner of B shows the number of flies averaged at each point in time. See also figure 2.10 for alternate conventions describing takeoff rotations.

Figure 2.10: (A) Both the individual time courses and mean (±s.e.m.) values for bank, elevation and heading. Blue traces correspond to voluntary takeoffs and red to escape responses (see figure 2.9 for the

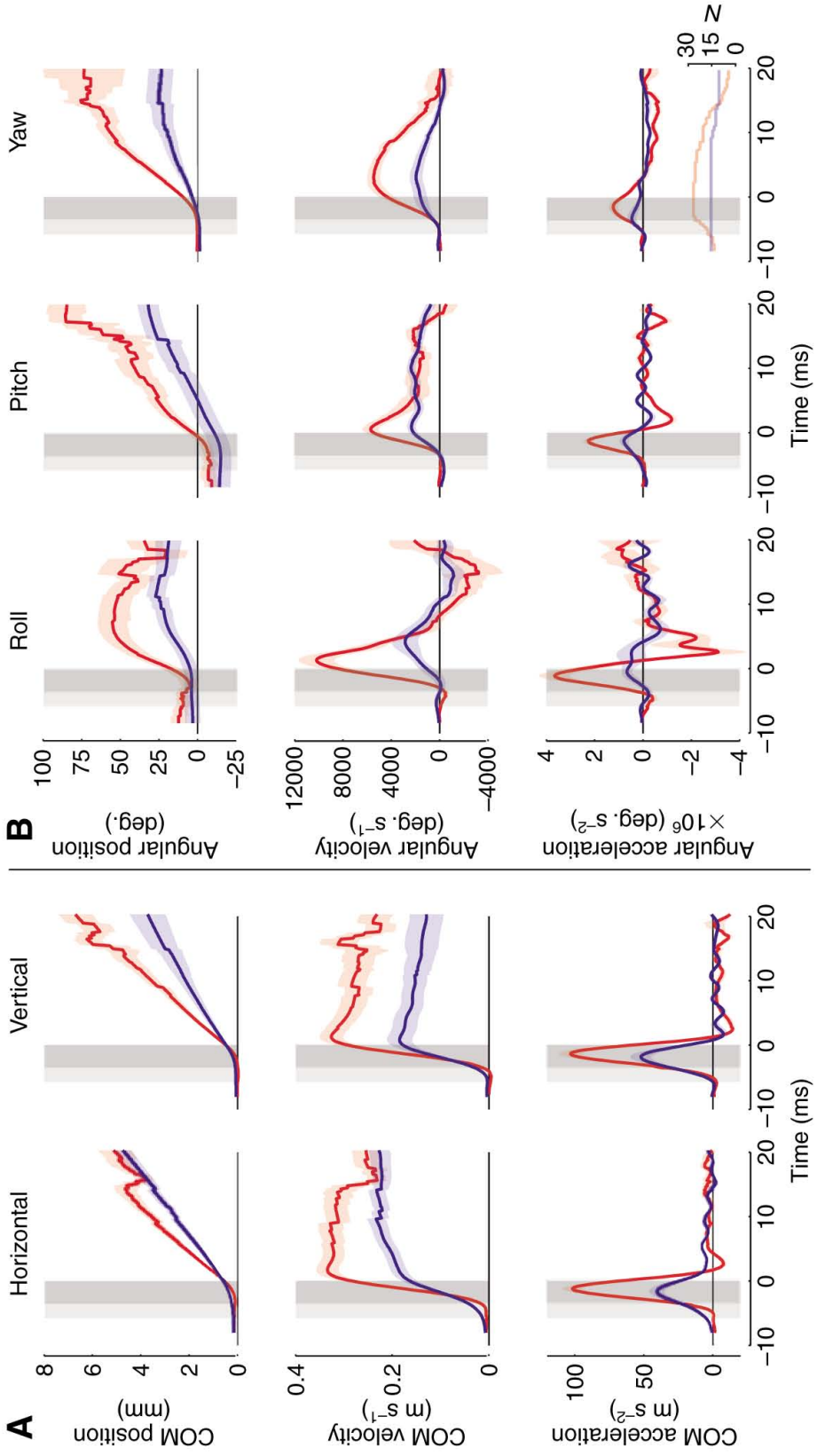

Figure 2.9. See p. 51 for caption.

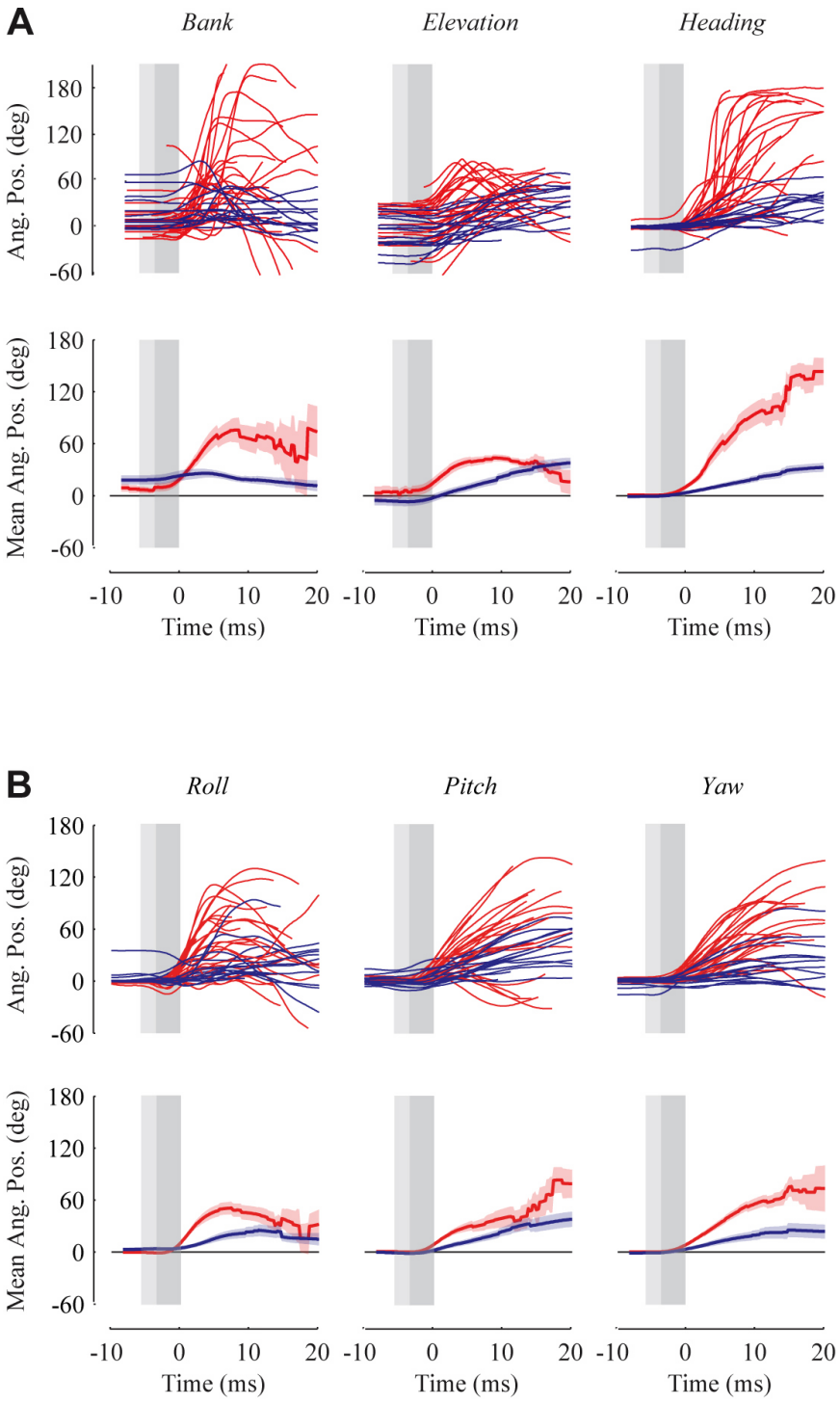

Figure 2.10. See p. 51 for caption.

2.4.5 Speed vs. Control

The differences in escape and voluntary takeoff performance can be characterized from the measured body kinematics by comparing their translational and rotational speeds. Translational speed relates to how quickly a fly is able to move away from an approaching threat, whereas rotational speed may indicate less stable flight, especially when it is composed of large roll and pitch components, as observed in escape flight (figure 2.9B). The speed of the fly along its flight path is simply the vector sum of the horizontal and vertical center of mass velocity components. We define a relative steadiness metric, S, that is a linear transformation of the fly's angular speed:

$$S = 1 - \frac{\| \boldsymbol{\omega} \|}{\| \boldsymbol{\omega} \|_{max}}, \tag{2.6}$$

where $\| \boldsymbol{\omega} \|$ is the vector sum of the angular velocity about all three body axes, and $\| \boldsymbol{\omega} \|_{max}$ is the largest angular speed observed in our experiments, 30,500 deg. s^{-1}. When $S = 1$, the fly was maximally stable, with angular speed 0 deg. s^{-1}, and when $S = 0$, the fly was maximally perturbed.

Figure 2.11A shows the time courses of COM speed for both voluntary and escape takeoffs. Escaping flies clearly accelerated more rapidly and achieved a higher initial velocity than those that took off voluntarily. Over the first 2 ms of flight, average COM speeds were 0.48 ± 0.01 m s^{-1} and 0.28 ± 0.02 m s^{-1} for escape and voluntary takeoffs, respectively ($P \ll 0.001$, ANOVA). Escape speeds approached the maximum flight speeds observed in *Drosophila* (0.6 m s^{-1}) (David, 1979; Budick and Dickinson, 2006), whereas voluntary launch velocity was closer to the average cruising speed of the fly (0.35 m s^{-1}) (Budick and

number of flies averaged at each time point). These Euler angles are difficult to interpret because when the fly reaches an elevation of 90° (corresponding to the long body axis pointing straight up, perpendicular to the ground), the heading and bank angles are displaced by 180°. Thus a fly flying 'upside down' is represented by an elevation angle of < 90°, but heading and bank angles 180° different from their 'right-side up' values. (B) For comparison, the individual and mean (±s.e.m.) roll, pitch and yaw values for the same data as shown in A and figure 2.9B. The only difference with the data presented in figure 2.9B is that the initial 'roll' and 'pitch' orientations for each fly have not been added, so the angles are expressed relative to the fly's starting posture rather than starting in the context of the lab frame. These 'position' values represent the cumulative amount of rotation about each of the body axes over time. The data in both A and B have been adjusted as in figure 2.9B so that initial banking/rolling and yawing/heading movements are to the right.

Dickinson, 2006). It is thus not surprising that, once in the air, flies that took off voluntarily were able to maintain a steady flight speed whereas those escaping slowed down over the first 5 ms of flight.

Figure 2.11B shows the time courses of our steadiness metric, S, for voluntary and escape takeoffs. For both conditions, angular speed peaked just after the fly left the ground, resulting in the lowest steadiness at this time. Flies taking off voluntarily, however, were more than 1.5 times as steady as escaping flies during the first 2 ms of flight ($S = 0.86 \pm 0.01$ voluntary vs. 0.55 ± 0.03 escape; $P \ll 0.001$, ANOVA) and still had greater steadiness nearly 20 ms into the flight. From the video sequences, it is evident that the angular speed of escaping flies was the result of uncontrolled tumbling around all three body axes. Many of these tumbling flies pitched up past 90° (figure 2.2B), such that they were essentially flying upside down.

A performance trade-off between speed and stability during takeoff is clear from figure 2.11. Whereas average takeoff velocity was greater for escapes compared to voluntary takeoffs, escapes also produced significantly more rotational velocity, resulting in unsteady flight. Other evidence confirms the priority of speed over control in escape responses. Figure 2.11A shows that escape flight speed declined for a short period immediately after takeoff, but was still higher than the speed of voluntary jumpers after 10–20 ms in the air. Also, tarsal contacts tended to slip more during escape takeoffs (38%) than during voluntary takeoffs (19%), a difference that is most likely due to faster leg extension. Although takeoffs in which the fly slipped were not analyzed, we observed from the video sequences that slipping during takeoff usually led to extensive tumbling once airborne, as would be expected since uneven force between the two legs tends to induce the fly to roll.

2.4.6 Clipped-wing Flies

To measure the effects of body drag and assess the role of the wings during takeoff, we clipped off the wings of eight flies and then elicited escape responses with the falling disk. Clipped-wing flies, not surprisingly, never exhibited a voluntary takeoff. Remarkably, however, they did respond to the looming stimulus used in our experiments. All eight of the

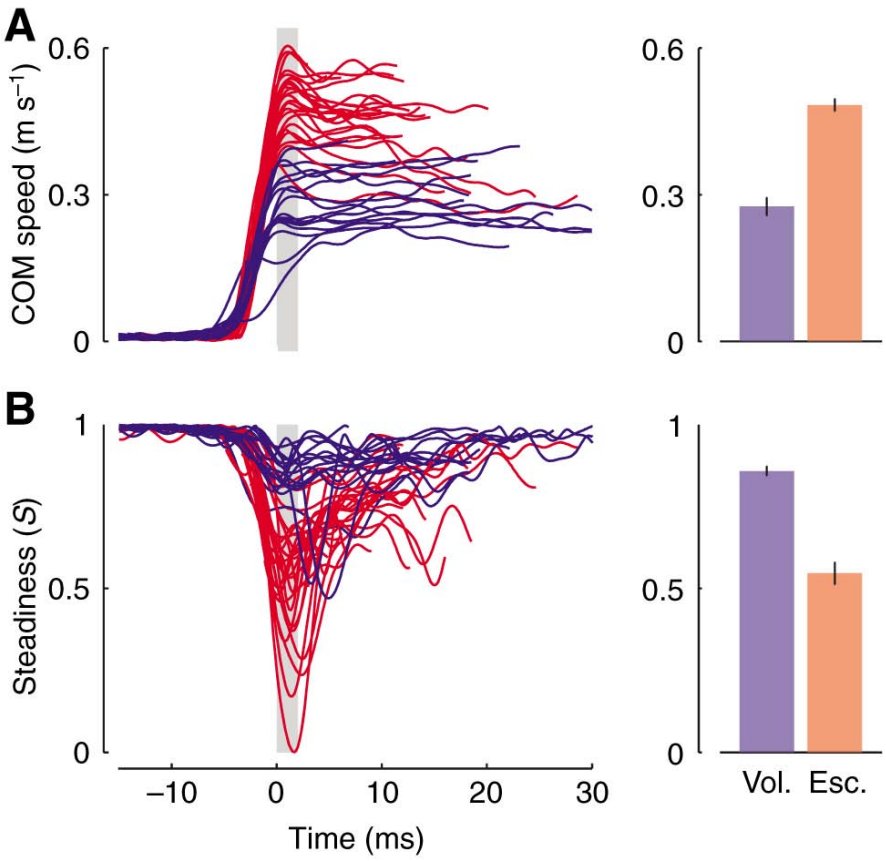

Figure 2.11. Speed vs. steadiness. (A) Time courses of center of mass (COM) speed shown for individual flies. Time courses are aligned so that liftoff occurred at 0 ms, and individual time courses end when the fly left the field of view of our cameras. The bar plot at the right indicates the COM speed (mean ± s.e.m.) for all flies over the first 2 ms of flight (grey region). (B) Time courses for steadiness (S) shown for individual flies. Steadiness was calculated from angular speed as described in the text, with large S-values corresponding to low angular speeds. Bar plots show steadiness (mean ± s.e.m.) over the first 2 ms of flight as in A. Voluntary (Vol.) trials are shown in blue, escape (Esc.) trials in red. Mean COM speed and steadiness are significantly different between voluntary and escape conditions, $P \ll 0.001$, ANOVA.

clipped-wing flies initiated 'flight' in response to the stimulus (figure 2.9A).

Time courses of kinematic parameters for all eight clipped-wing flies (means±s.e.m.) are shown in figure 2.12C. Clipped-wing takeoffs had a median leg extension time of 3.5 ms (IQR = 0.8) similar to that of escape takeoffs (NS, $P = 0.07$, Kruskal-Wallis test), but significantly shorter than that of voluntary takeoffs ($P \ll 0.001$ Kruskal-Wallis test). Note that, as expected from a simple ballistic model, the horizontal position of the fly's center of mass increased linearly while the vertical position described a roughly parabolic trajectory. Horizontal velocity was relatively constant once the fly was airborne, whereas vertical velocity declined linearly, becoming negative as the fly began to fall back toward the ground. The mean peak acceleration produced by the fly during leg extension was 46.9 ± 10.4 m s^{-1} in the horizontal direction, and 58.2 ± 10.1 m s^{-1} in the vertical direction, which is the same as that produced during voluntary takeoffs (NS, $P > 0.9$, ANOVA).

Clipped-wing takeoffs differed most prominently from both voluntary and escape responses in the time course of angular velocity. For the first 2 ms in the air, clipped-wing flies had a mean steadiness value of 0.38 ± 0.09 compared to 0.86 ± 0.01 for voluntary or 0.55 ± 0.03 for escape takeoffs. Figure 2.12D shows that the unsteady trajectory of clipped-wing flies was largely due to the extensive roll induced during the jump. Peak roll acceleration for the takeoff of clipped-wing flies occurred during leg extension, as with intact flies, further confirming that in both cases the roll moment was created by the legs. In wingless flies, roll velocity remains roughly constant once airborne, indicating that air friction generated by the body was insufficient to decelerate the animal substantially. The continuous rotation about the roll axis was in sharp contrast to what we observed in intact escaping flies, which appear to produce counterroll once airborne. Such counterroll might be generated either passively via wing drag or actively via compensatory reflexes.

Because clipped-wing flies cannot produce force once in the air, we can assume that any observable acceleration is due to gravity or body drag. We quantified the effect of body drag after takeoff by comparing the observed airborne COM velocity of each clipped-wing fly with the expected velocity if there was no effect of drag. In this frictionless model, the horizontal velocity of the airborne fly remains constant, and its vertical velocity declines at a constant

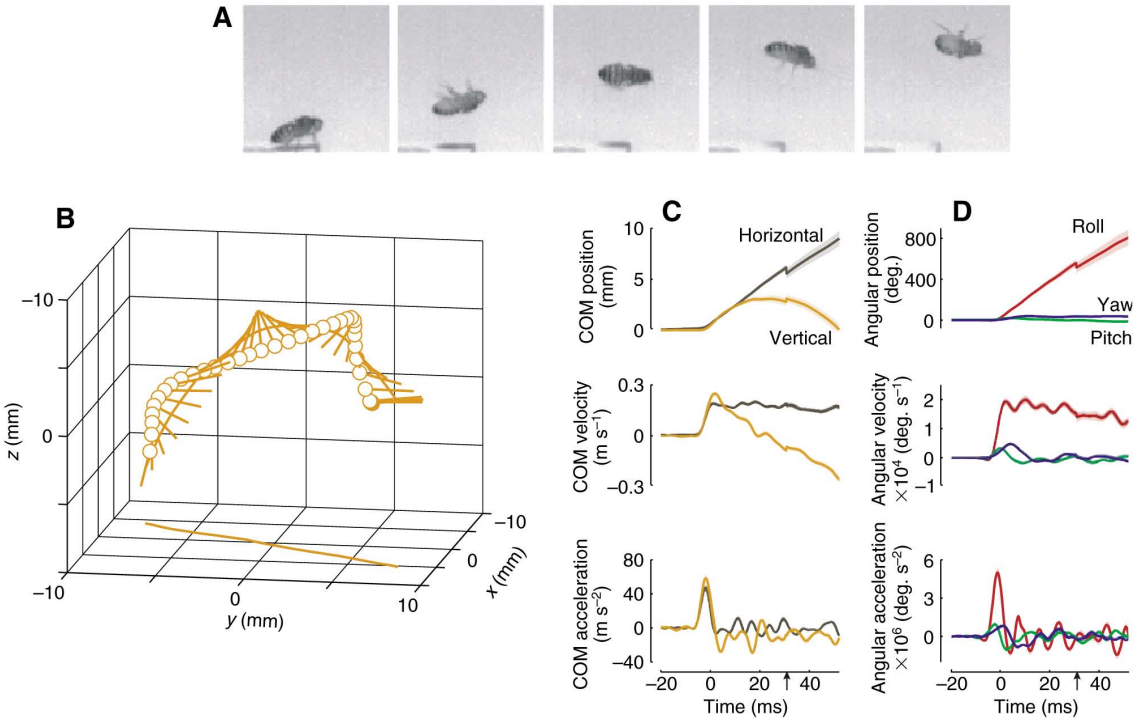

Figure 2.12. Kinematics of escape responses for clipped-wing flies. (A) Video sequence of an example clipped-wing fly escape response to a falling disk stimulus. (B) Lollipop diagram of an example clipped-wing escape response showing the 3D position of the fly every 2.5 ms. (C,D) Average time courses (solid line, mean; shaded area, ±s.e.m.) for translational and rotational kinematic variables during clipped-wing takeoff (as in figure 2.8). $N = 8$ before the arrow on the time axis, and $N = 7$ afterward.

rate of 9.8 m s^{-2} due to the effects of gravity. We found that the observed velocity of the clipped-wing flies deviated from the model with an average root mean square error (RMSE) of 0.04 ± 0.005 m s^{-1}. We also calculated the RMSE for the best polynomial fit to the horizontal and vertical velocity components. The best fit for both components was a linear model, and the resulting average RMSE for the velocity magnitude was 0.03 ± 0.004 m s^{-1}. The distributions of RMSE for the frictionless model and the best-fit polynomial model were not significantly different ($P = 0.12$, ANOVA), indicating that the effects of body drag are smaller than the noise in our kinematic data. However, the noise in the kinematic data for the clipped-wing flies was larger than in the other experiments due to the lower frame rate (2,000 frames s^{-1}) and lens magnification used to capture the entire jump of the flies. Also the clipped-wing flies rotated significantly more than the intact-wing flies, exacerbating any small errors in our estimation of the center of mass location. The average best-fit slope for the horizontal velocity component was -0.2 ± 0.20 m s^{-2}, which was only slightly different from the slope of 0 m s^{-2} predicted by the frictionless model ($P = 0.02$, one-sample t-test), and the average best-fit slope for the vertical velocity component was -10.2 ± 0.27 m s^{-2}, which was only slightly larger in magnitude than the expected -9.8 m s^{-2} if only gravity, and not drag, were affecting the fly's trajectory ($P = 0.004$, one-sample t-test). Based on this analysis, we conclude that the effects of drag are very small during takeoff and thus the body dynamics of wingless flies are dominated by inertia.

2.5 Discussion

Using high-speed videography we examined the flight performance of *Drosophila melanogaster* during two different kinds of flight initiation: escape responses elicited with a falling black disk and voluntary takeoffs that were not deliberately stimulated (figure 2.2). Voluntary takeoffs began with wing opening (rotation and elevation), followed, with quite a variable delay, by leg extension and simultaneous wing depression (figure 2.3). We observed that the wings were opened independently of each other, with the fly first raising whichever wing rests on top (Table 2.1). The largest time observed between the start of top and bottom

wing opening was 140 ms, representing a substantial neural delay, given the rapidity of the subsequent phases of takeoff behavior.

We were able to elicit escape takeoffs reliably in red-eyed, wild-type flies using a falling black disk as stimulus. Under these conditions, we observed that takeoffs, which were previously characterized by the absence of wing raising are, in fact, proceeded by variable degrees of wing elevation. This confirms the recent observations of Hammond and O'Shea, who used similar stimuli to elicit escape responses in *Drosophila* (Hammond and O'Shea, 2007a). In most escapes, however, we found that the fly did not fully raise its wings prior to the start of the jump, resulting in abnormal stroke kinematics during the first few cycles (figure 2.7). Instead, the wings were typically folded down against the body during leg extension and then, once airborne, bent ventrally at a joint distal to the wing hinge proper during the first few upstrokes. Although escape responses were somewhat variable, this peculiar pattern of wing motion during the first several stroke cycles was quite consistent.

We evaluated the two types of flight initiation and found that, although voluntary takeoffs produced very steady flight with little rotation once airborne, they were relatively slow both with respect to the time required to get off the ground and the initial takeoff velocity (figure 2.11). Escape takeoffs, by contrast, occurred rapidly and accelerated the fly to a faster initial speed, but resulted in high rotational velocities after launch. Roll velocity was the largest contributor to the elevated angular velocity during the initial stages of an escape takeoff and was quite distinct from the time course of roll during voluntary takeoffs (figure 2.9B). Collectively, these results suggest a fundamental trade-off between takeoff velocity and stability during flight initiation.

2.5.1 The Role of Wings

It seems paradoxical that voluntary takeoffs had lower speeds than escapes, even though during the former flies used two types of appendages, wings and legs, to launch themselves into the air, while during the latter flies typically used only their legs. Since we observed that voluntary takeoffs had greater steadiness (lower angular velocities) than escapes, we can rule out the possibility that this discrepancy in speed was the result of voluntary takeoff

forces not being directed through the fly's center of mass, producing more rotation and less forward speed. If anything, the greater steadiness of voluntary takeoffs suggests that the launch forces are directed more precisely through the center of mass in the voluntary case. The two more likely explanations are that either (1) the fly's outstretched wings during voluntary takeoff add a significant amount of drag, thereby slowing the fly during leg extension, or (2) the fly's legs do less work during voluntary takeoffs than during escapes.

To evaluate the magnitude of drag effects, we removed both wings from a set of flies that performed escape jumps. These flies were unable to produce force once in the air, so changes in their airborne velocity must be attributable to deceleration from body drag and gravity. Our analysis found that the effects of drag on flight speed were so small as to be within the noise of our kinematic measurements. The launch velocity of voluntary takeoffs, however, was 50% slower than that of escapes. Even if the effective area of the fly is tripled by the addition of outstretched wings—roughly tripling the effect of drag—drag alone cannot account for this lower velocity during voluntary takeoff.

Another way of testing the role of flapping wings in decelerating the fly at the onset of flight is to make use of the variability of escape takeoffs. If flapping wings substantially increase total drag compared to static wings, we would expect that in the subset of escape responses in which the flies successfully elevate both wings prior to the start of leg extension, the takeoff velocity would be slower than cases in which the wings were held down against the body. To examine this hypothesis, we divided the escape responses into three categories based on the position and action of the wings during leg-extension: (1) takeoffs in which both wings were elevated prior to leg extension and executed a downstroke similar to that during a voluntary takeoff, (2) takeoffs in which only one wing was completely elevated before leg-extension, or both wings reached only some intermediate opening position, and (3) takeoffs in which the wings were raised only a small amount before being pulled down against the back of the fly. Figure 2.13A shows the median takeoff velocity for these three conditions as well as for voluntary takeoffs and clipped-wing escapes. Escape responses in which the wings were successfully raised ('**Esc') had takeoff velocities indistinguishable from escapes in which the wings were closed ('Esc'), supporting the notion that increased

wing drag cannot explain the lower initial velocities during voluntary takeoffs. Furthermore, the takeoff velocity of clipped-wing flies was even lower than that of intact flies during escapes. We conclude that the wings do not appear to make a significant contribution to total drag during the jump.

2.5.2 The Role of Legs

If drag forces cannot account for the higher speed of escapes compared to voluntary takeoffs, could a difference in force production by the legs explain the discrepancy? If the legs are providing the only propulsive force during the majority of escape takeoffs, and their extension is coordinated by a single spike in TTM, one would expect the legs to produce roughly the same amount of force during every escape. We observed, however, that escapes by clipped-wing flies were slower than those by intact flies (figure 2.13A). In this case, the large angular speeds of clipped-wing fly takeoffs (figure 2.13B) indicate that it is possible the legs are providing the same amount of work as in intact flies, but that the line of force acts further from the center of mass. The result would be that the airborne fly rotates more and translates forward less quickly. To determine whether this explanation is feasible, we estimated the amount of translational and rotational kinetic energy the fly generated during takeoff, as well as the potential energy it had achieved during its first 2 ms in the air (see materials and methods, section 2.3). The average total energy of the fly during the first 2 ms after takeoff is the sum of translational, rotational and potential energies. From the airborne portion of our clipped-wing experiments, we know the effect of drag is minimal, so we neglect the effects of air resistance. Figure 2.13C shows that the clipped-wing flies have significantly more rotational energy immediately after takeoff than all intact-wing flies. The result of this rotation is that, although they have slower translational takeoff velocities, clipped-wing flies actually have the same amount of total energy after takeoff as other escaping flies (NS, $P > 2$, Mann-Whitney pairwise comparison with Bonferroni correction, figure 2.13D), and that all escaping flies have greater total energy than voluntarily jumping flies ($P \ll 0.026$, Mann-Whitney pairwise comparison with Bonferroni correction). Thus, the legs of clipped-wing and intact-wing flies perform the same amount of work during

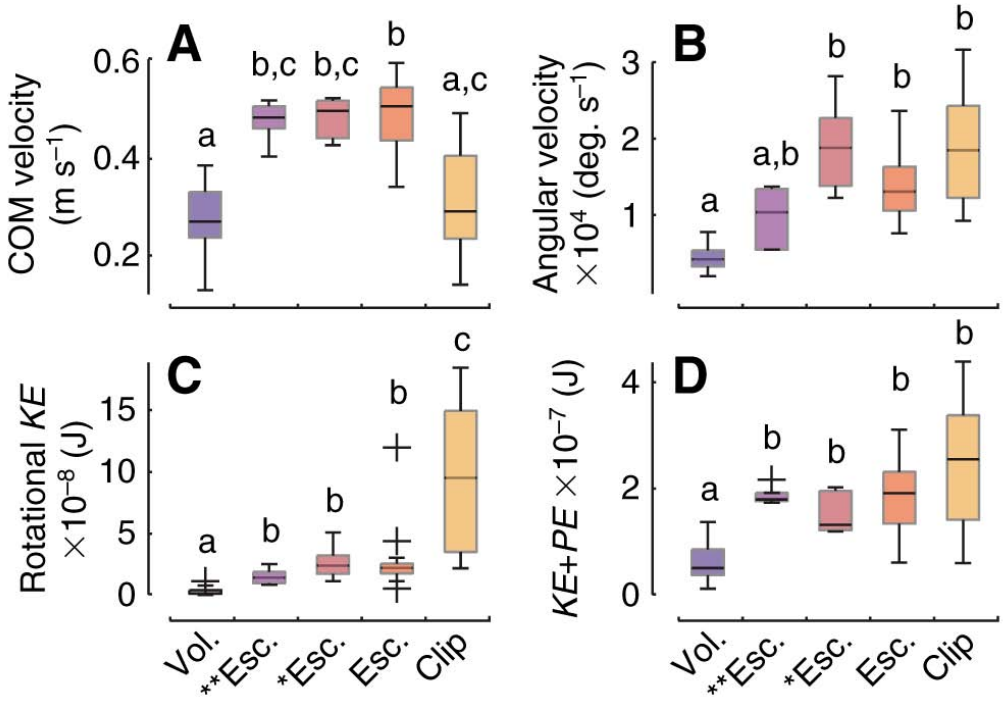

Figure 2.13. Distributions of kinematic variables under different wing-raising conditions: voluntary takeoff (Vol., $N = 16$), escape takeoffs with both wings raised before leg-extension (**Esc., $N = 5$), escape takeoffs with only one wing fully raised or wings only partially raised before leg-extension (*Esc., $N = 5$), remaining escape takeoffs in which wings move only minimally before leg-extension (Esc., $N = 17$), and escape takeoffs by flies with wings removed (Clip, $N = 8$). Box plots are of values averaged over the first 2 ms of flight for (A) center of mass (COM) speed, (B) angular speed, (C) rotational kinetic energy, calculated from the angular speed and assuming the fly to be an ellipsoid body, and (D) the sum of potential (PE) and kinetic energy (KE). Kinetic energy is the sum of rotational kinetic energy (C) and translational kinetic energy (see text for derivation). Statistically significant differences were determined using Mann-Whitney pairwise comparisons with Bonferroni correction for multiple comparisons. Comparisons for which $P \leq 0.05$ are marked by different lower case letters.

takeoff, but for clipped-wing flies a larger proportion goes into rotating the body rather than translating it. Such a difference might easily arise if, during takeoff, the leg forces of clipped-wing flies act through a point that is farther from the center of mass than in the intact-wing case. Flies taking off voluntarily both translate and rotate more slowly, indicating that the legs perform much less work in this case.

If the work produced by the legs during an escape is the result of a single twitch in each jump muscle, how could these muscles produce less force during a voluntary takeoff? One possibility is that the physiological state of the TTM muscle is different during the two behaviors. Octopamine has been suggested as a neuromodulator that can increase individual twitch strength in a jump muscle of locusts. In this system, octopamine is delivered by an octopaminergic midline neuron, DUM5A, at the correct time to enhance the contraction of the slow extensor tibia (SETi) muscle (Duch et al., 1999). Mutant *Drosophila* with defects either severely reducing the amount of octopamine available ($Tbhn^{M18}$) or lacking a strong octopamine receptor (TyR^{homo}) do not produce as much force with the mesothoracic legs when the GFs are stimulated and do not jump as far in assays where the wings are removed (Zumstein et al., 2004). This suggests that octopamine might enhance TTM force production during GF-mediated escapes but not during voluntary takeoffs. However, it is still unclear whether the octopaminergic system in *Drosophila* could deliver the neuromodulator to the muscle within the tens of milliseconds timescale required to make it effective during escapes.

A second possibility is that all the extensor muscles of the leg, including the large TTM, are coordinated more effectively to generate greater power during escapes. This hypothesis is supported by the observation that the period of leg extension is shorter during escape takeoffs. The GF is known to drive the tibial levator muscle (TLM), which extends the femur-tibia joint, with a characteristic latency of 0.6 ms after activation of the TTM (Trimarchi and Schneiderman, 1993). The TLM not only provides additional muscle force, but extension at the femur-tibia joint may help to keep the legs in contact with the substrate longer, prolonging the time during which leg muscle forces can act against the ground. The circuits underlying voluntary takeoffs might coordinate TTM and TLM muscles differently

to push the fly off the ground more slowly but with less rotation.

2.5.3 Components of the Flight Initiation System

Based on our observations and those in the literature, we propose a simple scheme of descending command pathways to explain the differences between voluntary and escape takeoffs in *Drosophila* (figure 2.14). Bilateral wing elevation pathways are required to explain how the fly can raise its left and right wings independently and with variable delay. In addition, the fly must possess two means of driving leg extension: the GFs and another, yet-to-be-identified, smaller diameter pathway. The existence of a second pathway is required by the evidence that flies can initiate takeoff even when the GFs are not active (Holmqvist, 1994; Trimarchi and Schneiderman, 1995a).

As has been suggested (Hammond and O'Shea, 2007a), the fact that wing motion precedes the jumping phase of escape challenges the notion that the large-diameter GF interneurons trigger the first response to a threatening stimulus. GF stimulation is known to activate indirect wing elevators (dorsoventral muscles, DVMs) and a direct wing opener, pa3 (also known as b2, see Wisser and Nachtigall, 1984), but with much longer latencies than the activation of the leg extensors (TTMs) and wing depressors (DLMs) (Tanouye and Wyman, 1980; Tanouye and King, 1983). Based on this well-characterized sequence of muscle activation, it is not possible for the GFs themselves to drive wing elevation prior to leg extension. One possible exception would be if the TTM muscle itself acts as a wing-

Figure 2.14: Model for achieving takeoff performance. (A) We hypothesize that a minimum of four independent pathways are required to coordinate takeoff behavior: one coordinating wing opening on either side of the body and two coordinating different types of leg extension. In our model, takeoff performance is determined by both the latency between activation of wing and leg pathways, τ, and the choice of leg pathway. In our diagram δ_1 represents the delay due to sensory and/or central processing before one or both wing pathways are activated, and δ_1 represents the delay before activation of one of the leg pathways. The difference between these two delay times is the observed wing-leg interval, We propose that which leg pathway is activated for a given takeoff determines the speed of that takeoff. Alt., alternate. (B) The latency, τ, between leg and wing pathway activation determines takeoff steadiness. This model is supported by our data: the graph shows the time, τ, between first wing and first leg motion plotted against the resulting takeoff steadiness, S, for each fly observed ($N = 43$). Upward-pointing triangles represent voluntary takeoffs, while upside-down triangles mark escape responses. The fill color of the upside-down triangles (escapes) indicates the conditions of the wings during takeoff, as defined in figure 2.13: black, **Esc. ($N = 5$); white, *Esc. ($N = 5$); gray, Esc. ($N = 17$). The green line is a best-fit linear regression to the data. The line has a positive slope, indicating a direct correlation between τ and steadiness. (C) Summary of how coordination of the hypothesized pathways leads to the observed differences in takeoff performance.

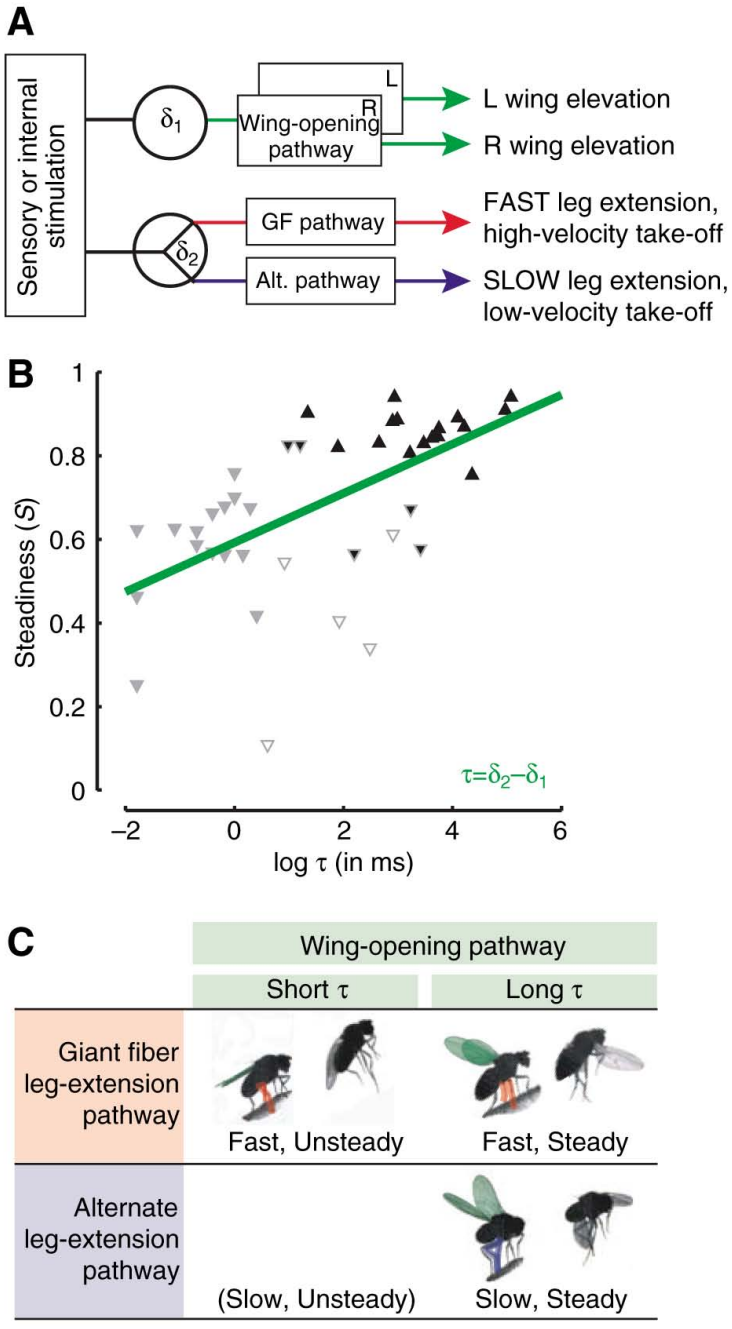

Figure 2.14. See p. 65 for caption.

opener, as has been suggested previously (Tanouye and King, 1983; Bacon and Strausfeld, 1986). If this is true, then some of the wing motion observed before the jump might be due to GF-driven TTM contraction. Even in this case, however, the GF pathway could not account for the cases in which the wings elevate several milliseconds or more before the onset of leg extension, a delay that is quite common during escapes (figure 2.3). Thus, the fact that the wings begin to open before the legs extend argues strongly for a small-diameter wing elevator pathway that is active before the GFs fire.

Although it seems unlikely that one or more spikes could travel more quickly along another axon than down the largest descending fibers in the neck connective, the initial activation of the GF system is temporally limited by the processing time within the visual system. A small-diameter descending interneuron that receives input from faster sensory modalities, such as the ocelli or antennae, might reach threshold much earlier, making up for its slower conduction speed and starting wing elevation before the GF spike arrives in the thorax. The descending interneurons of this putative pathway are likely to receive either local or ascending mechanosensory information because the circuit correctly raises the top wing first.

According to the scheme described in figure 2.14A, the functional performance of the takeoff depends critically on the latency between wing activation and leg activation. Kinematic results indicate that steadiness, S, increases directly with increasing latency between the start of wing elevation and leg extension, for both voluntary and escape takeoffs (figure 2.14A). Longer latencies presumably allow the fly to elevate its wings to a ready position before the start of the jump. Higher steadiness during takeoff might be advantageous to a fly because it allows the fly to maintain its initial heading relative to an odor plume or wind direction, and minimizes the likelihood of an uncontrolled crash at the onset of flight. In the case of a threatening stimulus, however, a faster launch velocity may be of primary importance. In these cases, the GF-system elicits a powerful jump before the wing raising program has time to finish, resulting in a short wing-leg latency τ and a 'tuck and jump' takeoff.

In addition, our data suggest that partially raised wings, or cases in which only one wing

is fully raised, lead to lower steadiness at takeoff than that predicted by their observed wing-leg latency (figure 2.14B, open triangles). This may explain why the giant fiber pathway activates the wing depressor muscles (DLMs) with such a short delay after the TTMs. Previous authors found the inclusion of the DLMs in the GF pathway paradoxical because they observed the wings to be closed before GF activation (Trimarchi and Schneiderman, 1995b). Hammond and O'Shea have revised this description, noting that the wings are typically elevated just before the escape jump (Hammond and O'Shea, 2007a). Our data further suggest that the functional role of pulling in the wings is not to lower translational drag (as might be assumed) but to reduce left-right wing differences, thus making takeoff a bit more stable. An alternative view is that the added tumbling of the fly during escape may actually help the fly to avoid capture—in which case the early role of the DLMs in escape would require another explanation. In either case, modulating the latency between wing and leg pathway activation could be the mechanism by which the fly controls steadiness during takeoff, trading it off against a faster reaction time when appropriate.

Another critical aspect of takeoff performance is initial flight speed. Our data suggest that translational takeoff velocity could be mediated by a choice between alternate leg-extension pathways. Body kinematics suggest that the mesothoracic legs produce more work during escape takeoffs than during voluntary takeoffs (figure 2.14D). If, as the literature suggests, escapes are mediated by the GF pathway and voluntary takeoffs by an alternate pathway, then we hypothesize that use of the GF leg-extension pathway results in a strong, fast jump and a high takeoff velocity. In contrast, use of the alternate leg-extension pathway results in a weaker, slower jump and a lower-velocity takeoff (figure 2.14A). Our hypothesized system is similar to the escape system found in the crayfish. The crayfish has two GF systems that coordinate stereotyped escape swimming either forward or backward, depending on the location of the stimulus. Both of these GF systems are activated by strong threatening visual or tactile stimuli. Milder stimuli, however, prompt a graded avoidance turn mediated by non-giant fiber pathways (Edwards et al., 1999). Together the GF systems and the non-giant pathways use the same musculature to create a range of responses to threatening stimuli, of which GF-mediated escape is at one extreme end. Our results

indicate that *Drosophila* may be similarly equipped to employ a range of escape behaviors best tuned to type and magnitude of the threat (figure 2.14C).

Chapter 3

Visually Mediated Motor Planning in the Escape Response of *Drosophila*

3.1 Summary

A key feature of reactive behaviors is the ability to spatially localize a salient stimulus and act accordingly. Such sensory-motor transformations must be particularly fast and well tuned in escape behaviors, in which both the speed and accuracy of the evasive response determine whether an animal successfully avoids predation (Eaton, 1984). We studied the escape behavior of the fruit fly, *Drosophila*, and found that flies can use visual information to plan a jump directly away from a looming threat. This is surprising, given the architecture of the pathway thought to mediate escape (King and Wyman, 1980; Levine and Tracey, 1973). Using high-speed videography, we found that approximately 200 ms before takeoff, flies begin a series of postural adjustments that determine the direction of their escape.

This chapter previously published as G Card and MH Dickinson (2008b) Visually mediated motor planning in the escape response of *Drosophila*. *Curr Biol* 18(17):1300-7.

These movements position their center of mass so that leg extension will push them away from the expanding visual stimulus. These preflight movements are not the result of a simple feed-forward motor program because their magnitude and direction depend on the flies' initial postural state. Furthermore, flies plan a takeoff direction even in instances when they choose not to jump. This sophisticated motor program is evidence for a form of rapid, visually mediated motor planning in a genetically accessible model organism.

3.2 Experimental Procedures

We used 3-day-old female *Drosophila melanogaster* from a laboratory culture as described in Card and Dickinson (2008a) (See section 2.3). In other animals, we excised the T2 legs near the femur-coxa joint. We used high-speed video cameras (Photron, San Diego, CA) to record images at 5,400 frames per second. The falling-disk stimulus and the methods for calibrating the high-speed video camera are described in Card and Dickinson (2008a), with the exception that flies emerged onto a flat 5-mm^2 plastic platform in the current study. The starting position of the disk was 420 mm from the center of the platform. The disk radius was 70 mm and accelerated toward the fly at an angle of 50° relative to horizontal. The disk fell toward the center of the platform for 250 mm (for a period of 300 ms) before it was stopped by a foam block. In some trials, this platform was replaced with a 5-mm^2 right-angle prism to enable imaging of the ground contact of all six tarsi. The entire imaging area was surrounded by backlit white cloth.

For each sequence, we marked the location of the fly's head and the end of its abdomen in the video frame 1.85 ms before the middle legs began to extend (t_{pre}) and in the frame when the tarsi first left the ground (t_{jump}). For data taken with the prism platform, we also marked the contact points of all six legs with the ground at t_{pre} and t_{jump}, and we marked body and leg points at stimulus onset (t_0). The fly's COM is well approximated by the halfway point between the head and abdomen. The fly's prestimulus heading vector was determined from the orientation of the head-abdomen line at t_{pre} (figure 3.1) or t_0 (figure 3.3 and 3.4). The jump direction was determined from the vector spanning the COM position

at t_{pre} to the COM position at t_{jump}. The leg and COM movements shown in figures 3.5C and 3.5D are the vectors oriented from the tarsal contact point (or COM) location at t_0 to the new contact point (or COM position) at t_{pre}. To make the vector fields shown in figure 3.6, we found the vector representing each fly's t_0-to-t_{pre} COM movement relative to the T2 tarsi. We then binned these vectors according to the COM location at t_0. Grid spacing for the bins was 0.2 mm in the longitudinal direction (x) and 0.1 mm in the lateral direction (y). We then interpolated these binned COM movement vectors to a finer mesh with 0.5×0.5 mm spacing by using a standard implementation of Delaunay triangulation in Matlab (The MathWorks, Natick, MA).

All statistical measures were taken with procedures appropriate for circular data (Zar, 1999). To assess the significance of our results in figure 3.1, we analyzed the distribution of jump directions for each experimental group (normal, clipped-wing, clipped-leg, and wind-blocked) in each of the five 36 bins for stimulus direction (θ). We used two tests for circular data to compare our results. To compare the observed mean jump direction to the hypothesis that the fly jumped forward ($\mu_a = 0$) or away from the stimulus ($\mu_a = \theta + 180°$), we used the one-sample test for mean angle, which is analogous to the one-sample t-test for linear data. The hypothesis that the observed mean direction, μ_0, is the same as a hypothesized mean direction, μ_a, was tested by determining whether μ_0 was within a 95% confidence interval around μ_a. To compare mean jump directions between experimental conditions (e.g., normal flies versus clipped-wing flies), we used the Watson-Williams test, which calculates the probability that two experimental groups are sampled from one population with a single mean. The reported p value in figure 3.1F is the probability that the observed variance in the two sample populations has occurred by chance. We consider $p \leq 0.05$ to indicate that the two populations have significantly different means.

3.3 Results

As described previously (Card and Dickinson, 2008a), we used a high-speed video camera to capture the motion of fruit flies in response to a 14-cm-diameter black disk that fell

toward the animals along a 50° downward trajectory. Individual flies were loaded into small opaque vials from which they climbed through a narrow tube onto the center of a 5×5 mm^2 platform. We triggered the descent of the black disk and started video capture once a fly had settled on the horizontal surface of the platform. Ninety-six percent of the flies responded to the descending disk by jumping into the air and initiating flight. A typical escape sequence is shown in Movie CB1, available in the supplementary material online. The mean delay between the start of the stimulus and the onset of flight (measured by the loss of tarsal contact of the mesothoracic legs) was 215 ± 42 ms (mean $\pm$ SD). Because we do not know when the flies first notice the stimulus, this value represents an upper limit on the time window, within which all of the sensory-motor processing for the escape behavior occurs.

Although the stimulus approached the platform from the same direction in each trial, the azimuthal angle of the stimulus relative to the fly's body axis (θ) varied across trials because the flies settled on top of the platform with different orientations (figure 3.1A). To determine whether flies bias their takeoff direction to avoid the threatening stimulus, we measured each fly's initial azimuthal angle heading over the duration of leg extension. As shown in figures 3.1B and 3.1C, flies tended to jump away from the looming stimulus, even when the stimulus approached from directly in front. We tested for bias in our experimental apparatus by dropping the disk from the opposite side of the platform, but we found no positional effect ($p \geq 0.05$, Watson-Williams test). In order to analyze our results with more statistical rigor, we reflected all the rightward approaches across a line of bilateral symmetry and parsed our data into five 36° bins of approach angle (figures 3.1D, 3.1E, and 3.1F). An analysis with circular statistics (Zar, 1999) indicated that flies jumped backward in response to looming objects in front of them and jumped forward in response to looming objects behind them (binned means not different from $\alpha = 0°$ and 180°, respectively; $p = 0.05$, one-sample test for mean angle). In response to stimuli approaching from the side, however, flies jumped at an angle that was approximately halfway between directly away ($\alpha = \theta + 180°$) and directly forward ($\alpha = 0°$) (binned means at $36° < \theta < 72°$ and $72° < \theta < 108°$ are significantly different from $\alpha = 0°$ and $\alpha = 180°$, $p = 0.05$; figure 3.1F).

This forward bias is not surprising, given that voluntary takeoffs elicited by either attractive odors or internal cues are almost always in the forward direction (data not shown).

An approaching predator (or, in our case, a falling disk) creates both visual and mechanosensory cues that a fly might use to compute the direction for an escape. To test whether visual cues alone are sufficient, we repeated our experiments with a clear acrylic windshield placed between the falling disk and the takeoff platform (Hammond and O'Shea, 2007b). For the five different binned values of stimulus direction, we found no significant difference in behavior in the presence or absence of the windshield ($p \leq 0.02$). We conclude that although mechanosensory cues might still play a role, visual information alone is sufficient for a fly to determine the direction of an approaching threat.

A fly might bias its initial heading by either modulating its leg motion so as to jump away from a threat or, alternatively, jumping forward but then quickly using its wings to steer while jumping. To test between these hypotheses, we repeated our analysis of takeoff direction on flies whose wings had been surgically removed. Ninety-seven percent of wingless flies (35 out of 36) jumped in response to the looming stimulus (see Movie CB2). As shown in figures 3.1E and 3.1F, the initial heading of wingless flies was statistically indistinguishable from normal winged flies in all 36° clusters of θ except $0° < \theta < 36°$. Although wing forces might still contribute, these experiments demonstrate that the leg motor system alone is

Figure 3.1: Flies control their escape direction in response to a visual looming threat. (A) We measured the azimuthal position of the stimulus (θ) and the direction moved by the fly's center of mass (COM) during the resulting escape jump (α) relative to the initial heading of the fly (indicated by the dotted line). (B and C) Each arrow shows the direction (α) jumped during one trial and is colored by stimulus direction (θ, see inset). (C) plots data from prism-platform experiments; see figures 3.3-3.6. (D) Assuming bilateral symmetry, we transformed all data to represent responses from left-side approaches ($0° < \theta < 180°$). We plotted α (black dots in 5° bins) for each of the five 36° ranges of θ (indicated by the light red wedge); the red arrow indicates the circular mean jump direction, and its length is inversely related to data angular dispersion. (E) A linear representation shows α as a function of θ for different experimental treatments: normal flies (black, as in D), flies with wings excised at the wing hinge (red), flies with T2 legs clipped (green), and normal flies behind a clear acrylic windshield (blue). The dashed lines indicate hypotheses for how the data should be distributed if the flies always jump forward ($\theta = 360°$) or backward ($\theta = 180°$), regardless of stimulus direction. Gray diagonal lines show where the data would be expected to fall if the flies always jumped directly toward the stimulus ($\theta = \alpha$). The black diagonal line indicates where the data would fall if the flies always jumped directly away from the stimulus ($\theta = \alpha + 180°$). (F) Circular means and standard deviations for each experimental treatment, grouped into the same 36° θ bins shown in (D). In each θ group, we compared the mean jump direction under normal conditions (black) to several hypotheses, as indicated by the symbols above each cluster: "†" The circular mean is significantly different from 0° or 360° ($p = 0.05$, one-sample test for the mean angle; Zar, 1999). "‡" The mean is significantly different from $\theta + 180°$ ($p = 0.05$, one-sample test for the mean angle). "∗" The normal fly mean was significantly different from the mean of the other treatment, indicated by color ($p \leq 0.02$, Watson-Williams test; Zar, 1999).

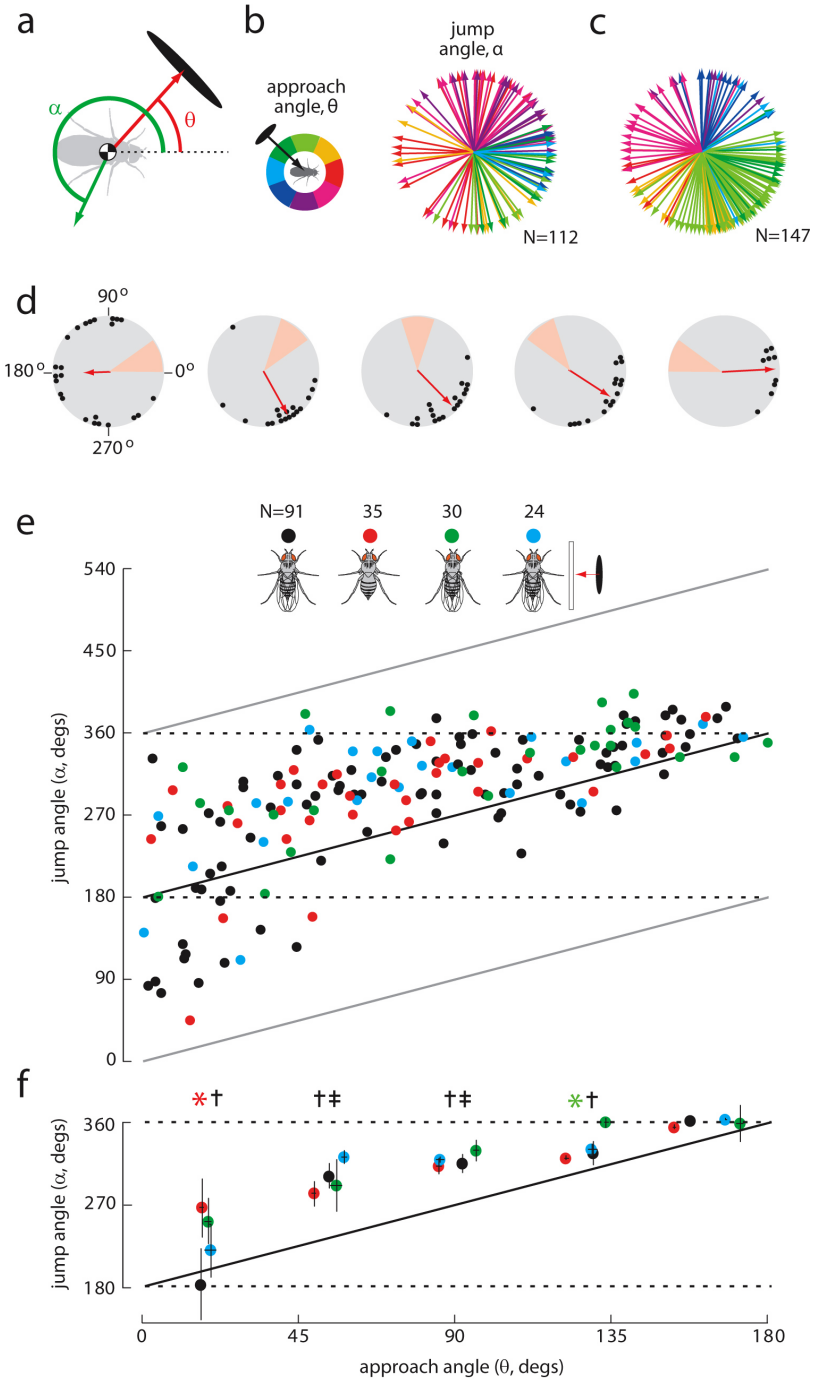

Figure 3.1. See p. 74 for caption.

sufficient to bias the direction of takeoff. We also performed the reverse experiment—testing the escape responses of flies with intact wings whose mesothoracic legs (T2) had been surgically removed (figures 3.1D and 3.1E and Movie CB3). Although they cannot jump, these flies were also able to escape away from the looming stimulus by "leaning" in the right direction before takeoff. These flies do not jump into the air, but the aerodynamic force created by their wings lifts them off the substratum in a direction determined by their leaning posture. The results were identical to controls in all θ groups except $108^\circ < \theta < 144^\circ$ (figure 3.1F). Together with the prior experiments, these results indicate that escaping from looming objects involves a sensory-to-motor transformation in which a visual estimate of the azimuthal orientation of the stimulus is transformed into postural changes that predominantly determine takeoff direction.

To better resolve the postural changes that precede flight, we modified our observational platform by replacing the opaque platform with a right-angle prism (figure 3.3 and Movie CB4) so that we could image both the side and underside of each fly. Using this arrangement, we could determine the position of the six tarsal contacts and each fly's center of mass (COM) at two time points: before release of the stimulus (t_0) and just prior to takeoff (t_{pre}) (figures 3.3 and 3.4A). Because only the T2 legs provide thrust during takeoff, we chose to measure the position of each fly's COM relative to a coordinate system determined by the line segment connecting the T2 tarsi and that segment's perpendicular bisector (figure 3.4A). The results indicate that flies actively reposition their COM away from the direction of the looming stimulus (figure 3.4A) and that this orientation accurately predicts the direction of their subsequent jump (figure 3.4B). Examples of these behaviors for stimulus approaches from the front, side, and back are provided in figure 3.2 and Movies CB4, CB5, and CB6.

Our analysis indicates that the COM motions elicited by different stimulus directions are brought about by different combinations of leg placement (lifting the legs and placing them in new locations) and leaning (shifting the body position by altering joint angles without changing tarsal position). The most prominent leg placements were the lateral movements of the T2 legs along an axis parallel to the longitudinal axis of the body, which shifted the

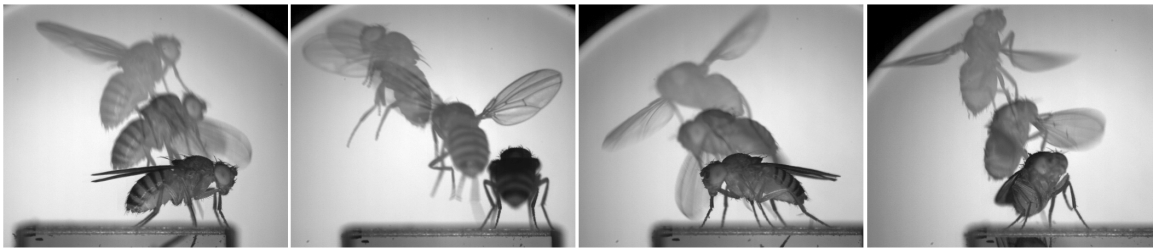

Figure 3.2. Photomontages of four different *Drosophila* escape jumps in response to a falling disk. Regardless of starting orientation, each fly jumped away from the stimulus, which approached from the right-hand side of the images. The video frames shown are the fly's starting position 17-130 ms before takeoff (darkest), the fly at the point of takeoff, when its tarsi first leave the ground (middle), and the fly in flight 2-5 ms after takeoff (lightest). Scale: Drosophila body length 2.5 mm.

COM forward or backward relative to the points of tarsi-ground contact. In contrast, the leaning movements primarily resulted in a sideways relocation of the COM, both in real-world coordinates and relative to the T2 tarsi. The magnitude and direction of both these motions varied strongly with the angular location of the looming stimulus. The functions shown in figures 3.5A and 3.5B amount to maps of the sensory-motor transformation that relates the azimuthal position of the looming stimulus in visual space to a set of motor actions that will determine jump direction. For example, a frontal stimulus position ($\theta = 0°$) elicits a large forward longiudinal motion of the T2 legs, whereas a rear position elicits a small rearward motion of the T2 legs. This visuomotor transformation results in a proper alignment of the COM so that the fly's subsequent jump will carry it away from the looming threat. In contrast, sideward stimulus directions ($\theta = 90°$ and $270°$) do not elicit lateral motions of the T2 legs, but rather lateral leaning movements that move the COM to an appropriate location for a sideward jump. The efficacy of these leaning movements in biasing jump direction is demonstrated by the performance of animals that are missing the T2 jump legs (figure 3.1 and Movie CB3).

The sensory-motor transformation that enables flies to jump away from looming threats might consist of a simple feed-forward motor program in which a stimulus arriving from a particular visual direction triggers a particular motor program for leg motion, regardless of the initial posture of the body. Alternatively, the motor program might take into account

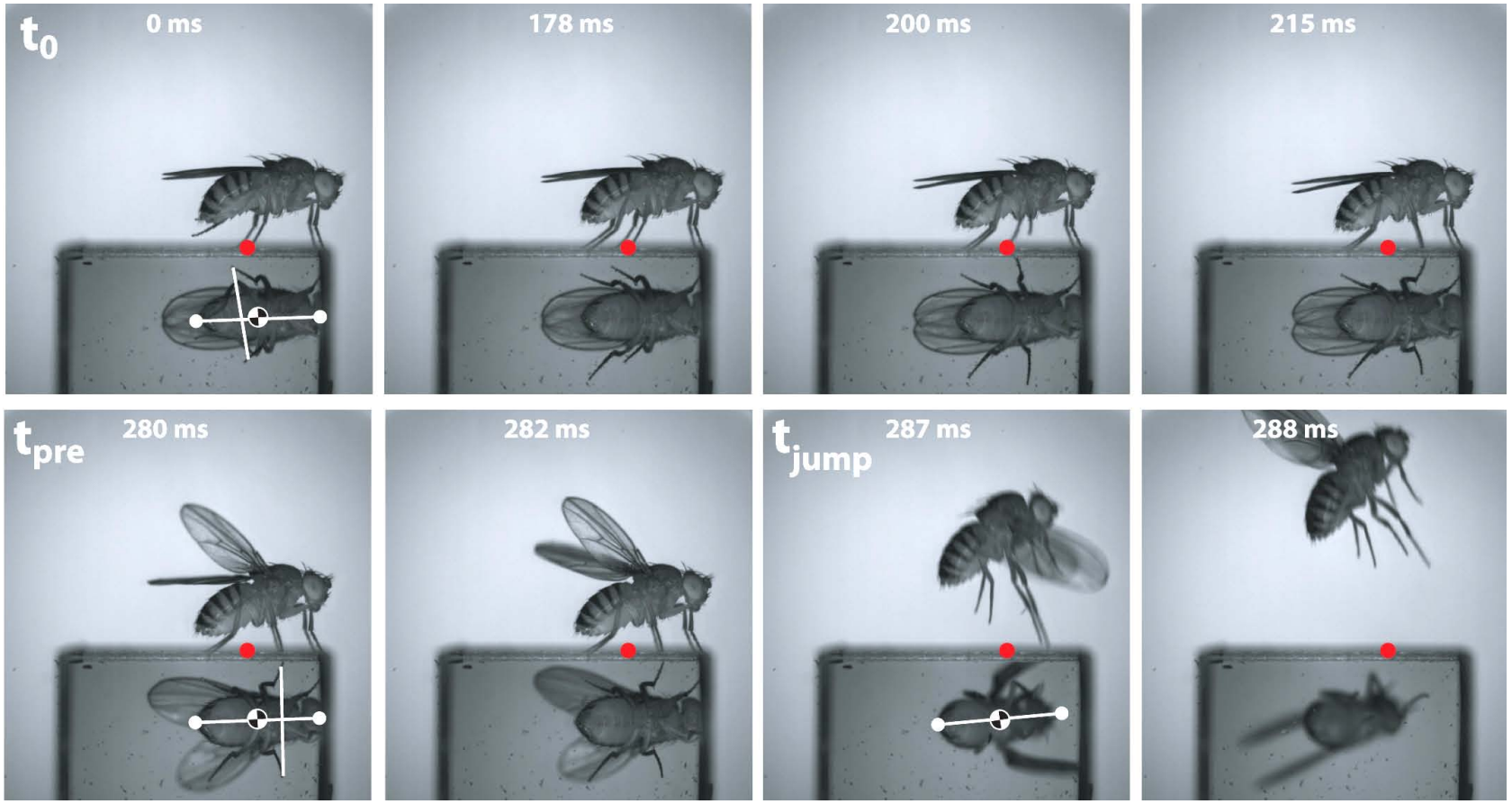

Figure 3.3. A video sequence with the prism platform shows a typical escape. The looming stimulus approaches from in front of the fly (right-hand side of the images). Time stamps denote milliseconds elapsed since stimulus onset. White dots on the prism image mark the head and abdomen points used to determine the fly's COM (black and white circle) at three time points: stimulus onset (t_0), immediately before the jump (t_{pre}), and the moment of takeoff at the end of the jump (t_{jump}). The red dot marks the contact point of the T2 tarsi with the surface at t_0.

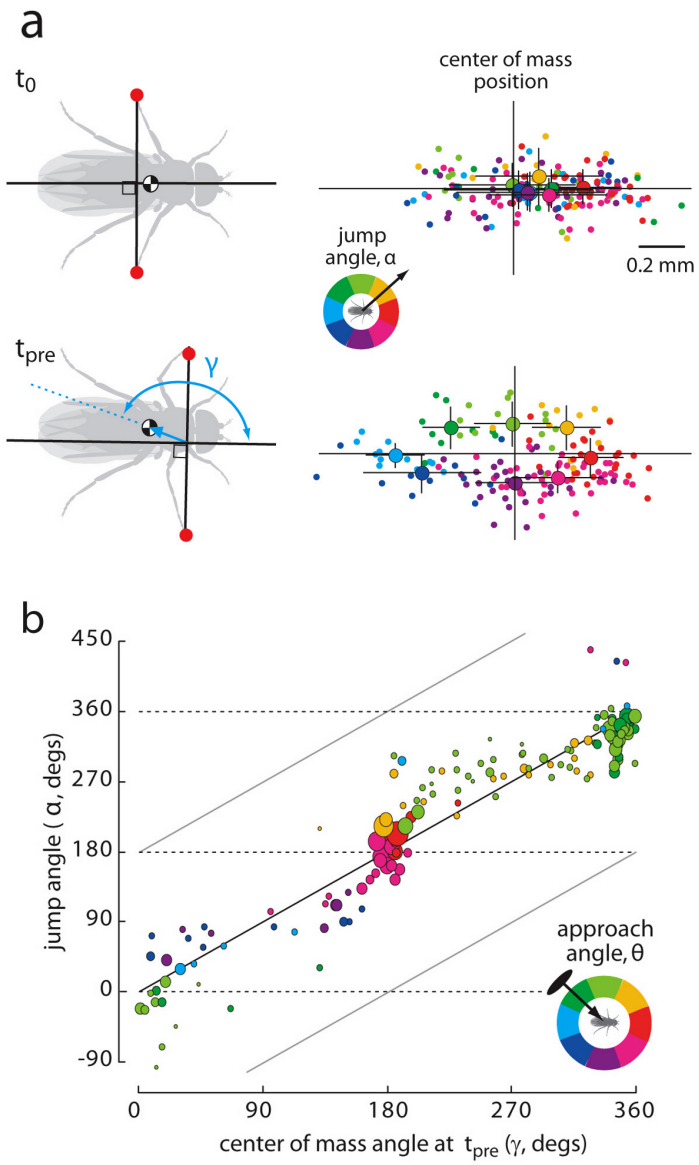

Figure 3.4. (A) We plot the COM locations ($n = 147$) relative to axes determined by a line connecting the left and right T2 tarsi and a perpendicular line that bisects that segment. Each colored dot represents the location of the COM of a fly during a single trial at t_0 (top) or t_{pre} (bottom). Colors indicate the direction the fly subsequently jumped (α, see inset). Large circles with error bars represent COM position (mean $\pm$ SD) for eight clusters of data, parsed according to the jump angle, α (45° bins). (B) Jump angle (α) as a function of the angle of the COM location at t_{pre} (γ). The size of each point is proportional to the length of the COM vector (γ), and the color indicates the angle of stimulus approach (θ, see inset). Dashed, gray, and black lines are used as in figure 3.1E.

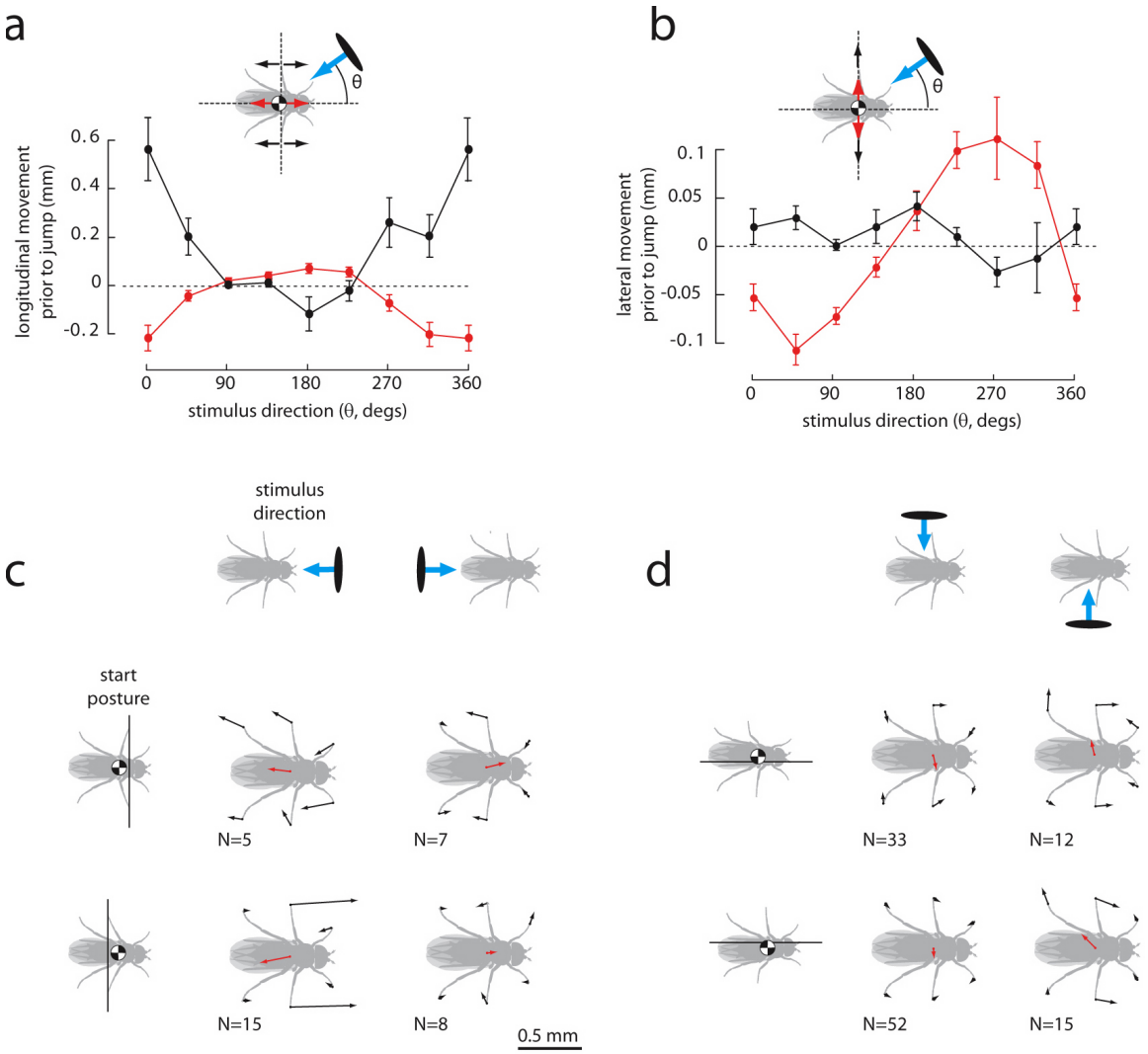

Figure 3.5. Preflight Movements Vary according to Postural State. (A) and (B) Longitudinal and lateral movements (mean ± SEM) of the T2 legs (black) and COM (red) in world frame, prior to the jump as a function of stimulus direction. (C and D) Vectors indicate motions of the legs (black) and COM (red) for different starting positions of the COM relative to the T2 tarsi. (C) shows responses to stimuli approaching from a 90° sector either in front of or behind the fly for flies whose COM at t_0 was either behind (top) or in front of (bottom) a line connecting the T2 tarsi. (D) shows responses to stimuli approaching from a 90° sector either to the left or right of the fly for flies whose COM at t_0 was either to the left (top) or right (bottom) of the midway point on the line connecting the T2 tarsi. The vectors represent the motion of the legs and COM between two time points: t_0 and t_{pre} (see figure 3.3). Each vector represents the vector mean for the indicated number of trials.

the fly's postural state before and during the preflight movements. In this case, a fly would not change its orientation if by chance its body happened to be in the correct posture for a directed escape before the threatening stimulus was detected, whereas the movement would be exaggerated if a fly was out of position when it first observed the stimulus. To test whether preflight motor programs compensate for initial posture, we parsed all takeoff sequences into two categories, those in which the COM was (1) anterior or (2) posterior to the line connecting the T2 tarsi (figure 3.5C). Within these two groups, we examined cases in which the looming disk approached from within the 90° sectors either in front of or behind the animal and measured the motion of each fly's tarsal contacts and COM in world coordinates (figure 3.5C). The results indicate that flies do indeed compensate for the initial posture of the body. The effect of prestimulus posture is most easily seen in the placement of the T2 legs along the anterior-posterior axis in response to stimuli approaching from the front ($\theta = 0°$). If their COM started anterior to the T2 tarsi, flies make a large forward corrective movement with their T2 legs prior to takeoff (figure 3.5C). This forward movement of the legs is accompanied by a backward motion of the body. In contrast, if the COM starts posterior to the T2 legs—closer to the "correct" position for a backward takeoff—the flies make small rearward leg movements. Thus, the polarity of the longitudinal leg motion is dependent on the flies' postural state when the stimulus is detected.

We repeated this analysis to examine motor planning for sideways escapes by parsing sequences according to whether each fly's COM was to the (1) left or (2) right of a longitudinal axis that was perpendicular to the line connecting the T2 tarsi (figure 3.5D). We then compared cases in which the looming stimulus approached from within the 90° sectors from the left or right of the fly. Although the leg movements in preparation for sideways takeoffs are more complicated than for forward or backward takeoffs, the analysis confirmed that a fly's preflight motor program compensates for initial posture. For example, when the disk approaches from the left, flies with a leftward-biased COM exhibit a large postural change to shift their COM to the right, whereas flies with a rightward-biased COM make a much smaller change in COM position. Further, the data show that the preflight motor program is distributed throughout all thoracic neuropils: Although the motion of the T2 legs tends

to be greatest, the pro- (T1) and meta- (T3) thoracic legs also contribute to the preflight postural changes.

We found that the dependence of preflight positioning movements on initial COM position holds at very fine resolution for all stimulus directions. Figure 3.6 shows vector maps of COM movement from each COM starting position for all eight stimulus directions (see Experimental Procedures, section 3.2). The COM movements in each panel appear to converge on a single location, which we suggest represents the target of the escape motor program for that stimulus direction. This interpretation is supported by the locations of the black dots in each panel of figure 3.6. These points, which are replotted from figure 3.4A, are the average COM locations at t_{pre} for trials in which flies jumped within particular 45° sectors. For example, in the top subpanel (light green vector field) in which the stimulus approached from the fly's left, the black dot represents the mean COM location for all jumps in a 45° sector to the right. In this and other subpanels, the movement vectors appear to converge on the COM location that would carry the animal away from the looming stimulus. According to this model, each stimulus position in visual space maps not to a stereotyped motor response, but rather to a COM target location.

A timeline for the various components of the escape behavior, aligned according to the time of takeoff (t_{jump}), is shown in figure 3.7B. The first manifestation of the flies' response to the looming stimulus is the positional changes of their T1 and T3 legs. Flies that were grooming at the time the stimulus was released placed their tarsi down on the platform during this period. Approximately 200 ms later, the flies begin to reposition their T2 legs. Just after the T2 legs start to move, flies start to raise their wings in preparation for takeoff. Prior to takeoff, there is a distinct pause in the motion of the T2 legs, which is followed by their rapid extension to power the jump. Throughout the course of these experiments, we observed many cases in which flies displayed early components of an escape without ever jumping. Out of the 147 individuals tested, five flies exhibited both leg and wing motion but never jumped, three flies moved their legs but never raised their wings or jumped, three flies adjusted only their wings but did not jump, and six flies exhibited no motion at all. The most parsimonious explanation for this behavioral timeline is that early

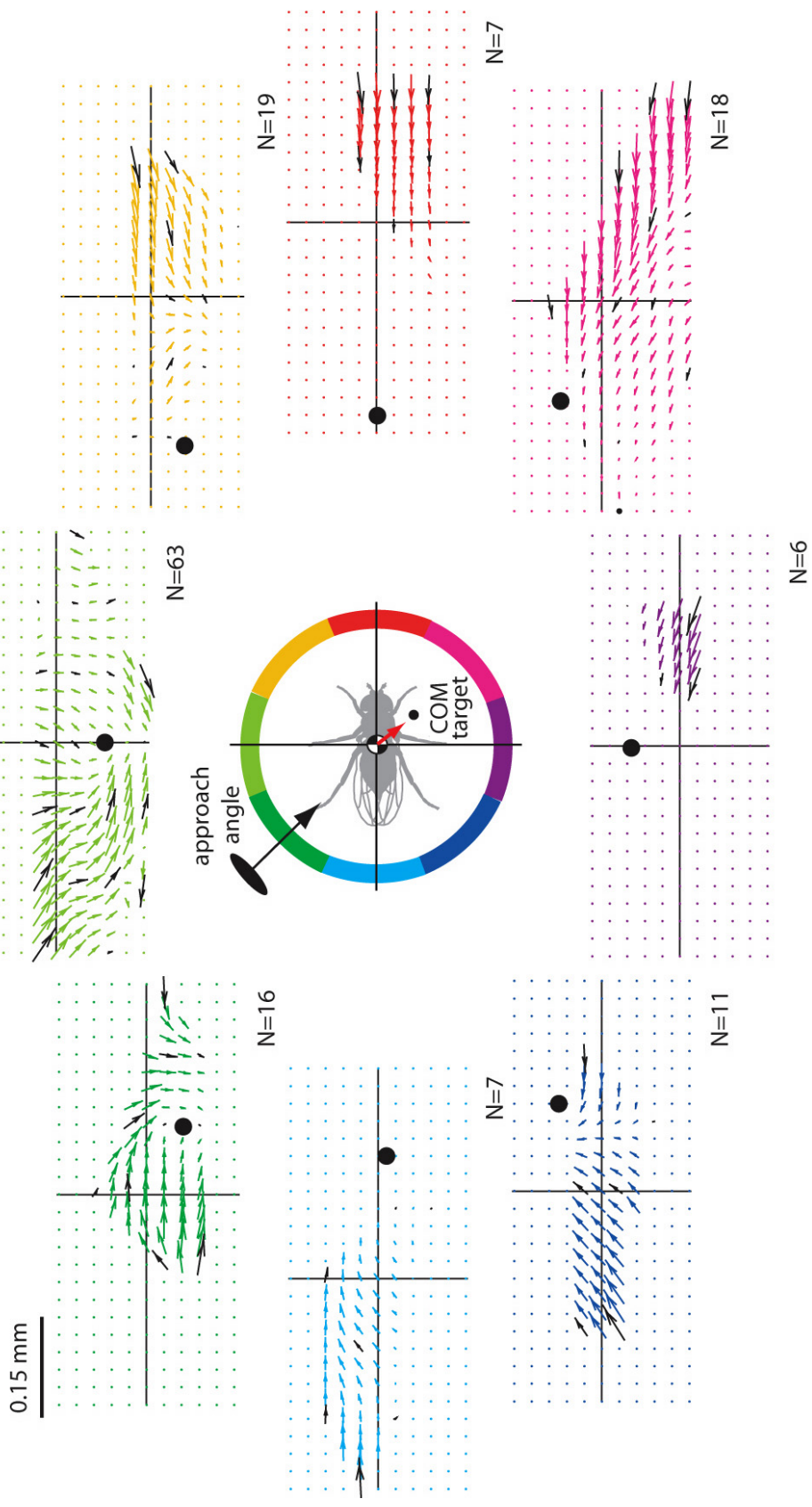

Figure 3.6. Preflight Movements Vary according to Postural State. Vector fields for relative COM motion for eight different stimulus directions (see center icon for color code). The origin of each vector indicates a fly's COM at t_0 relative to the T2 tarsi. Black vectors indicate the vector sum of COM movements, measured between t_0 and t_{pre}, over 0.2×0.1 mm rectangles centered on the vector origin. Colored lines are interpolated (see Experimental Procedures, section 3.2). Vector length is proportional to movement magnitude. Grid points without vectors are starting locations for which we could not interpolate expected movement given the limited data set. The large black circle in each plot represents a target location to which the fly might move its COM in order to jump directly away from the stimulus, determined on the basis of the data in figure 3.4A, which shows the mean location for the COM at t_{pre} for each of the eight relevant jump directions. The number of trials contributing to each vector field is indicated in each panel.

components (e.g., motion of front and back legs) are activated by the looming stimulus at lower thresholds, whereas later components (e.g., wing elevation and jumping) are activated at higher thresholds (figure 3.7C). The model indicates how a sophisticated motor behavior might be constructed from a simple set of separate motor actions (Flash and Hochner, 2005).

3.4 Discussion

We have shown that in response to a threatening stimulus, *Drosophila* exhibit a set of motor actions prior to flight initiation that are responsible for determining the initial direction of the escape. Within approximately 200 ms, the fly estimates the direction of an approaching visual stimulus and encodes a motor program that will move the body into an appropriate position to jump away from the looming threat. This behavior, which effectively plans the direction of takeoff, occurs approximately 100 ms earlier than all previously identified components of the escape response (Card and Dickinson, 2008a; Hammond and O'Shea, 2007a; Trimarchi and Schneiderman, 1995c), and it is not reflexively coupled to flight initiation because a fly can prepare for an escape without taking off. The involvement of all six legs indicates that this motor program coordinates leg movements across all three thoracic segments. The dependency of the behavior on initial postural state suggests that the fly uses either efference copy (Webb, 2004) or proprioceptive feedback in generating the leg-movement commands. Leg proprioceptors and associated local thoracic circuits might be sufficient to provide such feedback (Burrows, 1996), in which case descending commands from the brain might be identical regardless of initial posture. Alternatively, the proprio-

Figure 3.7: A Simple Model for Preflight Motor Planning (A) The cumulative probability of takeoff (indicated by the shaded area) in relation to the time course of increasing stimulus size (indicated by the blue line), $n = 177$. (B) The probability that a particular part of the fly was moving at time points prior to the jump: T1 and T3 legs (black), T2 legs (red), wings (blue), body (gray), $n = 50$. The green line indicates the takeoff itself, in which legs extend rapidly and wings stroke downwards. (C) A simple model for how flies may direct movement of their COM before takeoff. As stimulus energy increases with the increasing visual angle of the looming disk, it crosses the thresholds for different independent motor programs. T1 and T3 leg movement occurs first, indicating that this motor program may have the lowest activation threshold. In a typical backward-jumping sequence, motor commands to reposition the T2 legs are activated next, possibly followed by wing elevation. Finally, when the stimulus energy is very high, rapid leg extension of the middle legs is activated to complete the takeoff sequence.

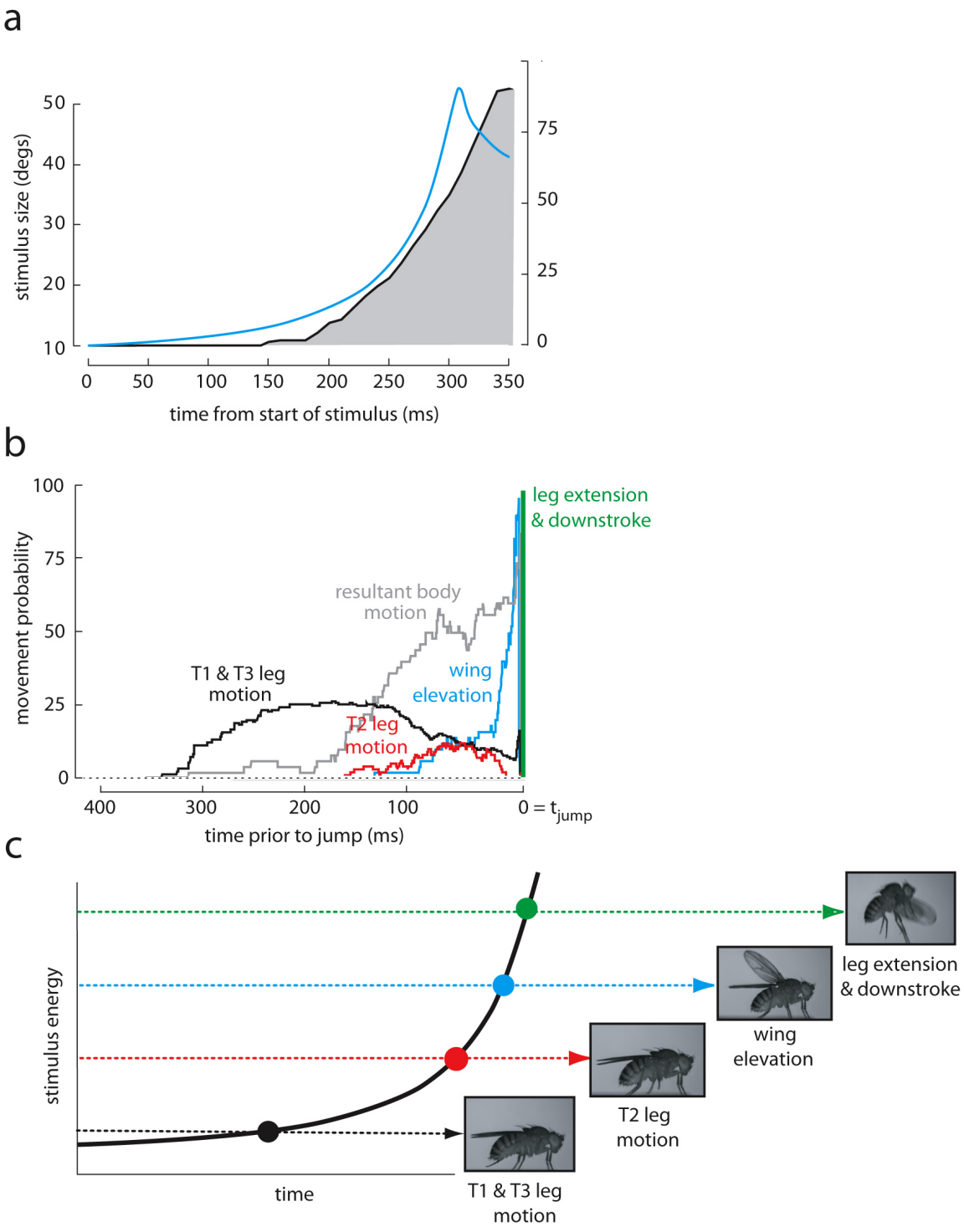

Figure 3.7. See p. 84 for caption.

ceptive feedback might project anteriorly to modify descending commands from the brain according to postural state.

A pair of large-diameter interneurons called the giant fibers (GF) (Levine and Tracey, 1973; Power, 1948; Allen et al., 2006) are thought to trigger visually mediated escape responses in flies by coordinating the rapid bilateral contraction of leg extensor and wing-depressor muscles (King and Wyman, 1980; Tanouye and Wyman, 1980; Lima and Miesenbock, 2005). An as-yet-unidentified small-diameter pathway is activated even earlier in the escape sequence to raise the wings prior to takeoff (Card and Dickinson, 2008a; Hammond and O'Shea, 2007a; Trimarchi and Schneiderman, 1995a). Neither the GF pathway nor the wing-raising pathway, however, could easily explain the behaviors we describe here. GF activation elicits immediate bilateral leg extension and thus could not activate early events within the escape sequence, and the preparatory leg movements occur with a variable delay prior to wing elevation and are thus unlikely to be triggered by the same pathway (figure 3.7). Further, we observed examples of animals shifting leg posture without raising their wings. We conclude that the early planning movements must be triggered by another as-yet-unidentified pathway that conveys visual information to thoracic circuits that control leg motion. This early component of the behavioral sequence presumably increases the effectiveness of escape by directing the animal away from a would-be predator. Such tactics do not guarantee success. For example, a recent comparative study shows how painted redstarts (*Myioborus pictus*) exploit flies' escape behaviors to flush them from the substrate into the air (Jabłoński and Strausfeld, 2001). It is even possible that such a predator might learn to anticipate the direction of the fly's takeoff, although we know of no such evidence.

Some features of this behavior are similar to those that have been described for jumping locusts. Before voluntary jumps, locusts can use motion-parallax cues to aim toward specific visual targets (Wallace, 1959). In response to looming visual objects, locusts exhibit directional "hiding responses," in which they lean their bodies away from the threat to hide behind a post they are grasping (Hassenstein and Hustert, 1999). Locusts can also direct their jumps away from looming stimuli (Santer et al., 2005), although their accuracy is coarser (forward $\pm 50^\circ$) than that reported here for flies, which can direct their jump

in any direction, including backward. The greater accuracy of flies is probably due to the fact that they use agile middle legs to jump, rather than powerful hind legs, and thus need not overcome as much of a biomechanical bias to jump forward as do locusts (Sutton and Burrows, 2008). Both locusts and flies direct their jumps with leg and body motions prior to leg extension. However, in locusts these postural adjustments occur after the start of cocontraction of the extensors and flexors of the femur-tibia joint, whereas the comparable movements of flies are the earliest components of the escape sequence. This sequence of aiming the jump prior to leg extension is possible because flies do not need to cocontract the muscles of their jump legs to store energy before takeoff. With respect to the flies' ability to adjust their escape motor program on the basis of initial position, there is no evidence that locusts compensate for their postural state in planning for jumps. However, locusts do exhibit load compensation (Matheson and Dürr, 2003) in their directed grooming movements (Matheson, 1998), indicating that their targeted leg motions do make use of proprioceptive feedback.

Collectively, the results from studies on flies and locusts suggest that the insect central nervous system is capable of transforming particular azimuthal positions in visual space to a set of spatially targeted trajectories in motor space (figure 3.6). We propose that this information is utilized by the motor system through a set of independent descending pathways with different thresholds of activation (figure 3.7B). A similar model has been suggested for the responses of locusts to looming stimuli, in which an unknown pathway activates early cocontraction of the jumping legs, whereas the descending contralateral movement detector (DCMD) may trigger subsequent events in the jump sequence (Santer et al., 2008). In structure, the fly's escape behavior fulfills the criteria for motor planning, which is considered a hallmark of vertebrate cortex (Wolpert and Ghahramani, 2000). Comparative neuroanatomical studies of insects suggest that such transformations may take place within the central complex (Loesel et al., 2002), a set of evolutionarily ancient midline neuropils in the arthropod brain. In the future, it will be of interest to dissect this behavior with the genetic and physiological approaches that are available in *Drosophila*.

Chapter 4

Conclusions

The previous chapters have described in detail the flight initiation behavior of the fruit fly, *Drosophila melanogaster*. The behavior has been analyzed with respect to both the timing of takeoff behaviors and the mechanical performance achieved by different takeoff sequences. Special attention has been paid to the directional control of escape takeoffs. Below is a summary of the main findings.

4.1 Summary of Findings

The fly uses both its wings and legs during the initiation of flight. First it begins to open and elevate its wings, then it extends its middle legs to push itself off the ground. In "voluntary" takeoffs, the fly raises its wings early before the takeoff jump, ensuring that the wings are unfurled and already stroking as the fly leaves the ground. In contrast, escaping flies start to raise their wings just before leg extension, and as a result, often the wings are still held close to the body when the fly leaves the ground. The fly must then open its wings in the air, resulting in significant wing bending. The takeoff jump is shorter for escaping flies (3 ms) compared to non-escaping flies (5 ms).

There is a trade-off in takeoff performance between the speed and steadiness of initial flight. Voluntary takeoffs tend to be slow and steady, while escapes achieve higher velocities but result in more tumbling once airborne. For both voluntary and escape takeoffs the main

acceleration is provided by the legs during their rapid extension, and the steadiness of initial flight is directly correlated with how early a fly begins to raise its wings before it initiates the takeoff jump. Escaping flies also produce a significant amount of roll velocity during leg extension, and then exhibit a counter roll torque immediately once airborne. This is especially evident in flies whose wings have been removed. These flies rotate continuously about their long body axis once airborne, indicating the roll can be generated by the legs alone, but without wings the fly cannot produce counter roll.

Escaping flies have more kinetic and potential energy than flies taking off voluntarily. For normal escaping flies, this excess energy is manifest in both increased linear and angular velocity compared to voluntary takeoffs, regardless of whether the wings are successfully raised before takeoff. When the wings are clipped, however, more energy is spent rotating the fly, and hence its linear speed is reduced. This indicates that the stabilizing effect of the wings may be advantageous in helping a fly to more rapidly move away from a predator.

Flies can control the direction in which they escape. The direction in which they move during the period of leg extension is a compromise between jumping directly away from a stimulus and jumping forward. Flies can still modulate their escape direction if their wings or their middle (jumping) legs are removed, and visual information from a looming stimulus is sufficient to elicit a directional escape. The fly modulates its takeoff direction by moving its center of mass relative to its two jumping legs before initiating the takeoff jump. To correctly position its center of mass for a sideways jump, the fly leans away from the stimulus, producing large lateral body movements but only small leg movements. To correctly position its center of mass for a forward or backward jump, the fly moves both its middle legs towards the stimulus, and makes only small movements of its body. These prejump movements of the fly are not strictly feed-forward, they take into account feedback about the fly's current position. In fact, regardless of starting posture, it appears that during the prejump movements the fly moves its center of mass towards an "ideal" location relative to the two jumping legs. This "ideal" location is well approximated by the center of mass position that would move the fly directly away from the stimulus during leg extension. Furthermore, the fly's prejump movements are independent of the takeoff jump. They occur

with variable time before the jump, often with 10s of milliseconds between pre-movements and the jump. In some instances, the fly makes prejump movements but then does not takeoff.

4.2 An Emerging Picture of Flight Initiation Control

Previously it was believed that the escape response of *Drosophila* was a hard-wired, stereotyped response that included only leg extension and the start of the flight motor, but my results suggest a new model for flight initiation, of which the actual escape jump is only one part. In this new view, flight initiation is composed of several behavioral modules that may be activated independently. Section 4.2.1 outlines the features of such a "modular" system for flight initiation, and Section 4.2.2 considers what might comprise the neural substrate of a "module."

4.2.1 Behavioral Modules

The idea that complex behaviors may be composed from the coordinated assemblage of simpler behaviors or "modules" is not new. As early as 1911, T. Graham Brown put forward the idea that the rhythmic pattern of limb placement during walking in the cat could be coordinated by alternating activity in limb flexion and extension motor units in the spinal cord (Brown, 1911). Since then, a modular organization of motor units in the spinal cord has been described in several flavors (half-centers, unit bursters, primitives, and muscle synergies) for a range of motor behaviors in the lamprey (Wallén, 1997), turtle (Stein, 2008), mudpuppy (Cheng et al., 1998), frog (Bizzi et al., 1991), and cat (Jordan, 1991; Grillner, 1981; for a review, see Tresch et al., 2002).

In the 1980s Rodney Brooks, a roboticist and computer scientist, demonstrated the efficacy of a modular architecture for behavior by applying the idea to to the building of machines with artificial intelligence (AI). Brooks revolutionized the AI field by suggesting that, rather than building systems that rely on central processing to form a representation of the world and coordinate actions, a better AI design is a layered, heirarchical architecture

of behaviors (Brooks, 1986; Brooks, 1989). One of the initial inspirations for this kind of architecture was the simple yet successful nervous systems of insects (Brooks, 1991). In this kind of system, behaviors were divided into simple, task-specific components, or modules, which were then arranged in layers such that higher layer behaviors (e.g. "find food," "explore") would subsume lower behaviors (e.g. "avoid obstacles," "move forward") when needed. Robots built using this subsumption architecture were the first to demonstrate animal-like speeds in responding to their environment and to autonomously navigate complex, dynamic environments (Brooks, 1989). In addition, lack of central processing meant that less processing power was required to operate these robots (Brooks and Flynn, 1989). The success of robots built using a subsumption architecture suggested that central processing of inputs into a perceptual framework for the world was not necessary for an artificial creature to produce emergent behavior that resembled that of simple insects.

Most recently, the concept of behavioral modules has become popular amongst molecular biologists who want to describe the function of the myriad proteins, DNA, RNA, and other small molecules that they have identified inside cells. Hartwell et al. (1999) have suggested that the critical level of organization at which to understand these molecular components is that of "functional modules," which are collections of molecular components that can be linked to a discrete behavior, such as chemotaxis in bacteria (Stock and Surette, 1996) or mating in yeast (Herskowitz, 1995; Posas et al., 1998).

Thus we see that behavioral modules emerge as an important unit whether behavior is being analyzed from the top down (breaking up complex robot behaviors into smaller components) or the bottom up (identifying the behavior that emerges from the activity of a specific set of molecules or neurons). From the three treatments of the concept described above, we may distill a few general aspects of modular behavior. First, individual modules are a collection of interacting components that directly connect sensory input to motor output. These components may be individual molecules, neurons, or populations of neurons. Second, modules are independent, separated by chemical specificity, physical locality, or, in some cases, time of activity. Third, modules interact with one another, exciting or inhibiting each another to produce the gross behavior of the animal. And finally, a module must be

functional, that is the smallest module must still coordinate some action of the animal.

As behavioral modules seem to be a feature of all organisms, from bacteria, yeast, and insects to the highest vertebrates, it is not surprising that *Drosophila* exhibit behaviors that can be decomposed into smaller modules. What I have demonstrated in the work of this thesis that is surprising, however, is that the real-world escape response of the fruit fly is not itself a single module (the giant fiber pathway), but appears to be composed of a handful of more limited behavioral units.

Instead of considering voluntary and escape takeoffs to be two completely separate "types" as previously suggested (Trimarchi and Schneiderman, 1995c), in a modular view of behavior, activation of one subset of behavioral modules occurs during a voluntary takeoff, and an overlapping subset is activated during escape. The individual modules may have different thresholds for stimulation, which means that a progressively more threatening stimulus, such as a looming disk, would tend to activate them in a consistent order (postural adjustments first, then wing raising, etc.). Still, the variability in timing between activation of the observed behaviors implies that they are independent. In some cases, there may be multiple modules for similar actions between which the fly must choose (e.g., "extend the legs quickly" vs. "extend the legs slowly"). Which module is activated thus determines the performance of the resulting takeoff. In other cases, performance is determined by the relative timing of module activation (e.g., the length of the interval between wing raising and leg extension determines takeoff steadiness). In the case of escape, visual information alone is enough to activate each of the modules, but either the modules themselves or the choice of module incorporates feedback about the current state of the fly.

In this thesis I have catalogued the following behavioral modules: grooming, cessation of grooming (signified by lowering all legs to the substrate), T2 leg motion toward the stimulus, leaning away from the stimulus, opening of the left wing, opening of the right wing, elevation of the left wing, elevation of the right wing, slow leg extension, rapid leg extension, and wing depression. It is possible that the "T2 leg motion" and "leaning" modules are just different manifestations of a more general module that directs the fly to "move [its] center of mass" to a specific location relative to the jumping legs. By incorporating feedback about

the current posture of the fly, this module might then be able to manifest the variety of leg and leaning motions we observe.

4.2.2 Neural Substrate of Behavioral Modules

The central nervous system of the fly is divided into two parts. In the head, the brain contains primary sensory afferents, sensory processing lobes, and central integration areas. A fused ganglion in the thorax is comprised primarily of interneurons and motoneurons, but also receives a large amount of local sensory information. Connecting these two neural structures is a thin bundle of fibers that traverses the neck via the central connective. Most of these fibers carry commands from sensory and integrative brain areas to motoneurons in the thorax. In general, however, these descending neurons (DNs) should not be thought of as command neurons for a specific action or behavior. DNs do not innervate muscles directly (they are not motoneurons) and tend to invade multiple regions of neuropil. Presumably, this means that a single DN contacts many different motoneurons in the thorax. Thus while it may be inappropriate to associate each DN with a single behavior (the GF being a noteable exception), it is likely that signature combinations of DNs are active during specific behaviors. Thus a "behavioral module" might be represented neurally by a code of activated DNs.

Some support for this notion comes from the architecture of DNs observed in blowflies. These flies are larger than *Drosophila* and therefore the anatomy of their nervous system is more easily described. At the same time, their neuroanatomy is very similar to that of *Drosophila*, especially with regard to the giant fiber system (see Section 1.2.7). Milde and Strausfeld (1990) have observed that the descending neurons of *Calliphora vicina* are organized in clusters. Within a cluster, the DNs all have dendritic arbors that integrate information from the same regions of the brain. Individual DNs in a cluster, however, invade very different regions of the thoracic ganglion. For example, the giant fiber belongs to a descending cluster that contains seven other neurons: four giant neurons (the giant fiber, GF; lateral giant, LG; inferior giant, IG; and contralateral giant, CLG), two medium-sized neurons (the ipsilateral giant mimic, IGM; and the contralateral giant mimic, CGM), and

two small-axon fibers (the ipsilateral small neuron and the contralateral small neuron). Each of these descending neurons has dendrites that share at least one dendritic domain with the GF. In some cases, such as the IGM and CGM, their dendrites follow all of those of the GF. All the neurons in this cluster also share all common target in the T2 thoracic neuromere: neuropil areas containing the three motor neurons of the TTM. But there is more diversity in the breadth of their thoracic targets. Whereas the GFs make only limited contacts in the T2 neuromere, the LG additionally send axon collaterals to the T1 neuromere, and the CLG, IGM, and CGM make connections in all three leg neuromeres. The IG has the most complex terminus, branching bilaterally to extend terminals throughout the entire thoracic ganglia. Both the IG and the IGM extend dorsally into the neuropil of indirect flight muscles.

Clearly the GFs are not alone in relaying visual and mechanosensory information to motor circuits. Rather they are one component of a group of cells that integrate similar sensory information and drive a variety of actions. It is possible that the slightly different dendritic arborizations of the different DNs within a cluster lend each DN a different thresholds to activation, or that a stimulus such as a looming object will activate different DNs at different times. This would be a system in which a pattern of incoming sensory information could trigger different actions in a sequence. In this case a behavioral module is represented by a specific combination of DNs in a cluster that are activated at the same time to coordinate leg or wing movements in response to a looming stmulus.

4.3 Similar Architecture in Other Systems

The modular system hypothesized above for flight initiation in *Drosophila* is similar in structure to the control of escape responses found in other organisms. The crayfish tail-flip, cockroach cercal wind response, goldfish C-start, and leech shortening and swimming behaviors are all controlled by networks of modules, each tuned to respond to threatening stimuli from a particular direction and to generate motor responses that move the animal in the opposite direction. These directional circuits, which span sensory input to motor

output using a unique subset of neurons, can each be thought of as a behavioral module. For example, the crayfish has separate giant interneurons, medial and lateral, that mediate backwards and forwards escape swimming respectively (Edwards et al., 1999). In the cockroach, the paired ventral giant interneurons are wired to three different classes of thoracic interneuron that either receive bilateral sensory input from wind-sensitive hair cells, or input from hair cells on either the left or right side of the animal only. These thoracic interneurons then connect to leg motor circuits and drive an escape turn away from a sharp puff of air (Ritzmann and Eaton, 1997). The Mauthner cells in the brainstem of the goldfish are perhaps the best known escape neurons. Each one of the bilateral pair mediates a rapid turn response on the contralateral side of the body (Ritzmann and Eaton, 1997). Finally, in the leech, stimulation at the anterior end of an isolated nerve cord preparation triggers the shortening motor circuit, while stimulation at the posterior end activates the crawling motor circuit (Kristan et al., 2005).

A further similarity of some of these systems to our hypothesized architecture for fly escape is the use of a combination of both giant fiber and non-giant fiber mediated modules. In the crayfish system, the lateral and medial giant interneurons are only activated in response to abrupt simuli. Slower or less salient stimulation prompts a graded avoidance turn that is coordinated by selective activation of a population of fast flexor motor neurons withought giant interneuron activation (Edwards et al., 1999). The C-start of the fish can also be coordinated by alternate pathways not requiring Mauthner cell activation. One hypothesis is that one population of reticulospinal neurons controls the initial turn away from the stimulus, while another population of reticulospinal neurons controls the following counterturn. These pathways can work in tandem with Mauthner cell activity, and activation of additional cells which are the segmental homologues to the Mauthner cells, to generate the variability in escape responses observed. As in the system I describe for the fly, the performance of the goldfish escape system (in this case measured by escape direction) is determined by the selection of which behavioral module to activate (Mauthner cell or reticulospinal cells) and by the relative timing of module activation (timing between the initial turn and the counter turn; Ritzmann and Eaton, 1997).

A feature of the *Drosophila* escape system that seems to be unique among the examples described is the sequential activation of the response modules and how early in the response the fly begins to prepare. Goldfish are known to execute two sequential turns (the initial turn and the counterturn) during escape, but in this case the second behavior (counterturn) occurs after the escape movement (turn). I found that the fly performed a series of behaviors (cessation of grooming, leg and body placement, wing opening) before the main escape motion (jump). This sequence more closely resembles the responses of locusts to looming stimuli. In response to a looming disk, locusts first flex their hind legs, then cocontract the muscles that flex and extend the femur in order to store power. Finally, they rapidly extend their rear legs for the escape jump. During the periods of co-contraction and leg extension, locusts can position their forelegs so as to bias the direction of their jump away from the stimulus (Santer et al., 2005). Whereas the locust is only able to bias its jump slightly around the forward direction ($\pm 50^{\circ}$), however, the fly can jump in any direction.

4.4 The Unanswered Question: What Role Does the GF Play?

Though fly escape involves many behaviors that are clearly not mediated by the giant fibers, the modular architecture we have outlined leaves open the possibility that the GFs may still play a role in fruit fly escape. For example, other pathways might coordinate preliminary movements directing the fly's center of mass and preparing the wings for flight. Then, if the stimulus continues to be threatening, the GFs could be triggered to release the takeoff jump. There is evidence that this is unlikely to be the case. In houseflies (*Musca domestica*) a looming disk stimulus that causes free flies to initiate flight fails to elicit a spike in the TTM of tethered flies (Holmqvist, 1994). A new study indicates that this is also the case in *Drosophila* (Fotowat et al., 2008). And we know that both leg extension and flapping flight can commence without GF activity (Trimarchi and Schneiderman, 1995a). The TTMn appears to have arborizations in the thoracic ganglia beyond its direct contact with the GF, and so undoubtably receives input from other descending neurons. In addition to the TTMn,

the TTM is also innervated by two other small motor neurons whose inputs are unknown. In blowflies, other descending fibers that receive sensory information similar to that input to the GFs terminate in the neuropil shared by all three of the TTM motor neurons. Yet though this evidence shows the GFs are not necessary to produce the escape jump, this is not proof that, in unrestrained flies, under different visual stimulation regimes they are not activated. One study suggests that this may indeed be the case. If *shaking-B* flies, which have disrupted GF connections, are presented with a physical looming disk stimulus, they show abnormal escape responses compared to wild type. Leg extension is either delayed or absent, and the flies occasionally attempt to take off using only the flapping of their wings (Hammond and O'Shea, 2007b). Yet voluntary takeoffs are normal. These results suggest that the GF pathways is being used during escape in wild type flies, though it is possible that *shaking-B* flies have other neural defects that affect descending pathways other than just the GFs. Still, it seems unlikely that the giant fiber pathway persists in the central nervous system of the fly if it is entirely unused. Further experiments either monitoring GF activity in response to a wider range of stimuli or modulating it using molecular genetic techniques are required to ascertain what natural stimuli activate it.

4.5 The Role of Neuromodulation

I have hypothesized in the modular behavior model that there could be different modules for similar behaviors such as "fast extension" or "slow extension" of the jumping legs. The anatomy suggests, for example, that these modules could be represented by different descending pathways, one of which innervated the TTMn, a large motor neuron with extensive articulation amongst the TTM fibers, and the other which contacted one of the smaller motor neurons innervating the TTM. These motor neurons are not as well described as the TTM, but in my hypothesized system could excite fewer of the TTM fibers directly, leading to a more prolonged and potentially less forceful muscle contraction.

However, there is an alternative hypothesis for how similar actions of this kind may be differentiated. Neuromodulators, such as octopamine, can act at a neuromuscular junction

to increase the incoming motor neuron signal. For example, octopamine is known to increase the power of muscle contraction in the flight muscles of the locust (Malamud et al., 1988; Stevenson and Meuser, 1997; Duch et al., 1999). In *Drosophila*, Zumstein et al. (2004) have shown that mutants that lack octopamine can only produce half as much force in their TTM jumping legs as compared to wild-type. These flies also cannot jump as far. Thus an alternative possibility is that, rather than multiple pathways, leg extension is mediated by a single descending pathway that is modulated by octopamine.

4.6 Future Directions

The flight initiation system of *Drosophila* provides a unique opportunity to assess how different components of the takeoff circuit, or different behavioral modules, affect the biomechanical performance of the animal. Many questions regarding the biomechanics of takeoff require further investigation. How do the wings provide stability at the start of takeoff, even when they are not open? How much lift do the wings contribute when they are open and flapping during the takeoff jump? Is there active control of escape direction by the mesothoracic legs during extension? How do flies recover from the tumbling initiated during escape jumps, and is this recovery visually mediated, haltere-controlled, or do the ocelli have a role?

On the neural side, the work presented here is a first step toward "cracking" the behavioral circuit that controls flight initiation in the fly. However, it is already very suggestive of which cells previously described in larger flies are likely to be involved. Future work should look for these cells in *Drosophila* and take advantage of the molecular genetic techniques available in the fruit fly to selectively activate or silence them during free behavior. Such an approach will hopefully move us closer toward understanding the secrets of how brains work.

Appendix A

Species List for cervical connective sections

Full species identification for cervical connective cross-section images taken by David King (King, 2007), as shown in figure 1.3.

	Species	Determined by (source)
Row 1		
Tipulidae	*Tipula bicornis* Forbes	GW Byers, Univ. Kansas
Psychodidae	*Psychoda* sp.	FC Thompson, SEL USDA
Tabanidae	*Tabanus calens* Linneaus	DW Webb, IL Nat. Hist. Surv.
Rhagionidae	*Rhagio mystaceus* (Macquart)	RV Peterson, SEL USDA
Row 2		
Asilidae	*Diogmites misellus* Loew	FC Thompson, SEL USDA
Bombyliidae	*Poecilanthrax* sp.	DG King
Bombyliidae	*Sparnopolius* sp.	DG King
Empididae	*Rhamphomyia* sp.	FC Thompson, SEL USDA
Row 3		
Dolichopodidae	*Condylostylus sipho* (Say)	FC Thompson, SEL USDA
Syrphidae	*Helophilus fasciatus* Walker	FC Thompson, SEL USDA
Micropezidae	*Rainieria antennaepes* (Say)	AL Norrbom, SEL USDA
Lauxaniidae	*Minettia magna* (Coquillett)	AL Norrbom, SEL USDA
Sphaeroceridae	*Copromyza equina* Fallén	AL Norrbom, SEL USDA

	Species	Determined by (source)
Row 4		
Drosophilidae	*Drosophila melanogaster*	EM courtesy J. Coggshall
(Drosophilidae)		
Ephydridae	*Ochthera* sp.	WN Mathis, SEL USDA
Row 5		
Anthomyiidae	*Delia platura* (Meigen)	FC Thompson, SEL USDA
Muscidae	*Muscina pascuorum* (Meigen)	RJ Gagne, SEL USDA
Muscidae	*Musca domestica* Linnaeus	(Carolina Biol. Supply Co.)
Glossinidae	*Glossina morsitans* Newstead	(Tsetse Research Lab, Bristol)
Row 5		
Glossinidae	*Glossina morsitans* Newstead	(Tsetse Research Lab, Bristol)
Sarcophagidae	*Sarcophaga bullata* Parker	(Carolina Biol. Supply Co.)
Tachinidae	*Archytas apicifer* (Walker)	NE Woodley, SEL USDA
(Cuttlefish)		

Appendix B

Kine

B.1 What is Kine?

Kine [Kee·nay] is a Graphical User Interface (GUI) that enables the user to determine the coordinates of objects captured in a video sequence. Kine relies on the Digital Linear Transform (DLT) method to calibrate two or more camera views in order to extract the coordinates in three dimensions. Kine was written in Matlab (The Mathworks, Natick, MA) by G. Card, and was inspired by a similar program by Stephen Fry and incorporates functions written by Will Dickson.

B.1.1 Kine is a Hand-digitization Program

Kine does not currently incorporate any automatic tracking of video features. This makes Kine flexible enough to use with any properly calibrated video sequence. There are no requirements for lighting, field of view, size of object, etc. Future development of Kine will add some basic tracking features that are compatible with common uses of the program. For example, a program written by Ebraheem Fontaine (Fontaine, et al., 2008, in preparation) to automatically track the body and wing kinematics of fruit flies during flight initiation currently uses Kine to hand digitize a starting position for the animal. This program could be incorporated to be run by the user directly from Kine.

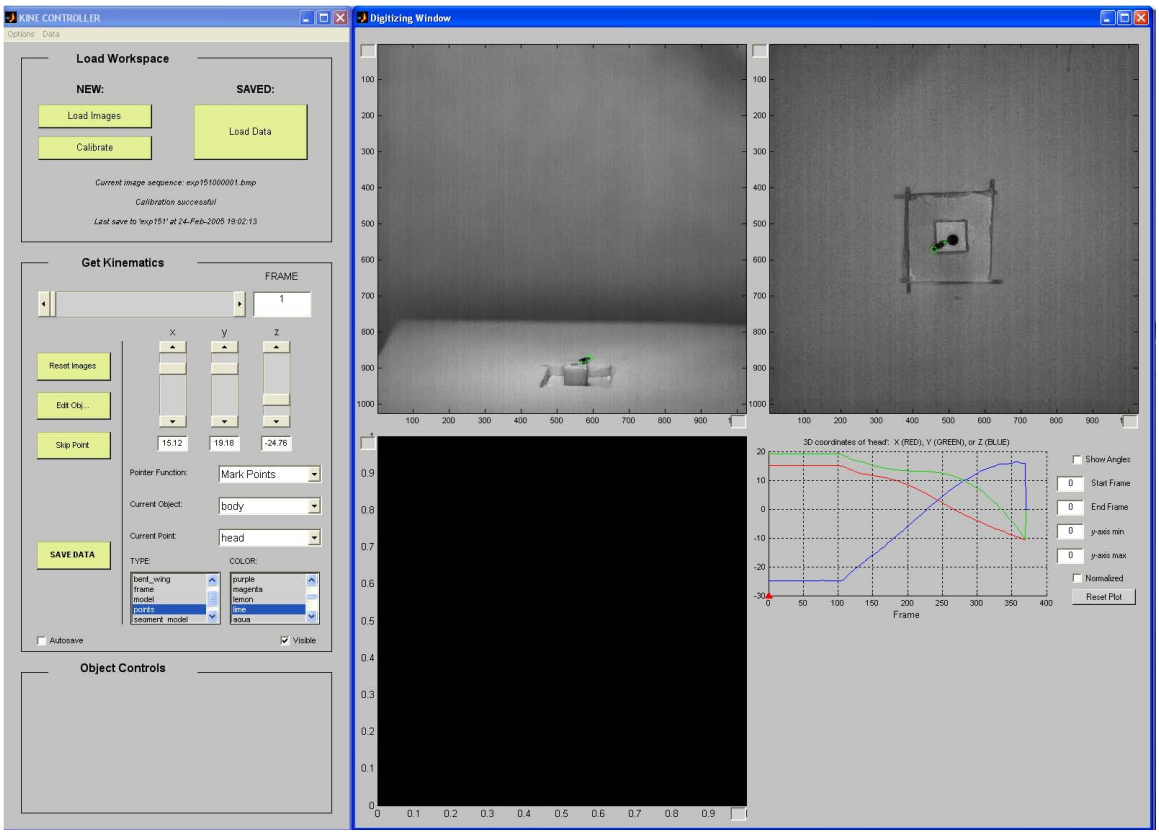

Figure B.1. A Screen shot of "Kine," a hand-digitization GUI I programmed in Matlab.

B.1.2 Kine Offers a Flexible, Object-based Platform

The main advantage of Kine over other hand-digitization software is its object-based structure, which permits the creation of a large range of objects that can be digitized. Users can either click on individual points of interest in their video images, or they can group these points together in "objects." Objects are defined with a set of parameters whose values are assigned by the user. For example, the user can create an object of type "model" that is composed of the two points "wing-hinge" and "wing-tip." Once these two points are defined, Kine then uploads a model frame specified by the user (in this case, a 2D wing shape), and the user can adjust any parameters associated with the model (in this case, angle of attack). Kine already has programs for several different types of object installed, but, in addition, users can easily incorporate new object modules written in Matlab to aid

rapid digitization of objects to fit their specific task.

B.2 How Does Kine Work?

Kine strives to make hand digitizing as efficient as possible for the user by minimizing the number of actions required to digitize a given point or object. To determine the 3D coordinates of a point from a calibrated video, the user clicks on a view of that point (e.g., the tip of the fly wing) in one of the camera images. Kine then projects this point as a line in all the remaining camera views. The point is resolved when the user clicks on the object in a second camera view.

B.3 Kine Features

- Manual digitization of objects in 3D using multiple camera views.
- Object-based environment allows the user to create digitization object protocols for rapid digitization of novel structures.
- Visual feedback is provided to the user in three ways: 1) Digitized objects can be drawn on top of the images in all camera views; 2) The 3D coordinates of the current point are plotted as a time course for all the frames in the sequence; 3) Digitized objects can also be shown in a body-centered view.

Bibliography

Abdel-Aziz Y, Karara H (1971) Direct linear transformation from comparator coordinates into object space coordinates in close-range photogrammetry. In: *Proceedings of the Symposium on Close-Range Photogrammetry,* pp 1-18. Urbana, Illinois.

Allen MJ, Drummond JA, Moffat KG (1998) Development of the giant fiber neuron of *Drosophila melanogaster*. *J Comp Neurol* 397:519–531.

Allen MJ, Godenschwege TA, Tanouye M, Phelan P (2006) Making an escape: Development and function of the *Drosophila* giant fibre system. *Semin Cell Dev Biol* 17:31–41.

Allen MJ, Shan X, Caruccio P, Froggett SJ, Moffat KG, Murphey RK (1999) Targeted expression of truncated glued disrupts giant fiber synapse formation in *Drosophila*. *J Neurosci* 19:9374–9384.

Andersen RA, Burdick JW, Musallam S, Pesaran B, Cham JG (2004) Cognitive neural prosthetics. *Trends in Cognitive Sciences* 8:486–93.

Armstrong JD, Texada MJ, Munjaal R, Baker DA, Beckingham KM (2006) Gravitaxis in *Drosophila melanogaster*: A forward genetic screen. *Genes Brain Behav* 5:222–239.

Bacon JP, Strausfeld NJ (1986) The Dipteran 'giant fibre'pathway: Neurons and signals. *J Comp Physiol A* 158:529–548.

Baird DH, Schalet AP, Wyman RJ (1990) The *Passover* locus in *Drosophila melanogaster*: Complex complementation and different effects on the giant fiber neural pathway. *Genetics* 126:1045–1059.

Balint CN, Dickinson MH (2001) The correlation between wing kinematics and steering muscle activity in the blowfly *Calliphora vicina*. *J Exp Biol* 204:4213–4226.

Balint CN, Dickinson MH (2004) Neuromuscular control of aerodynamic forces and moments in the blowfly, *Calliphora vicina*. *J Exp Biol* 207:3813–3838.

Bauer R, Loer B, Ostrowski K, Martini J, Weimbs A, Lechner H, Hoch M (2005) Intercellular communication: The Innexin multiprotein family of gap junction proteins. *Chem Biol* 12:515–526.

Bennet-Clark HC, Ewing A (1968) The wing mechanism involved in the courtship of *Drosophila*. *J Exp Biol* 49:117–128.

Benshalom G, Dagan D (1985) *Drosophila* neural pathways. *J Comp Physiol A* 156:13–23.

Bizzi E, Mussa-Ivaldi FA, Giszter S (1991) Computations underlying the execution of movement: A biological perspective. *Science* 253:287–291.

Blagburn JM, Alexopoulos H, Davies JA, Bacon JP (1999) Null mutation in *shaking-B* eliminates electrical, but not chemical, synapses in the *Drosophila* giant fiber system: A structural study. *J Comp Neurol* 404:449–458.

Boettiger E (1960) Insect flight muscles and their basic physiology. *Annu Rev Entomol* 5:1–16.

Boettiger E, Furshpan E (1952) The mechanics of flight movements in Diptera. *Biol Bull* 102:200–211.

Borst A, Haag J (2002) Neural networks in the cockpit of the fly. *J Comp Physiol A* 188:419–437.

Brand AH, Perrimon N (1993) Targeted gene expression as a means of altering cell fates and generating dominant phenotypes. *Development* 118:401–415.

Briggman KL, Abarbanel HDI, Kristan WB (2006) From crawling to cognition: Analyzing the dynamical interactions among populations of neurons. *Curr Opin Neurobiol* 16:135–144.

Brooks R (1986) A robust layered control system for a mobile robot. *Robotics and Automation* RA-2:14–23.

Brooks R (1989) A robot that walks; Emergent behaviors from a carefully evolved network. *Neural Comput* 1:253–262.

Brooks R (1991) How to build complete creatures rather than isolated cognitive simulators. In: *Architectures for Intelligence* (VanLehn K, ed), pp 225-239. Hillsdale, NJ: Lawrence Erlbaum Associates.

Brooks R, Flynn A (1989) Fast, cheap, and out of control: A robot invasion of the solar system. *J Brit Inter Soc* 42:478–485.

Brown TG (1911) The intrinsic factors in the act of progression in the mammal. *P R Soc B* 84:308–319.

Budick SA, Dickinson MH (2006) Free-flight responses of *Drosophila melanogaster* to attractive odors. *J Exp Biol* 209:3001–3017.

Bullock T (1984) Comparative neuroethology of startle, rapid escape, and giant fiber-mediated responses. In: *Neural Mechanisms of Startle Behavior* (Eaton R, ed), 1-13. New York, NY: Plenum Press.

Bullock T, Horridge G (1965). *Structure and Function in the Nervous Systems of Invertebrates,* vol. 1-2. San Francisco, CA: W.H. Freeman.

Burkhardt D (1960) Action potentials in the antennae of the blowfly (*Calliphora erythrocephala*) during mechanical stimulation. *J Insect Physiol* 4:138–145.

Burrows M (1996). *The Neurobiology of an Insect Brain.* Oxford, New York: Oxford University Press.

Card G, Altshuler D, Dickinson MH (2005) A directional escape response in *Drosophila melanogaster*. *Society for Neuroscience* Program No. 176.14, Washington, D. C.

Card G, Dickinson MH (2008a) Performance trade-offs in the flight initiation of *Drosophila*. *J Exp Biol* 211:341–353.

Card G, Dickinson MH (2008b) Visually mediated motor planning in the escape response of *Drosophila*. *Curr Biol* 18:1300–1307.

Certel SJ, Savella MG, Schlegel DCF, Kravitz EA (2007) Modulation of *Drosophila* male behavioral choice. *Proc Natl Acad Sci USA* 104:4706–4711.

Cheng J, Stein R, Jovanovic K, Yoshida K (1998) Identification, localization, and modulation of neural networks for walking in the mudpuppy (*Necturus maculatus*) spinal cord. *J Neurosci* 18:4295–4304.

Claparede E (1869) Histologische untersuchungen über den regenwurm (*Lumbricus terrestris*). *Z Wiss Zool* 19:163–205.

Coggeshall RE, Coulter JD, Willis WD (1973) Unmyelinated fibers in the ventral root. *Brain Res* 57:229–233.

Coggshall JC (1978) Neurons associated with the dorsal longtitudinal flight muscles of *Drosophilla melanogaster*. *J Comp Neurol* 177:707–720.

Dagan D, Parnas I (1970) Giant fibre and small fibre pathways involved in the evasive response of the cockroach, *Periplaneta americana*. *J Exp Biol* 52:313–324.

David CT (1979) Optomotor control of speed and height by free-flying *Drosophila*. *J Exp Biol* 82:389–392.

Dickinson MH, Tu M (1997) The function of Dipteran flight muscle. *Comp Biochem Phys A* 116A:223–238.

Duch C, Mentel T, Pflüger HJ (1999) Distribution and activation of different types of octopaminergic DUM neurons in the locust. *J Comp Neurol* 403:119–134.

Duffy JB (2002) GAL4 system in *Drosophila*: A fly geneticist's swiss army knife. *genesis* 34:1–15.

Eaton RC (1984). *Neural Mechanisms of Startle Behavior.* New York, NY: Plenum Press.

Eberl DF, Boekhoff-Falk G (2007) Development of Johnston's organ in *Drosophila*. *Int J Dev Biol* 51:679–687.

Eberl DF, Hardy RW, Kernan MJ (2000) Genetically similar transduction mechanisms for touch and hearing in *Drosophila*. *J Neurosci* 20:5981–5988.

Edwards DH, Heitler WJ, Krasne FB (1999) Fifty years of a command neuron: The neurobiology of escape behavior in the crayfish. *Trends Neurosci* 22:153–161.

Elliott C, Brunger HL, Stark M, Sparrow JC (2007) Direct measurement of the performance of the *Drosophila* jump muscle in whole flies. *Fly* 1:68–74.

Engel JE, Wu CF (1996) Altered habituation of an identified escape circuit in *Drosophila* memory mutants. *J Neurosci* 16:3486–3499.

Engel JE, Wu CF (1998) Genetic dissection of functional contributions of specific potassium channel subunits in habituation of an escape circuit in *Drosophila*. *J Neurosci* 18:2254–2267.

Engel JE, Xie X, Sokolowski M, Wu CF (2000) A cGMP-dependent protein kinase gene, foraging, modifies habituation-like response decrement of the giant fiber escape circuit. *Learning & Memory* 7:341–352.

Fan SF, Hsu K, Chen FS, Hao B (1961) On the high conduction velocity of the giant nerve fiber of shrimp, *Penaeus orientalis*. *Kexue Tongbao* 4:160–172.

Fayyazuddin A, Zaheer MA, Hiesinger PR, Bellen HJ (2006) The nicotinic acetylcholine receptor Dalpha7 is required for an escape behavior in *Drosophila*. *Plos Biol* 4:422–431.

Flash T, Hochner B (2005) Motor primitives in vertebrates and invertebrates. *Curr Opin Neurobiol* 15:660–666.

Fotowat H, Fayyazuddin A, Bellen HJ, Gabbiani F (2008) A novel neuronal pathway for visually guided escape in *Drosophila*. *Society for Neuroscience* Program No. 198.17, Washington, DC.

Franz MO, Krapp HG (2000) Wide-field, motion-sensitive neurons and matched filters for optic flow fields. *Biol Cybern* 83:185–197.

Friedländer B (1889) Über die markhaltigen nervenfasern und neurochorde der crustaceen und anneliden. *Mitt. Zool. Sta. Neapel* 9:205–265.

Fry SN, Sayaman R, Dickinson MH (2003) The aerodynamics of free-flight maneuvers in *Drosophila*. *Science* 300:495–498.

Fry SN, Sayaman R, Dickinson MH (2005) The aerodynamics of hovering flight in *Drosophila*. *J Exp Biol* 208:2303–2318.

Gilbert C, Strausfeld NJ (1991) The functional organization of male-specific visual neurons in flies. *J Comp Physiol A* 169:395–411.

Glasscock E, Tanouye MA (2005) *Drosophila couch potato* mutants exhibit complex neurological abnormalities including epilepsy phenotypes. *Genetics* 169:2137–2149.

Grillner S (1981) Control of locomotion in bipeds, tetrapods, and fish. In: *Handbook of Physiology,* vol. 2 (Brooks VB, ed), pp 1179-1236. Bethesda, MD: American Physiological Society.

Gronenberg W, Strausfeld NJ (1990) Descending neurons supplying the neck and flight motor of Diptera: Physiological and anatomical characteristics. *J Comp Neurol* 302:973–991.

Hammond S, O'Shea M (2007a) Escape flight initiation in the fly. *J Comp Physiol A* 193:471–416.

Hammond S, O'Shea M (2007b) Ontogeny of flight initiation in the fly *Drosophila melanogaster*: Implications for the giant fibre system. *J Comp Physiol A* 193:1125–1137.

Hartline D, Colman D (2007) Rapid conduction and the evolution of giant axons and myelinated fibers. *Curr Biol* 17:R29–R35.

Hartwell LH, Hopfield JJ, Leibler S, Murray AW (1999) From molecular to modular cell biology. *Nature* 402:C47–C52.

Harvey J, Brunger H, Middleton CA, Hill JA, Sevdali M, Sweeney ST, Sparrow JC, Elliott C (2008) Neuromuscular control of a single twitch muscle in wild type and mutant *Drosophila*, measured with an ergometer. *Invert Neurosci* 8:63–70.

Hassenstein B, Hustert R (1999) Hiding responses of locusts to approaching objects. *J Exp Biol* 202(Pt12):1701–1710.

Hassler S (2008) Winged vitory: Fly-size wing flapper lifts off. *Spectrum, IEEE* 45:9.

Hausen K (1984) The lobula-complex of the fly: Structure, function and significance in visual behaviour. In: *Photoreception and Vision in Invertebrates* (Ali MA, ed), pp 523-559. New York, NY: Plenum Press.

Hegde AN, Diantonio A (2002) Ubiquitin and the synapse. *Nat Rev Neurosci* 3:854–861.

Heide G (1968) Flight control by non-bibrillar (direct) flight muscles in the blowfly *Calliphora*. *Z vergl Physiol* 59:456–460.

Heide G (1971) Die funktion der ruchtnbrillaren flugmuskeln von *Calliphora*. Teil I. Lage, insertionsstellen und innervierungsmuster der muskeln. *Zool Jb (Physiol)* 76:87–98.

Herskowitz I (1995) MAP kinase pathways in yeast: For mating and more. *Cell* 80:187–197.

Hicke L (2001) A new ticket for entry into budding vesicles—Ubiquitin. *Cell* 106:527–530.

Hodgkin A (1954) A note on conduction velocity. *J Physiol (Lond)* 125:221–224.

Hodgkin A, Huxley A (1939) Action potentials recorded from inside a nerve fibre. *Nature* 144:710–711.

Holmqvist MH (1994) A visually elicited escape response in the fly that does not use the giant fiber pathway. *Vis Neurosci* 11:1149–1161.

Holmqvist MH, Srinivasan MV (1991) A visually evoked escape response of the housefly. *J Comp Physiol A* 169:451–459.

Homyk T, Szidonya J, Suzuki DT (1980) Behavioral mutants of *Drosophila melanogaster*. III. Isolation and mapping of mutations by direct visual observations of behavioral phenotypes. *Mol Gen Genet* 177:553–565.

Hummon MR, Costello WJ (1987) Induced disruption in the connectivity of an identified neuron in the *Drosophila* ts mutant *shibire*. *J Neurosci* 7:3633–3638.

Hummon MR, Costello WJ (1989) Giant fiber activation of flight muscles in *Drosophila*: Asynchrony in latency of wing depressor fibers. *J Neurobiol* 20:593–602.

Hursh J (1939) Conduction velocity and diameter of nerve fibers. *Am J Physiol* 127:131–139.

Ikeda K, Koenig JH, Tsuruhara T (1980) Organization of identified axons innervating the dorsal longitudinal flight muscle of *Drosophila melanogaster*. *J Neurocytol* 9:799–823.

Ikeda K, Ozawa S, Hagiwara S (1976) Synaptic transmission reversibly conditioned by single-gene mutation in *Drosophila melanogaster*. *Nature* 259:489–491.

Jabłoński PG, Strausfeld NJ (2001) Exploitation of an ancient escape circuit by an avian predator: Relationships between taxon-specific prey escape circuits and the sensitivity to visual cues from the predator. *Brain Behav Evol* 58:218–240.

Jacobs K, Todman MG, Allen MJ, Davies JA, Bacon JP (2000) Synaptogenesis in the giant-fibre system of *Drosophila*: Interaction of the giant fibre and its major motorneuronal target. *Development* 127:5203–5212.

Johnson G (1924) Giant nerve fibers in crustaceans with special reference to *Cambarus* and *Palaemonetes*. *J Comp Neurol* 36:323–373.

Johnson G (1926) Studies on the functions of the giant nerve fibers of crustaceans, with special reference to *Cambarus* and *Palaemonetes*. *J Comp Neurol* 42:19–33.

Jordan L (1991) Brainstem and spinal cord mechnanisms for the initiation of locomotion. In: *Neurological Basis of Human Locomotion* (Shimamura M, Grillner S, Edgerton VR, eds), pp 3-20. Tokyo, Japan: Japan Scientific Societies Press.

Josephson RK (2006) Comparative physiology of insect flight muscle. In: *Nature's Versatile Engine: Insect Flight Muscle Inside and Out* (Vigoreaux JO, ed), pp 34-43. Georegetown, TX: Landes Bioscience.

Kaas JH, Collins CE (2004). *The Primate Visual System.* Boca Raton, FL: CRC Press.

Kamikouchi A, Shimada T, Ito K (2006) Comprehensive classification of the auditory sensory projections in the brain of the fruit fly, *Drosophila melanogaster*. *J Comp Neurol* 499:317–356.

Kaplan WD, Trout WE (1974) Genetic manipulation of an abnormal jump response in *Drosophila*. *Genetics* 77:721–739.

Katsov A, Clandinin T (2008) Motion processing streams in *Drosophila* are behaviorally specialized. *Neuron* 59:322–335.

Kern R, Petereit C, Egelhaaf M (2001) Neural processing of naturalistic optic flow. *J Neurosci* 21:RC139.

King DG (1983) Evolutionary loss of a neural pathway from the nervous system of a fly (*Glossina morsitans*/Diptera). *J Morphol* 175:27–32.

King DG (2007) What's so special about giant fibers? Presented at: *National Evolutionary Synthesis Center Catalysis Meeting Duke University,* September 16-19. Available at: www.zoology.siu.edu/king/DGKing-GiantFibers.ppt.

King DG, Tanouye M (1983) Anatomy of motor axons to direct flight muscles in *Drosophila*. *J Exp Biol* 105:231–239.

King DG, Valentino KL (1983) On neuronal homology: A comparison of similar axons in *Musca*, *Sarcophaga*, and *Drosophila* (Diptera: Schizophora). *J Comp Neurol* 219:1–9.

King DG, Wyman RJ (1980) Anatomy of the giant fibre pathway in *Drosophila*. I. Three thoracic components of the pathway. *J Neurocytol* 9:753–770.

Knudsen EI, Konishi M (1978) A neural map of auditory space in the owl. *Science* 200:795–797.

Koto M, Tanouye M, Ferrus A, Thomas J, Wyman RJ (1981) The morphology of the cervical giant fiber neuron of *Drosophila*. *Brain Res* 221:213–217.

Krapp HG, Hengstenberg B, Hengstenberg R (1998) Dendritic structure and receptive-field organization of optic flow processing interneurons in the fly. *J Neurophysiol* 79:1902–1917.

Krieger R (1879) Ueber das centralnervensystem des flusskrebses. *Z Wiss Zool* 33:527–594.

Krishnan SN, Frei E, Swain GP, Wyman RJ (1993) *Passover*: A gene required for synaptic connectivity in the giant fiber system of *Drosophila*. *Cell* 73:967–977.

Kristan WB, Calabrese RL, Friesen WO (2005) Neuronal control of leech behavior. *Prog Neurobiol* 76:279–327.

Kuebler D, Tanouye M (2000) Modifications of seizure susceptibility in *Drosophila*. *J Neurophysiol* 83:998–1009.

Kuebler D, Zhang H, Ren X, Tanouye M (2001) Genetic suppression of seizure susceptibility in *Drosophila*. *J Neurophysiol* 86:1211–1225.

Kuipers JB (2002). *Quaternions and Rotation Sequences: A Primer with Application to Orbits, Aerospace, and Virtual Reality.* Princeton, NJ: Princeton University Press.

Kusano K (1965) Electrical characteristics and fine structure of the *Kuruma*-shrimp nerve fibres (*Penaeus japonicus*). *Proc Jpn Acad* 41:952–957.

Kusano K (1966) Electrical activity and structural correlates of giant nerve fibers in *Kuruma* shrimp (*Penaeus japonicus*). *J Cell Physiol* 68:361–384.

Kusano K, LaVail M (1971) Impulse conduction in the shrimp medullated giant fiber with special reference to the structure of functionally excitable areas. *J Comp Neurol* 142:481–494.

Lee J, Wu CF (2002) Electroconvulsive seizure behavior in *Drosophila*: Analysis of the physiological repertoire underlying a stereotyped action pattern in bang-sensitive mutants. *J Neurosci* 22:11065–11079.

Levine J (1974) Giant neuron input in mutant and wild type *Drosophila*. *J Comp Physiol A* 93:265–285.

Levine J, Hughes M (1973) Stereotaxic map of the muscle fibers in the indirect flight muscles of *Drosophila melanogaster*. *J Morphol* 140:153–158.

Levine J, Tracey D (1973) Structure and function of the giant motorneuron of *Drosophila melanogaster*. *J Comp Physiol A* 87:213–235.

Levine JD, Wyman RJ (1973) Neurophysiology of flight in wild-type and a mutant *Drosophila*. *Proc Natl Acad Sci USA* 70:1050–1054.

Lima S, Miesenbock G (2005) Remote control of behavior through genetically targeted photostimulation of neurons. *Cell* 121:141–152.

Loesel R, Nässel DR, Strausfeld NJ (2002) Common design in a unique midline neuropil in the brains of arthropods. *Arthropod Struct Dev* 31:77–91.

Malamud J, Mizisin A, Josephson RK (1988) The effects of octopamine on contraction kinetics and power output of a locust flight muscle. *J Comp Physiol A* 162:827–835.

Manoli DS, Foss M, Villella A, Taylor BJ, Hall JC, Baker BS (2005) Male-specific *fruitless* specifies the neural substrates of *Drosophila* courtship behaviour. *Nature* 436:395–400.

Matheson T (1998) Contralateral coordination and retargeting of limb movements during scratching in the locust. *J Exp Biol* 201(Pt13):2021–2032.

Matheson T, Dürr V (2003) Load compensation in targeted limb movements of an insect. *J Exp Biol* 206:3175–3186.

Milde JJ, Strausfeld NJ (1990) Cluster organization and response characteristics of the giant fiber pathway of the blowfly *Calliphora erythrocephala*. *J Comp Neurol* 294:59–75.

Miller A (1950) The internal anatomy and histology of the imago of *Drosophila melanogaster*. In: *Biology of Drosophila* (Demerec M, ed), pp 420-534. London: Wiley and Sons.

Mulloney B (1969) Interneurons in the central nervous system of flies and the start of flight. *Z vergl Physiologie* 64:243–253.

Muralidhar MG, Thomas J (1993) The *Drosophila bendless* gene encodes a neural protein related to ubiquitin-conjugating enzymes. *Neuron* 11:253–266.

Murphey RK, Froggett SJ, Caruccio P, Shan-Crofts X, Kitamoto T, Godenschwege TA (2003) Targeted expression of *shibire* ts and *semaphorin 1a* reveals critical periods for synapse formation in the giant fiber of *Drosophila*. *Development* 130:3671–3682.

Murphey RK, Godenschwege TA (2002) New roles for ubiquitin in the assembly and function of neuronal circuits. *Neuron* 36:5–8.

Nachtigall W, Wilson DM (1967) Neuro-muscular control of Dipteran flight. *J Exp Biol* 47:77–97.

Nakashima-Tanaka E, Matsubara K (1979) An anomalous response (jumping behaviour) to light in *Drosophila melanogaster*. *Jap J Genet* 54:345–357.

Offner F, Weinberg A, Young G (1940) Nerve conduction theory: Some mathematical consequences of Bernstein's model. *B Math Biol* 2:86–103.

Oh CE, McMahon R, Benzer S, Tanouye M (1994) *bendless*, a *Drosophila* gene affecting neuronal connectivity, encodes a ubiquitin-conjugating enzyme homolog. *J Neurosci* 14:3166–3179.

Olsen SR, Wilson RI (2008) Cracking neural circuits in a tiny brain: New approaches for understanding the neural circuitry of *Drosophila*. *Trends Neurosci* 31:512–520.

Pavlidis P, Ramaswami M, Tanouye M (1994) The *Drosophila easily shocked* gene: a mutation in a phospholipid synthetic pathway causes seizure, neuronal failure, and paralysis. *Cell* 79:23–33.

Pavlidis P, Tanouye M (1995) Seizures and failures in the giant fiber pathway of *Drosophila* bang-sensitive paralytic mutants. *J Neurosci* 15:5810–5819.

Phelan P, Bacon JP, Davies JA, Stebbings LA, Todman MG, Avery L, Baines RA, Barnes TM, Ford C, Hekimi S, Lee R, Shaw JE, Starich TA, Curtin KD, Sun YA, Wyman RJ (1998) Innexins: A family of invertebrate gap-junction proteins. *Trends Genet* 14:348–349.

Phelan P, Nakagawa M, Wilkin MB, Moffat KG, O'Kane CJ, Davies JA, Bacon JP (1996) Mutations in *shaking-B* prevent electrical synapse formation in the *Drosophila* giant fiber system. *J Neurosci* 16:1101–1113.

Phelan P, Starich TA (2001) Innexins get into the gap. *Bioessays* 23:388–396.

Phelan P, Stebbings LA, Baines RA, Bacon JP, Davies JA, Ford C (1998) *Drosophila Shaking-B* protein forms gap junctions in paired *Xenopus* oocytes. *Nature* 391:181–184.

Phillips WF (2002) Aircraft flight simulation. In: *Mechanics of Flight,* pp 867-890. Hoboken, NJ: Wiley and Sons.

Pick S, Strauss R (2005) Goal-driven behavioral adaptations in gap-climbing. *Curr Biol* 15:1473–1478.

Pitman RM, Tweedle CD, Cohen MJ (1972) Branching of central neurons: Intracellular cobalt injection for light and electron microscopy. *Science* 176:412–414.

Politoff A, Pappas GD, Bennett MV (1974) Cobalt ions cross an electrotonic synapse if cytoplasmic concentration is low. *Brain Res* 76:343–346.

Posas F, Takekawa M, Saito H (1998) Signal transduction by MAP kinase cascades in budding yeast. *Curr Opin Microbiol* 1:175–182.

Power M (1948) The thoracico-abdominal nervous system of an adult insect, *Drosophila melanogaster*. *J Comp Neurol* 88:347–409.

Pringle JWS (1949) The excitation and contraction of the flight muscles of insects. *J Physiol (Lond)* 108:226–232.

Pringle JWS (1957). *Insect flight.* Cambridge, MA: Cambridge University Press.

Pringle JWS (1968) Comparative physiology of the flight motor. In: *Advances in Insect Physiology* (Beament JWL, ed), pp 163-228. London: Academic Press.

Reichardt W (1987) Evaluation of optical motion information by movement detectors. *J Comp Physiol A* 161:533–547.

Ritzmann RE, Eaton RC (1997) Neural substrates for initaion of startle responses. In: *Neurons, Networks, and Motor Behavior* (Stein P, Stuart D, Selverston A, Grillner S, eds), pp 33-44. Cambridge, MA: MIT Press.

Roeder K (1951) Movements of the thorax and potential changes in the thoracic muscles of insects during flight. *Biol Bull* 100:95–106.

Rushton W (1951) A theory of the effects of fibre size in medullated nerve. *J Physiol (Lond)* 115:101–122.

Santer RD, Yamawaki Y, Rind FC, Simmons PJ (2005) Motor activity and trajectory control during escape jumping in the locust, *Locusta migratoria*. *J Comp Physiol A* 191:965–975.

Santer RD, Yamawaki Y, Rind FC, Simmons PJ (2008) Preparing for escape: An examination of the role of the DCMD neuron in locust escape jumps. *J Comp Physiol A* 194:69–77.

Schilstra C, Hateren J (1999) Blowfly flight and optic flow. I. Thorax kinematics and flight dynamics. *J Exp Biol* 202(Pt11):1481–1490.

Schneiderman AM, Tao ML, Wyman RJ (1993) Duplication of the escape-response neural pathway by mutation of the *bithorax*-complex. *Dev Biol* 157:455–473.

Schouest LP, Anderson M, Miller TA (1986) The ultrastructure and physiology of the tergotrochanteral depressor muscle of the housefly, *Musca domestica*. *J Exp Zool* 239:147–158.

Siddiqi O, Benzer S (1976) Neurophysiological defects in temperature-sensitive paralytic mutants of *Drosophila melanogaster*. *Proc Natl Acad Sci USA* 73:3253–3257.

Soler C (2004) Coordinated development of muscles and tendons of the *Drosophila* leg. *Development* 131:6041–6051.

Sotavalta O (1953) Recordings of high wing-stroke and thoracic vibration frequency in some midges. *Biol Bull* 104:439–444.

Stein PSG (2008) Motor pattern deletions and modular organization of turtle spinal cord. *Brain Res Rev* 57:118–124.

Stevenson P, Meuser S (1997) Octopaminergic innervation and modulation of a locust flight steering muscle. *J Exp Biol* 200:633–642.

Stock JB, Surette MG (1996) Chemotaxis. In: *Escherichia coli and Salmonella Cellular and Molecular Biology* (Neidhardt FC, ed), pp 1103-1129. Washington, DC: ASM Press.

Strausfeld NJ, Bassemir U (1983) Cobalt-coupled neurons of a giant fibre system in Diptera. *J Neurocytol* 12:971–991.

Strausfeld NJ, Bassemir U, Singh R, Bacon JP (1984) Oraganizational principles of outputs from Dipteran brains. *J Insect Physiol* 30:77–93.

Strausfeld NJ, Obermayer M (1976) Resolution of intraneuronal and transynaptic migration of cobalt in the insect visual and central nervous systems. *J Comp Physiol A* 110:1–12.

Strausfeld NJ, Singh RN (1980) Peripheral and central nervous system projections in normal and mutant (*bithorax*) *Drosophila melanogaster*. *Basic Life Sci* 16:267–291.

Strauss R (2002) The central complex and the genetic dissection of locomotor behaviour. *Curr Opin Neurobiol* 12:633–8.

Sun YA, Wyman RJ (1996) *Passover* eliminates gap junctional communication between neurons of the giant fiber system in *Drosophila*. *J Neurobiol* 30:340–348.

Sutton GP, Burrows M (2008) The mechanics of elevation control in locust jumping. *J Comp Physiol A* 194:557–563.

Tanouye MA, Wyman RJ (1980) Motor outputs of giant nerve fiber in *Drosophila*. *J Neurophysiol* 44:405–421.

Tanouye M, Ferrus A, Fujita S (1981) Abnormal action potentials associated with the *Shaker* complex locus of *Drosophila*. *Proc Natl Acad Sci USA* 78:6548–6552.

Tanouye M, King DG (1983) Giant fibre activation of direct flight muscles in *Drosophila*. *J Exp Biol* pp. 241–251.

Thomas J, Wyman RJ (1982) A mutation in *Drosophila* alters normal connectivity between two identified neurones. *Nature* 298:650–651.

Thomas JB, Wyman RJ (1984) Mutations altering synaptic connectivity between identified neurons in *Drosophila*. *J Neurosci* 4:530–538.

Tiegs OW (1955) The flight muscles of insects–their anatomy and histology; with some observations on the structure of striated muscle in general. *Philos T Roy Soc B* 238:221–348.

Tobalske BW, Altshuler DL, Powers DR (2004) Take-off mechanics in hummingbirds (Trochilidae). *J Exp Biol* 207:1345–1352.

Tresch MC, Saltiel P, d'Avella A, Bizzi E (2002) Coordination and localization in spinal motor systems. *Brain Res Rev* 40:66–79.

Trimarchi J, Murphey RK (1997) The *shaking-B2* mutation disrupts electrical synapses in a flight circuit in adult *Drosophila*. *J Neurosci* 17:4700–4710.

Trimarchi J, Schneiderman AM (1993) Giant fiber activation of an intrinsic muscle in the mesothoracic leg of *Drosophila melanogaster*. *J Exp Biol* 177:149–167.

Trimarchi J, Schneiderman AM (1995a) Different neural pathways coordinate *Drosophila* flight initiations evoked by visual and olfactory stimuli. *J Exp Biol* 198:1099–1104.

Trimarchi J, Schneiderman AM (1995b) Flight initiations in *Drosophila melanogaster* are mediated by several distinct motor patterns. *J Comp Physiol A* 176:355–364.

Trimarchi J, Schneiderman AM (1995c) Initiation of flight in the unrestrained fly, *Drosophila melanogaster*. *J Zool (Lond)* 235:211–222.

Vrontou E, Nilsen SP, Demir E, Kravitz EA, Dickson BJ (2006) *fruitless* regulates aggression and dominance in *Drosophila*. *Nat Neurosci* 9:1469–1471.

Wallace GK (1959) Visual scanning in the desert locust, *Schistocerca Gregaria* Forskål. *J Exp Biol* 36:512–525.

Wallén P (1997) Spinal networks and sensory feedback in the control of undulatory swimming in lamprey. In: *Neurons, Networks, and Motor Behavior* (Stein P, Stuart D, Selverston A, Grillner S, eds), pp 75-81. Cambridge, MA: MIT Press.

Webb B (2004) Neural mechanisms for prediction: Do insects have forward models? *Trends Neurosci* 27:278–282.

Williams C, Williams M (1943) The flight muscles of *Drosophila repleta*. *J Morphol* 72:589–599.

Williamson R, Kaplan WD, Dagan D (1974) A fly's leap from paralysis. *Nature* 252:224–226.

Wisser A, Nachtigall W (1984) Functional-morphological investigations on the flight muscles and their insertion points in the blowfly *Calliphora erythrocephala* (Insecta, Diptera). *Zoomorphology* 104:188–195.

Wolpert DM, Ghahramani Z (2000) Computational principles of movement neuroscience. *Nat Neurosci Suppl* 3:1212–1217.

Wyman RJ, Thomas J (1983) What genes are necessary to make an identified synapse? *Cold Spring Harb Sym* 48(Pt2):641–652.

Wyman RJ, Thomas J, Salkoff LB, King DG (1984) The *Drosophila* giant fiber system. In: *Neural Mechanisms of Startle Behavior* (Eaton R, ed), pp 133-161. New York, NY: Plenum Press.

Yang CH, Belawat P, Hafen E, Jan LY, Jan YN (2008) *Drosophila* egg-laying site selection as a system to study simple decision-making processes. *Science* 319:1679–1683.

Young J (1936) The structure of nerve fibres in cephalopods and crustacea. *P R Soc B* 121:319–337.

Zalokar M (1947) Anatomie du thorax de *Drosophila melanogaster*. *Rev Suisse Zool* 54:17–53.

Zar J (1999). *Biostatistical Analysis,* 4th ed. Upper Saddle River, NJ: Prentice Hall.

Zhang H, Tan J, Reynolds E, Kuebler D, Faulhaber S, Tanouye M (2002) The *Drosophila slamdance* gene: a mutation in an aminopeptidase can cause seizure, paralysis and neuronal failure. *Genetics* 162:1283–1299.

Zumstein N, Forman O, Nongthomba U, Sparrow JC, Elliott C (2004) Distance and force production during jumping in wild-type and mutant *Drosophila melanogaster*. *J Exp Biol* 207:3515–3522.